

UNIVERSITÉ DU QUÉBEC À MONTRÉAL

STUDY OF LAKE-RIVER-ATMOSPHERE INTERACTIONS FOR
NORTHEAST CANADA IN CURRENT AND FUTURE CLIMATES

THESIS
PRESENTED
AS PARTIAL REQUIREMENT
FOR PHD DEGREE IN EARTH AND ATMOSPHERIC SCIENCES

BY
OLEKSANDR HUZİY

JUNE 2016

UNIVERSITÉ DU QUÉBEC À MONTRÉAL
Service des bibliothèques

Avertissement

La diffusion de cette thèse se fait dans le respect des droits de son auteur, qui a signé le formulaire *Autorisation de reproduire et de diffuser un travail de recherche de cycles supérieurs* (SDU-522 – Rév.07-2011). Cette autorisation stipule que «conformément à l'article 11 du Règlement no 8 des études de cycles supérieurs, [l'auteur] concède à l'Université du Québec à Montréal une licence non exclusive d'utilisation et de publication de la totalité ou d'une partie importante de [son] travail de recherche pour des fins pédagogiques et non commerciales. Plus précisément, [l'auteur] autorise l'Université du Québec à Montréal à reproduire, diffuser, prêter, distribuer ou vendre des copies de [son] travail de recherche à des fins non commerciales sur quelque support que ce soit, y compris l'Internet. Cette licence et cette autorisation n'entraînent pas une renonciation de [la] part [de l'auteur] à [ses] droits moraux ni à [ses] droits de propriété intellectuelle. Sauf entente contraire, [l'auteur] conserve la liberté de diffuser et de commercialiser ou non ce travail dont [il] possède un exemplaire.»

UNIVERSITÉ DU QUÉBEC À MONTRÉAL

ÉTUDE DES INTERACTIONS LAC-RIVIÈRE-ATMOSPHÈRE DANS LE
CLIMAT PRÉSENT ET FUTUR SUR LE NORD-EST DU CANADA

THÈSE
PRÉSENTÉE
COMME EXIGENCE PARTIELLE
DU DOCTORAT EN SCIENCES DE LA TERRE ET DE L'ATMOSPHÈRE

PAR
OLEKSANDR HUZİY

JUIN 2016

ACKNOWLEDGEMENTS

First, I would like to thank my supervisor, Laxmi Sushama, for introducing me to the domain of land surface modelling, for her patience, honesty, encouragement and kind advice.

I would like to thank Naveed Khaliq, for help and advice with statistical questions, Bernhard Lehner, for help with the development of the river flow direction upscaling algorithm and for sharing the high resolution dataset used by the algorithm, René Laprise and René Roy, for fruitful discussions and advice at the start of the project.

I would also like to thank NSERC, Hydro-Québec and Ouranos for funding the project and centre ESCER for providing the infrastructure, which made this project possible.

I am very grateful to my wife, Tanya, and son, Mark, for their love, encouragement, patience and understanding; to my parents, Misha and Nelya, for their support and trust in me from the start of my path into science.

Also, special thanks to Andrey Martynov, who told me about UQÀM and made my transition to the new learning and research environment quick and easy.

It was a pleasure to work with such helpful people like Michel Valin, Katja Winger, Bernard Dugas, Nadjat Labassi, George Huard, Adelina Alexandru and Delphine Person. Thank you for your support and help.

I would also like to thank all my friends and colleagues at UQÀM for friendly talks and discussions.

CONTENTS

LIST OF FIGURES	vii
LIST OF TABLES	xiii
LIST OF ACRONYMS	xv
RÉSUMÉ	xvii
ABSTRACT	xxi
INTRODUCTION	1
CHAPTER I	
ANALYSIS OF STREAMFLOW CHARACTERISTICS OVER NORTH- EASTERN CANADA IN A CHANGING CLIMATE	7
1.1 Introduction	9
1.2 Model and experiments	12
1.3 Methodology	15
1.4 Results	18
1.4.1 Model verification	18
1.4.2 Projected changes based on ensemble averaging approach . . .	24
1.4.3 Projected changes based on merged longer samples	39
1.5 Discussion and conclusions	43
CHAPTER II	
IMPACT OF LAKE-RIVER CONNECTIVITY AND INTERFLOW ON THE CANADIAN RCM SIMULATED REGIONAL CLIMATE AND HY- DROLOGY FOR NORTHEAST CANADA	47
2.1 Introduction	48
2.2 Models, experimental configuration and data	51
2.2.1 River-lake routing model	52
2.2.2 Experimental configuration and observation data	53

2.3	Methodology	57
2.4	Results	59
2.4.1	Impact of lakes on regional climate and hydrology	59
2.4.2	Direct impact of lakes on streamflow	66
2.4.3	Impact of interflow	71
2.5	Summary and conclusions	74
CHAPTER III		
LAKE-RIVER AND LAKE-ATMOSPHERE INTERACTIONS IN A CHANG-		
ING CLIMATE OVER NORTHEAST CANADA		77
3.1	Introduction	79
3.2	Models and methods	83
3.2.1	Model	83
3.2.2	Methods	85
3.3	Results	89
3.3.1	Performance and boundary forcing errors	89
3.3.2	Projected regional climate and streamflow changes	99
3.3.3	Influence of lakes on projected climate change	106
3.3.4	Influence of interflow on projected climate change	108
3.4	Conclusions	111
CONCLUSION		115
REFERENCES		119

LIST OF FIGURES

Figure	Page
I.1 Study region with basins of interest, topography [m] and lakes. The lakes information was taken from the Level1 of the Global Lakes and Wetlands Database (GLWD) (Lehner and Döll, 2004).	3
1.1 (a) Study domain with its 21 watersheds along with the flow directions. Watersheds are marked using their abbreviated names (Table 1.1). Simulation domain of the CRCM is shown in the inset. (b) Location of the gauging stations (red triangles) used in the evaluation of CRCM simulated streamflow characteristics. Station identification numbers assigned by CEHQ are also shown.	14
1.2 Comparison of observed and modelled hydrographs (mean daily streamflows). The length of the observed record varies from 10–20 years within the 1970 to 1999 period. The values of the Nash-Sutcliffe (ns) index and correlation coefficient (r) based on mean daily streamflow comparisons, station identification number and longitude-latitude values of station location are also shown.	21
1.3 Biases in the (a) mean winter (DJF) snow water equivalent (in mm) and (b) mean spring (MAM) 2-m temperature (in °C).	22
1.4 Scatter plots of selected observed and modelled (a) high and (b) low flow return levels (in m ³ /s).	23
1.5 Ensemble averaged projected changes to mean a annual and b-e seasonal streamflow. Grid cells where the changes are not significant at the 5 % significance level are masked in grey.	29
1.6 Ensemble averaged projected changes to mean a-d seasonal 2-m temperature. Grid cells where the changes are not significant at the 5 % significance level are masked in grey.	30
1.7 Ensemble averaged projected changes to mean a-d seasonal precipitation (in mm/day), and e winter (DJF) SWE (in mm). Grid cells where the changes are not significant at the 5 % significance level are masked in grey.	31

1.8	Ensemble averaged normalized frequency of occurrence of 1-day high flow events for current 1970–1999 (left y-axis) and future 2041–2070 (right y-axis) period for northern (top panel), central (middle panel) and southern (bottom panel) watersheds. The numbers correspond to watershed indices given in Table 1.1. Inset shows changes to normalized frequency of occurrence from current to future climate.	32
1.9	Same as in Fig. 1.8 but for low flow events.	33
1.10	a–e Projected changes (in %) to 10-year return levels of 1-day high flows derived from five future and current period simulation pairs (F1–C1, F2–C2, . . . , F5–C5). f Ensemble averaged changes to 10-year return levels of high flows. Grid cells where the changes are not significant at the 5 % significance level are shown in grey. . .	34
1.11	Same as in Fig. 1.10 but for 30-year return levels of high flows. . .	35
1.12	a–e Projected changes (in %) to 2-year return levels of 15-day low flows derived from five future and current period simulation pairs (F1–C1, F2–C2, . . . , F5–C5). f Ensemble averaged changes to 2-year return levels of low flows. Grid cells where the changes are not significant at the 5 % significance level are shown in grey.	36
1.13	Same as in Fig. 1.12 but for 5-year return levels of low flows. . . .	37
1.14	Coefficient of variation (ratio of standard deviation to the mean absolute value based on the five ensemble members) of projected changes to selected return levels of high and low flows.	38
1.15	<i>p</i> values of the Kruskal–Wallis test for a mean annual flows, b 15-day low flows, and c 1-day high flows for current (left column) and future (right column) climates.	40
1.16	Projected changes (in %) to mean (a) annual and (b–e) seasonal streamflows. Grid cells where the changes are not significant at the 5% significance level are shown in grey.	41
1.17	Projected changes (in %) to 10- and 30-year return levels of high flows (left column) and 2- and 5-year return levels of low flows (right column) derived using longer samples (consisting of 150 values) for each grid-cell both for current and future climates. Grid cells where the changes are not significant at the 5% significance level are shown in grey.	42

2.1	Representation of local and global lakes in the lake-river routing scheme.	52
2.2	(a) Simulation domain; the dashed line separates the blending and free zones. The colours correspond to topography (m). Ocean and inland water bodies are shown in blue. Geophysical fields used in the simulations: (b) lake fraction, (c) depth to bedrock, (d) percentage of sand and (e) percentage of clay.	56
2.3	Inclined soil layer and saturation front at the critical time ($t = t_c$) when the interflow regime changes from linear to exponential function of time.	57
2.4	Upper row: CRCM5-NL simulated seasonal mean 2-m air temperatures ($^{\circ}\text{C}$), for the 1991–2010 period. Lower row: difference between CRCM5-L1 and CRCM5-NL simulated mean seasonal 2-m air temperature. Black dots are used to show grid points where the differences are statistically significant at 10% significance level.	60
2.5	Same as Fig. 2.4 but for down-welling long-wave radiation at the surface in W/m^2	60
2.6	Same as Fig. 2.4 but for total precipitation (mm/season).	61
2.7	Same as Fig. 2.4 but for streamflow (m^3/s).	61
2.8	(a) Locations of streamflow gauging stations (red dots) and their corresponding upstream areas. (b) Differences between modelled (CRCM5-L1 and CRCM5-NL simulations) and observed (Brown et al., 2003) SWE (mm) for winter (DJF) and for spring 2-m temperature.	64
2.9	Comparison of the climatologic streamflow from experiments CRCM5-NL, CRCM5-L1 and observations at selected gauging stations. The panels are sorted according to the station latitude, i.e. the northernmost (southernmost) stations are shown in the top (bottom) panels.	65
2.10	Mean seasonal streamflow (upper row, for simulation CRCM5-L1) and changes to the mean streamflow due to lake routing (bottom row, i.e. CRCM5-L2 minus CRCM5-L1). All values are in m^3/s . Dots show grid cells where the differences are statistically significant at 10% significance level.	66

2.11	(a) Same as Fig. 2.9 but for simulations CRCM5-L1 and CRCM5-L2, (b) Scatter plots of 90 th (left) and 10 th percentiles (right) of the daily mean climatologic streamflows derived from observed and modelled (CRCM5-L1 and CRCM5-L2) streamflows.	69
2.12	(a) Locations and identification numbers of lake level gauging stations. (b) Mean seasonal cycle of observed and simulated lake level variability. CRCM5-L2 (red), CRCM5-L2(P-E) (blue), and observed (black, taken from CEHQ dataset).	70
2.13	Zonally averaged mean interflow rate for the first soil layer, for the 1991–2010 period, for CRCM5-L2I.	71
2.14	Differences between CRCM5-L2I and CRCM5-L2 simulated fields; from top to bottom are streamflow, surface runoff, moisture in the first soil layer, total precipitation, subsurface runoff and latent heat flux. Black dots indicate grid cells with statistically significant differences at 10% significance level.	72
2.15	Correlations between CRCM5-L2I variables, for the 1991–2010 period (INTF – interflow rate in the top soil layer, PR – total precipitation rate, SI – soil ice fraction in the top soil layer, SWE – snow water equivalent, LHF – latent heat flux), for spring and summer seasons.	73
3.1	The simulation domain, with the topography shown in color. The black solid line separates the free zone from the blending zone, while the black dashed line separates the blending and outer halo zones. The grey lines show every 20 th grid point. The bottom left panel shows the free domain with the basins of interest, while zonally averaged lake fractions are shown in the bottom right panel. The grey circles show basin outlets determined from the flow direction field used for streamflow simulation. Basin boundaries are shown in red.	80
3.2	Seasonal mean 2-m air temperature [°C] from CRU (first row), Hopkinson et al. (2011) (second row) and the differences between ERAI-CRCM5-L and CRU (third row) and ERAI-CRCM5-L and Hopkinson et al. (2011) (fourth row), for the 1980–2010 period. CRU values are masked over the Great Lakes, since station data from over the lakes were not used to produce this dataset.	90
3.3	Same as in Fig. 3.2 but for the total precipitation in mm/day. . .	91

3.4	Observed (from Brown et al. (2003); top panels) and ERAI-CRCM5-L simulated (middle panels) SWE [mm] for winter and spring for the 1980–1996 period. Differences between ERAI-CRCM5-L simulated SWE and that observed are shown in the bottom panels for the same period.	92
3.5	(a) Locations and identification numbers (IDs) of the gauging stations considered for validation, with their upstream areas (determined from the flow directions field) shown shaded. (b) Comparison of observed (black) and modelled (blue and red correspond to ERAI-CRCM5-L and CanESM2-CRCM5-L simulations, respectively) mean annual hydrographs [m^3/s] at selected stations. The analysed time intervals are based on the availability of observation data during the 1980–2010 period.	93
3.6	Scatter plots of 10- and 50-year observed and modelled return levels of 1-day high flow (top panels) and 2- and 5-year observed and modelled return levels of 15-day low flow, at the six selected gauging stations shown in Fig. 3.5.	94
3.7	Boundary forcing errors, i.e. differences between CanESM2-CRCM5-L and ERAI-CRCM5-L simulations for the 1980–2010 period, for 2-m air temperature [$^{\circ}\text{C}$] (first row), total precipitation [mm/day] (second row), SWE [mm] (third row) and streamflows [m^3/s] (fourth row).	95
3.8	Simulated mean annual hydrographs [m^3/s] for the reanalysis-driven ERAI-CRCM5-L (blue) and the GCM-driven CanESM2-CRCM5-L (red) simulations, for the period 1980–2010, at the outlets of the WAS, SAG, RDO, PYR, LGR and ARN basins.	96
3.9	Projected changes for the 2070–2100 period with respect to the 1980–2010 period to 2-m temperature [$^{\circ}\text{C}$], total precipitation [mm/day], SWE [mm], latent heat flux [W/m^2] and streamflows [m^3/s]; the grid-cells where the changes are not significant at the 5% significance level are indicated with dots. The changes are based on CanESM2-CRCM5-L simulation results between 1980–2010 and 2070–2100 periods.	100

- 3.10 Projected changes for the 2070–2100 period with respect to the 1980–2010 period to the 10- and 50-year return levels of 1-day high flow (upper panel) and of 2- and 5-year return levels of 15-day low flow (bottom panel) for CanESM2-CRCM5-L. Changes that are not significant at the 5% significance level (evaluated using bootstrap procedure) are hatched over. 101
- 3.11 Zonally averaged projected changes to (a) lake surface water temperature, (b) lake ice thickness and (c) fraction of lake ice and (d) lake levels for the period 2070–2100 with respect to 1980–2010 from the CanESM2-CRCM5-L simulation. 102
- 3.12 Impact of lakes on projected changes for the period 2070–2100 with respect to the period 1980–2010 (i.e. differences between projected changes based on CanESM2-CRCM5-L and CanESM2-CRCM5-NL projected changes) to seasonal mean 2-m air temperature [°C], total precipitation [mm/day], SWE [mm], latent heat flux [W/m²], streamflow[m³/s]. 105
- 3.13 Projected changes to mean hydrographs at the outlets of the ARN, PYR, LGR, WAS, SAG, RDO basins for CanESM2-CRCM5-NL (blue) and CanESM2-CRCM5-L (red) simulations and the difference in projected changes (green). Northern (southern) basins are shown in the top (bottom) panel. All values are in m³/s. The left axis indicates projected changes (red and blue lines) and the right axis indicates differences in projected changes. 106
- 3.14 Zonally averaged interflow rates (for the first soil layer, mm/day) simulated by CanESM2-CRCM5-LI are shown for current (1980–2010) and future climates (2070–2100) (upper row). The difference between the future and current climate, i.e. projected changes, is shown in the second row. 109
- 3.15 Projected changes to mean hydrographs at the outlets of the ARN, PYR, LGR, WAS, SAG, RDO basins for CanESM2-CRCM5-L (blue) and CanESM2-CRCM5-LI (red) simulations and the difference in projected changes (green). Northern (southern) basins are shown in the top (bottom) panel. All values are in m³/s. The left axis indicates projected changes (red and blue lines) and the right axis indicates differences in projected changes. 110

LIST OF TABLES

Table	Page
1.1 Description of 21 watersheds used in the study	11
2.1 List of simulations used in the current study.	58
3.1 List of simulations used in the current study.	88
3.2 Names, abbreviations and drainage areas (km ²) of the studied watersheds; the areas are calculated based on the flow direction field. The asterisk (*) indicates compound basins (PYR contains CAN and MAN is a sub-basin of BOM).	89
3.3 Annual mean biases [%] and correlations for the mean hydrographs at the 6 selected stations compared to those observed. All the correlation coefficients are significant at the 1% significance level	98

LIST OF ACRONYMS

CanESM2	Canadian Earth System Model, 2nd generation
CEHQ	Centre d'Expertise Hydrique du Québec
CGCM	Canadian Global Climate Model
CRCM	Canadian Regional Climate Model
CRU	Climatic Research Unit
ERA	European Centre for Medium-Range Weather Forecasts re-analysis
GCM	Global Climate Model
GLCC	Global lake cover characteristics
IPCC	Intergovernmental Panel on Climate Change
LHF	Latent Heat Flux
LSS	Land Surface Scheme
MCG	Modèles Climatiques Globaux
MCR	Modèles Climatiques Régionaux
MRCC	Modèle Régional Canadien du Climat
NARCCAP	North American Regional Climate Change Assessment Program
RCM	Regional Climate Model
RCP	Representative Concentration Pathway
SWE	Snow water equivalent
UDel	University of Delaware
USGS	United States Geological Survey

RÉSUMÉ

Le cycle hydrologique de la terre devrait être modifié par le changement climatique. Des études précédentes basées sur des modèles climatiques globaux (MCG) ont montré une future intensification dans la moyenne globale des précipitations et de l'évaporation. Cependant, à l'échelle régionale, des augmentations et diminutions significatives sont prédites. L'étude des réponses régionales au changement climatique requiert le plus souvent l'utilisation de simulations à plus haute résolution que celle employée dans les modèles globaux. Par conséquent, les modèles climatiques régionaux (MCR) sont de plus en plus utilisés dans le but de comprendre les interactions et rétroactions entre les différentes composantes du système climatique dans le cadre du climat présent et futur. La résolution des MCR est en constante augmentation rendant nécessaire la prise en compte des surfaces d'eau intérieures ainsi que leurs interactions avec les autres composantes du système climatique. L'objectif de cette étude est l'implémentation d'un module rivière-lac ainsi que la paramétrisation de l'écoulement latéral dans le sol (écoulement hypodermique) dans la cinquième génération du modèle climatique canadien du climat (MRCC5). Le nouveau système ainsi développé sera ensuite validé par l'évaluation des interactions rivière-lac-atmosphère ainsi que les changements projetés dans l'hydrologie de surface et le climat dans les régions de latitudes élevées. Le domaine considéré dans cette étude couvre 21 bassins versants du nord-est Canadien localisés principalement dans la province du Québec avec quelques parties situées dans les provinces avoisinantes (Ontario et Terre-Neuve-et-Labrador). Le choix du domaine est justifié par la multitude des lacs et rivières dont l'importance est cruciale pour la population à bien des égards, on pourrait citer l'hydro-électricité, transports, tourisme. Cette étude est donc d'intérêt scientifique mais aussi économique.

La première partie de cette thèse est consacrée à l'analyse des caractéristiques des débits, c'est à dire la moyenne annuelle, les écoulements saisonniers ainsi que les extrêmes dans un cadre de climat présent et futur. Aux fins d'analyse, les débits sont dérivés à partir de simulations d'ensemble de 10 membres produites par la quatrième génération du modèle régional canadien du climat (MRCC4) piloté par des sorties du modèle global canadien du climat (cinq représentant le climat présent 1970–1999 et les cinq restant le climat futur 2041–2070). Pour développer les changements projetés dans les caractéristiques des débits, deux approches sont utilisées: l'une basée sur le concept de la moyenne d'ensemble alors que la

deuxième est basée sur la fusion de membres de simulations du climat courant et futur selon des tests de comparaison multiples. La vérification des caractéristiques des débits simulés par le MRCC pour la période 1970–1999 suggère que les hydrographes moyens simulés ainsi que les caractéristiques des hauts débits sont raisonnablement comparables à ceux observés à l’exception de certaines déficiences dans la représentation des extrêmes dans les faibles écoulements. Les résultats des changements projetés dans les débits annuels moyens montrent une augmentation statistiquement significative sur la majorité du domaine d’étude alors que pour les débits saisonniers, on note des augmentations ou diminutions selon la saison. On note également que les valeurs de période de retour de 2 et 5 ans pour les débits moyennés sur 15 jours affichent une augmentation significative même si ces changements sont faibles en valeur absolue. En se basant sur l’approche de la moyenne d’ensemble, les changements obtenus pour les valeurs de période de retour 10 et 30 ans ne sont généralement pas significatifs. Cependant, une analyse similaire effectuée sur des échantillons plus longs révèle des augmentations significatives dans les périodes de retour des hauts débits principalement dans les bassins versants septentrionaux. Ces résultats suggèrent, pour le développement de projections robustes, d’utiliser des échantillons plus longs et particulièrement pour les événements extrêmes. Il est important de fournir de l’information sur les projections futures des caractéristiques des débits mais il est surtout important de comprendre les mécanismes physiques derrière ces changements projetés. Ceci a incité à des développements supplémentaires au MRCC ainsi qu’à la conduite des expériences de sensibilité afin de répondre à d’importantes questions scientifiques. Ceci fait l’objet de la deuxième et la troisième partie de cette thèse.

Dans la deuxième partie de la thèse, d’importants processus tels que la connectivité lac-rivière et l’écoulement hypodermique, c’est à dire l’écoulement latéral de l’eau dans les couches superficielles du sol, sont implémentés dans le MRCC5. En utilisant plusieurs expériences avec le modèle régional, les interactions entre lacs et rivières ont été évaluées ainsi que leur impact sur le climat régional et l’hydrologie nord-est Canadien; lors de ces simulations les lacs sont représentés par un modèle unidimensionnel (Hostetler), alors que les rivières sont modelées à l’aide d’un schéma de routage distribué (WATROUTE-modifié). La comparaison des simulations du MRCC5 avec et sans lacs pour le climat présent montre de large différences dans les précipitations hivernales et estivales et les température hivernales et met en évidence l’importance des lacs. Les simulations du MRCC5 avec et sans interactions lac-rivière suggèrent une meilleure représentation des débits dans le premier cas. L’inclusion du processus d’écoulement hypodermique induit des augmentations des débits de plusieurs rivières pendant l’été et l’automne causant des changements modestes dans les interactions sol-atmosphère à travers la modification de l’humidité du sol. L’impact de l’écoulement latéral sur les débits dans la zone d’étude est comparable à celui obtenu en incluant les interactions

lac-atmosphère.

Finalement, la troisième partie de la thèse est consacrée à l'évaluation de l'impact du changement climatique sur les lacs et l'hydrologie ainsi que l'influence des lacs sur les changements projetés sur le climat régional et l'hydrologie du nord-est du Canada. À cette fin, des simulations de changement climatique transitoire ont été réalisées avec le MRCC5 pour la période 1950–2100 avec et sans lacs avec le scénario RCP8.5. Les conditions aux frontières latérales sont fournies par des sorties du modèle canadien du système terre (CanESM2). La comparaison des changements projetés basés sur les simulations avec et sans lacs révèle que l'inclusion des lacs amortit les changements pour la température à 2-m et ceci pour toutes les saisons. Comme pour les débits, les lacs atténuent les changements des débits printaniers durant la fonte à cause de l'effet de leur effet de stockage. De façon similaire, on note que les lacs augmentent les changements projetés dans les débits estivaux du à la libération progressive de l'eau provenant de la fonte de neige qu'ils emmagasinent.

La contribution scientifique principale de ce travail est une meilleure compréhension des interactions lac-rivière-atmosphère sur la région d'étude. Ce travail est innovateur dans le sens où c'est la première fois que les interactions lac-rivière-atmosphère sont examinées au sein d'un système régional de modélisation climatique. Ces processus sont également étudiés dans un contexte de changement climatique régional dans le but de quantifier leur impact sur le signal de changement climatique sur les variables de surface ainsi que variables atmosphériques proches de la surface. Un résultat quelque peu technique de l'étude est l'exécution on-line du schéma de routage au sein d'un cadre complexe de calcul parallèle sur lequel tourne le MRCC5. Des améliorations additionnelles pourraient être apportées à ce système en incluant l'hydrologie thermique et la modélisation de la glace des rivières, ceci serait très bénéfique pour adresser d'autres questions scientifiques.

Mots clé: Changement climatique; Modélisation climatique régionale; Modélisation des débits; Modélisation des rivières; Modélisation des lacs, Interactions lac-rivière; Interactions lac-atmosphère; Débits extrêmes.

ABSTRACT

Climate change is expected to modify the Earth's hydrological cycle. As shown in previous studies using Global Climate Models (GCMs), an intensification of the global hydrological cycle is projected for the future climate, with both global average precipitation and evaporation increasing in the future. However, there will be significant increases or decreases at regional scales. To study regional responses to climate change, higher resolution simulations than those provided by GCMs are often required. Therefore, Regional Climate Models (RCMs) are being used more and more to understand interactions and feedbacks between various components of the climate system in current and future climates. The resolutions of RCMs are on the rise and at high resolution it becomes important to consider inland water bodies and their interactions with other components of the climate system. This study is aimed at implementing a river-lake module and interflow parametrization in the fifth generation Canadian Regional Climate Model (CRCM5), and assessing river-lake-atmosphere interactions and projected changes to the surface hydrology and climate for a high latitude region using this newly developed system. The study region considered in this study covers 21 northeast Canadian watersheds, located mainly in Quebec province and some parts of adjoining Ontario, Newfoundland and Labrador provinces. This domain is selected, given its innumerable lakes and rivers, that are crucial to the population in many respects, i.e. hydropower generation, transportation, tourism, thus making it interesting both from scientific and economic points of view.

The first part of this thesis focuses on the analysis of streamflow characteristics, i.e. mean annual and seasonal flows and extreme high and low flows, in current and future climates. For the analysis, streamflows are derived from a 10-member ensemble of the fourth generation Canadian Regional Climate Model (CRCM4) simulations, driven by the Canadian Global Climate Model outputs, of which five correspond to current 1970–1999 period, while the other five correspond to future 2041–2070 period. For developing projected changes to streamflow characteristics, two different approaches are used: one based on the concept of ensemble averaging, while the other approach is based on merged samples of current and similarly future simulations following multiple comparison tests. Verification of the CRCM simulated streamflow characteristics for the 1970–1999 period suggests that the model simulated mean hydrographs and high flow characteristics compare reasonably well with those observed, albeit some deficiencies in representing

the low flow extremes. Results of projected changes to mean annual streamflows suggest statistically significant increases nearly all over the study domain, while those for seasonal streamflow show increases/decreases depending on the season. Two- and five-year return levels of 15-day low flows are projected to increase significantly over most part of the study domain, although the changes are small in absolute terms. Based on the ensemble averaging approach, changes to 10- and 30-year return levels of high flows are not generally found significant. However, when a similar analysis is performed using longer samples, significant increases to high flow return levels are found mainly for northernmost watersheds. This part highlights the need for longer samples, particularly for extreme events, in the development of robust projections. Although important information on projected changes to streamflow characteristics are developed, it is important to understand the physical mechanisms behind these projected changes. This led to further developments of the CRCM and sensitivity experiments to focus on important science questions. This constitute parts two and three of this thesis.

In part two of the thesis important land processes such as lake-river connectivity and interflow, i.e. the lateral flow of water in the surface soil layers, were implemented in the CRCM5. Using a suite of experiments performed with the regional climate model, the interactions between lakes and rivers and their impact on the regional climate and hydrology of northeast Canada are assessed; in these simulations lakes are represented by a one-dimensional model (Hostetler), while the rivers are modelled using a distributed routing scheme (WATROUTE-modified). Comparison of CRCM5 simulations with and without lakes for current climate suggests large differences in winter/summer precipitation and winter temperature, highlighting the importance of lakes. CRCM5 simulations performed with and without lake-river interactions suggest improved representation of streamflows and lake levels in the former case. Inclusion of the interflow process leads to increases in streamflows during summer and fall seasons for many rivers, causing modest changes to land-atmosphere interactions via modified soil moisture. The impact of interflow on streamflows, obtained in the study region, is comparable to the impact of lake-atmosphere interactions on streamflows.

Finally, the third part of the thesis focuses on the assessment of the impact of climate change on lakes and hydrology as well as on the influence of lakes on projected changes to regional climate and hydrology for Northeast Canada. To this end, transient climate change simulations spanning the 1950–2100 period, with and without lakes, are performed with CRCM5, for the RCP8.5 scenario, using the Canadian Earth System Model (CanESM2) outputs as driving data at the lateral boundaries. Comparison of projected changes based on the simulations with and without lakes suggests that lakes dampen projected changes to 2-m temperature for all seasons. As for streamflows, lakes attenuate projected changes

to spring streamflow and this is due to the storage effect of lakes. Similarly lakes augment projected changes to summer streamflows due to the gradual release of snowmelt water stored in lakes.

In summary, the main scientific contribution of this work is improved understanding of lake-river-atmosphere interactions over the study region. This work is innovative in that it is for the first time that lake-river-atmosphere interactions are investigated within a single regional modelling system. These processes are also studied in the context of regional climate change to quantify their impact on the simulated climate change signal in the near-surface atmospheric and selected surface hydrologic fields. A somewhat technical outcome of the study is the on-line routing scheme within a complex parallel framework of CRCM5, which might be further improved by including thermal hydrology and river ice modelling that would be beneficial to address other science questions.

Keywords: Climate change; Regional climate modelling; Streamflow modelling; River modelling; Lake modelling; Lake-river interactions; Lake-atmosphere interactions; Extreme flows.

INTRODUCTION

Context and motivation

Earth's climate system is complex and its components interact on a wide range of temporal and spatial scales. Global Climate Models (GCMs), with extensive representation of physical processes within the atmospheric and oceanic components of the climate system, are the most comprehensive tools available to address these interactions and anticipated changes in future climate. Several recent studies based on GCMs report important regional differences in the response to the increased greenhouse gas forcing, either through changes in the hydrological cycle (Held and Soden, 2006) or atmospheric circulation patterns (Vallis et al., 2014). For example, Held and Soden (2006) report an intensification of the poleward moisture transfer and an enhancement of precipitation minus evaporation patterns in future climate. To better understand the regional changes, higher spatial resolution than traditionally used by GCMs (≥ 100 km), is necessary. Regional Climate Models (RCMs) offer higher spatial resolution than GCMs, since the simulation domains are much smaller in the case of RCMs, allowing for greater topographic complexity and finer-scale atmospheric dynamics to be simulated (Giorgi and Bates, 1989; Laprise, 2008). Therefore RCMs are more suitable for generating information required for many water related regional impact studies (Leung et al., 2003; Jha et al., 2004; Sushama et al., 2006; Poitras et al., 2011; Huziy et al., 2013; Clavet-Gaumont et al., 2013).

RCMs as well as GCMs use land surface schemes (LSSs) to represent heat and humidity exchanges between the land surface and the atmosphere. The LSSs have evolved from simplified energy and water budget equations (bucket scheme) into sophisticated physically based models, representing soil moisture and temperature profiles, snow and vegetation components (Pitman, 2003). Even though the importance of land surface has been recognized since a long time, the parametrization of lakes was not adequately addressed in majority of GCMs (Dutra et al., 2010;

Subin et al., 2012) and RCMs (Martynov et al., 2012; Samuelsson et al., 2010) until recently. In addition to the obvious impacts of lakes (warming in winter, increased humidity and precipitation, spring and summer cooling), they can also lead to decreases in precipitation by stabilizing overlaying air masses depending on the depth and size of lakes, changes in radiative fluxes through cloud cover modification and other indirect impacts on the regional climate. Although these feedbacks seem to be well captured by the sub-grid lake parametrization, the realism of the simulations is still limited when applied to very deep or large lakes (Bennington et al., 2014), mainly due to the lack of representation of circulation and related processes in the 1D lake models.

In the context of a changing climate, the stability of freshwater resources, is a major concern for various economic sectors, requiring detailed and reliable information of projected changes to the surface hydrology and climate. For example, information related to changes in river flow/lake characteristics is important in the management and planning/adaptation, notably for energy and agriculture sectors. Currently, most of the impact and adaptation studies use climate model outputs to drive lake/river (hydrological) models offline, to study changes to lake and river flow characteristics. However, with the improved representation of land processes in climate models, it is possible to obtain streamflows directly from many GCMs and RCMs. RCMs and GCMs, with their complete closed water budget including the atmospheric and land surface branches, are ideal tools to understand better the linkages and feedbacks between climate and hydrologic systems. However, many studies (Music et al., 2009; Sushama et al., 2006; Muerth et al., 2013) have identified biases in climate model simulated surface hydrology, particularly streamflows. This is primarily due to the lack of representation of processes in the models. For example, realistic simulation of streamflows requires adequate representation of lakes and lake-river connectivity in models. Other important processes include interflow, i.e. lateral flow of water in the upper soil layers along the topographic slopes, and surface-groundwater interactions. These processes when incorporated in climate models, in addition to the surface hydrology, may also impact the surface climate through modification of the surface energy and water budgets. This research thus makes an important contribution by bridging the gap between regional climate and hydrology by considering lakes, rivers, river-lake connectivity,

interflow and the atmosphere within the same regional climate modeling system.

Region of study and background information

The focus region of this study consists of 21 basins (Arnaud, Feuilles, M  l  zes, Caniapiscou, Caniapiscou (Pyrite), Grande rivi  re de la Baleine, Baleine, George, Churchill Falls, La Grande Riv  re, Natashquan, Romaine, Moisie, Manicouagan, Rupert, Bell, Saint Maurice, Ottawa, Saguenay, Bersimis-Outardes-Manic, Waswanipi) covering parts of northeastern Canadian provinces: Qu  bec, Newfoundland and Labrador, and Ontario (Fig. I.1). The most important of these basins is the La Grande, with an installed total power generation capacity of 17,000 MW. Ninety percent of this capacity comes from reservoir-type power stations, while the rest is generated by the run-of-river stations. For comparison,

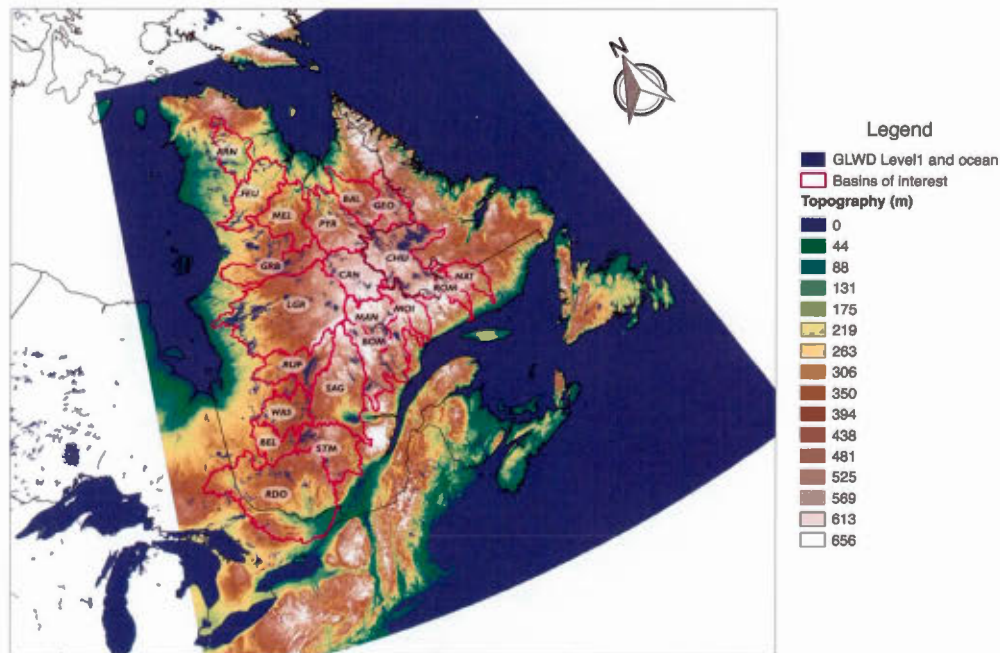


Figure I.1: Study region with basins of interest, topography [m] and lakes. The lakes information was taken from the Level1 of the Global Lakes and Wetlands Database (GLWD) (Lehner and D  ll, 2004).

Québec's summer peak demand is around 21000 MW and it goes up to 39000 MW in winter.

The largest natural lake by area in Québec is the lake Mistassini (around 2164 km², with the maximum depth of 183 m). It is located in the central part of the study region and drains mostly into the Rupert River. However, there are no major hydropower generation facilities downstream of the lake. On the contrary, Manicouagan lake, the fifth largest lake in the world by volume, located to the east of Lake Mistassini, is a very important reservoir for hydropower generation in the region. It serves as storage for downstream rivers Manicouagan and Outardes, where around 7000 MW of hydropower generation capacity is installed.

Streamflows and lake levels for these regions exhibit substantial variability within the year. The highest streamflows occur primarily during the melting season. Therefore, understanding streamflow regimes and streamflows is of interest to understand flooding risks. As for low streamflows, they are mostly observed during winter, with lakes and groundwater being the main sources. Assessing low flows is of interest to facilitate better management of hydropower generation, due to the higher electricity demand during winter.

Scientific objective and outline

This research is aimed at studying lake-river-atmosphere interactions and their evolution in future climate, for Northeastern Canada, using the fifth generation Canadian Regional Climate Model (CRCM5). The main science questions addressed are: (1) What is the impact of the increased greenhouse gas concentration in the atmosphere on the climate and hydrology of Northeastern Canada? (2) What is the role of lake-river and lake-atmosphere interactions in modifying the regional climate and hydrology for the study region? (3) What is the impact of lakes, lake-river connectivity and interflow on projected changes to the surface climate and hydrology? To answer these questions using a single regional modelling system, a river model and lake-river interactions and interflow parametrization are implemented first in CRCM5. Using carefully designed CRCM5 experiments, with and without the newly introduced modules/processes, for current and future climates, the answers to the above posed questions are sought. This research is

innovative in that it is the first time that a single regional modelling system is used to address the above indicated questions, which is crucial information for many impact and adaptation studies.

To model river flows in CRCM5, the distributed routing scheme WATROUTE (Soulis et al., 2000) is used. The lake model considered is the Hostetler's model (Hostetler et al., 1993), which is a 1D column model based on a vertical temperature diffusion equation. Lakes and rivers exchange water fluxes, via river and lake routing, and this is important for the realistic representation of streamflows.

The outline of the thesis is presented below:

Chapter one focuses on the analysis of streamflow characteristics, i.e. mean annual and seasonal flows and extreme high and low flows, in current and future climates (Question 1 above). For the analysis, an ensemble of simulations from the fourth generation Canadian Regional Climate Model (CRCM4), for current and future climates, is considered. For developing projected changes to streamflow characteristics, two different approaches are used: one based on the concept of ensemble averaging, while the other approach is based on merged samples of current and similarly future simulations, following multiple comparison tests. This work has been published in *Climate Dynamics*.

In the second chapter of the thesis, important land processes such as lake-river connectivity and interflow, i.e. the lateral flow of water in the surface soil layers, are implemented in CRCM5. Using a suite of experiments performed with the regional climate model, the interactions between lakes and rivers and their impact on the regional climate and hydrology of Northeastern Canada are assessed (Question 2 above). This work has been submitted to *Climate Dynamics*.

In the concluding third part of this work, the regional model, with and without the newly implemented modules is applied in transient climate change experiments over the study region. The climate change experiments are used to assess the impacts of lake-river-atmosphere interactions and of interflow on projected changes, as well as the impact of climate change on these processes (Question 3 above). This work is presented in the form of an article that has been submitted

to Climate Dynamics.

CHAPTER I

ANALYSIS OF STREAMFLOW CHARACTERISTICS OVER NORTHEASTERN CANADA IN A CHANGING CLIMATE

This chapter is presented in the format of a scientific article that has been published in the peer-reviewed journal *Climate Dynamics*. The design of the research and its performance together with the analysis of data and the redaction of this article are entirely based on my work, with the co-authors involved in the supervision of all these tasks. The detailed reference is:

Huziy, O., Sushama, L., Khaliq, M., Laprise, R., Lehner, B. et Roy, R. (2013). Analysis of streamflow characteristics over northeastern Canada in a changing climate. *Climate Dynamics*, 40(7-8), 1879–1901. <http://dx.doi.org/10.1007/s00382-012-1406-0>

Abstract

An analysis of streamflow characteristics (i.e. mean annual and seasonal flows and extreme high and low flows) in current and future climates for 21 watersheds of northeastern Canada covering mainly the province of Quebec is presented in this article. For the analysis, streamflows are derived from a 10-member ensemble of Canadian Regional Climate Model (CRCM) simulations, driven by the Canadian Global Climate Model simulations, of which five correspond to the current 1970–1999 period, while the other five correspond to the future 2041–2070 period. For developing projected changes of streamflow characteristics from current to future periods, two different approaches are used: one based on the concept of ensemble averaging while the other approach is based on merged samples of current and similarly future simulations following multiple comparison tests. Verification of the CRCM simulated streamflow characteristics for the 1970–1999 period suggests that the model simulated mean hydrographs and high flow characteristics compare well with those observed, while the model tends to underestimate low flow extremes. Results of projected changes to mean annual streamflow suggest statistically significant increases nearly all over the study domain, while those for seasonal streamflow show increases/decreases depending on the season. Two- and five-year return levels of 15-day low flows are projected to increase significantly over most part of the study domain, although the changes are small in absolute terms. Based on the ensemble averaging approach, changes to 10- and 30-year return levels of high flows are not generally found significant. However, when a similar analysis is performed using longer samples, significant increases to high flow return levels are found mainly for northernmost watersheds. This study highlights the need for longer samples, particularly for extreme events in the development of robust projections.

Keywords: Climate change; Extreme flows; Regional climate modelling; Statistical analysis

1.1 Introduction

Reliable information about various streamflow characteristics in a changing climate is critical for planning of adaptation measures, particularly for the energy and agriculture sectors. According to the Fourth Assessment Report (AR4) of the Intergovernmental Panel on Climate Change (IPCC) (2007), global mean precipitation and evaporation rates are projected to increase in a future climate, or in other words an intensification of the global hydrological cycle is to be expected in a future warmer climate. However, there will be important regional differences in changes to precipitation and evaporation. Held and Soden (2006), based on their analysis of the coupled climate models that participated in the AR4, suggests that the poleward vapour transport and the pattern of evapotranspiration minus precipitation will increase proportionally to the lower-tropospheric vapour if the lower-tropospheric relative humidity and flow is assumed unchanged. In other words, the current wet (dry) regions, i.e. regions where precipitation (evaporation) exceeds evaporation (precipitation), will become wetter (drier) in a future climate. Northeastern Canada, the region considered in this study, has an excess of precipitation over evaporation, with mean annual precipitation of the order of 800 mm according to the 1980–2010 normals based on the Global Precipitation Climatology Centre (Rudolf et al., 2010), and average annual evaporation of the order of 200 mm according to the 1980–2010 normals calculated using the European Centre for Medium-Range Weather Forecasts (ECMWF)’s ERA interim reanalysis data (Berrisford et al., 2009). According to the Global Climate Models (GCMs) participating in AR4 (IPCC, 2007), the mean annual precipitation rate for this region is projected to increase by $0.4\text{--}0.5\text{ mm}\cdot\text{day}^{-1}$, while mean annual evaporation and runoff increase by $0.1\text{--}0.2\text{ mm}\cdot\text{day}^{-1}$ and $0.1\text{--}0.3\text{ mm}\cdot\text{day}^{-1}$, respectively, in the future 2080–2099 period with respect to the 1980–1999 period. This northeastern part of Canada with its large number of hydroelectric power generation stations plays a very important role in the economy of the provinces located in the region, particularly the province of Quebec. Therefore, information on projected changes to various streamflow characteristics and associated uncertainties would be beneficial for better management of these mega-projects, including the "Plan Nord" recently initiated by the Government of Quebec (<http://plannord.gouv.qc.ca>).

The conventional approach to study projected changes to streamflow is based on hydrological models driven by climate model outputs for various scenarios. Few studies so far have looked at streamflow directly from climate models: Global Climate Models (GCMs) and Regional Climate Models (RCMs). RCMs and GCMs, with their complete closed water budget including both the atmospheric and land surface branches, are ideal tools to understand better the linkages and feedback between climate and hydrological systems, and to evaluate the impact of climate change on streamflows. RCMs offer higher spatial resolution than GCMs, allowing for greater topographic complexity and finer-scale atmospheric dynamics to be simulated and thereby representing a more adequate tool for generating the information required for regional impact studies. In a number of recent studies, RCMs have been used to study projected changes to various components of the hydrological cycle including streamflows (Jha et al., 2004; Wood et al., 2004; Sushama et al., 2006; Kay et al., 2006a,b; Graham et al., 2007a,b; Dadson et al., 2011; Poitras et al., 2011).

In this study, climate change impacts on selected streamflow characteristics for 21 northeast Canadian watersheds, located mainly in the Quebec province and some parts of the adjoining Ontario and Newfoundland and Labrador provinces of Canada, are considered. A ten-member ensemble of the Canadian RCM (CRCM), of which five correspond to the current 1970–1999 period and the other five correspond to the future 2041–2070 period, driven by five different members of a Canadian GCM (CGCM) initial condition ensemble is used for this purpose. RCM simulations in general are associated with several uncertainties including structural uncertainties associated with regional model formulation, uncertainties associated with the lateral boundary conditions from the driving GCM, emission scenarios, as well as the RCM’s own internal variability. de Elía et al. (2008) quantified some of these uncertainties using larger CRCM ensembles. Although it is very desirable to assess the various sources of uncertainties in streamflow projections as in Arnell (2011) and Kay et al. (2009), given the nature of the ensemble used in this study, it is not possible to address or quantify all uncertainties since the simulations considered here have been performed with the same model and configuration for one SRES (Special Report on Emissions Scenario) scenario. However, it can be used to quantify uncertainty associated with the natural variability of the driving

No.	Name of the watershed	Abbreviation	Area (km ²)
1	Arnaud	ARN	26,872
2	aux Feuilles	FEU	42,068
3	aux Mélèzes	MEL	40,624
4	Caniapiscau	CAN	37,566
5	Caniapiscau (Pyrite)	PYR	48,431
6	Grande Rivière de la Baleine	GRB	34,314
7	Baleine	BAL	29,896
8	George	GEO	24,159
9	Churchill Falls	CHU	69,632
10	La Grande Rivière	LGR	140,374
11	Natashquan	NAT	15,468
12	Romaine	ROM	13,212
13	Moisie	MOI	19,101
14	Manicouagan	MAN	29,343
15	Rupert	RUP	41,115
16	Bell	BEL	22,238
17	Saint Maurice	STM	42,843
18	Ottawa	RDO	143,241
19	Saguenay	SAG	72,678
20	Bersimis-Outardes-Manic	BOM	87,511
21	Waswanipi	WAS	31,691

Table 1.1: Description of 21 watersheds used in the study

GCM and the internal variability of the RCM combined.

For the northeast Canadian region considered in this work, no study has so far addressed projected changes to streamflow characteristics for all the 21 watersheds in a systematic way as presented in this study. Some studies focusing on individual watersheds in this northeast region of Canada such as Dibike and Coulibaly (2007), Quilbé et al. (2008), Minville et al. (2008, 2009), among others, based on hydrological models driven by temperature and precipitation data from climate models, are available. Recently Frigon et al. (2010) studied projected changes to mean annual runoff for the same region considered in this study and suggested increases in runoff in future climate for the northern part of the region. The main value of this work is in the detailed statistical analysis of mean annual, seasonal and extreme (low/high) flows and their associated uncertainties and timings of

extreme flows, topics that were not covered by earlier studies for this area in the context of a changing climate.

The article is organized as follows: description of the CRCM and simulations are presented in Section 1.2 and methodology is presented in Section 1.3. Evaluation of the CRCM simulated streamflow and assessment of projected changes to selected but important streamflow characteristics using two approaches are presented in Section 1.4 followed by conclusions in section 1.5.

1.2 Model and experiments

The streamflows considered in this study are simulated by the fourth generation of the CRCM (de Elia and Côté, 2010). The CRCM is a limited-area nested model based on the fully elastic non-hydrostatic Euler equations, solved with a semi-implicit and semi-Lagrangian scheme. Vertical resolution is variable with a Gal-Chen scaled-height terrain following coordinate (29 levels, with model top at 29 km) (Gal-Chen and Somerville, 1975). The CRCM lateral boundary conditions are provided through a one-way nesting method inspired by Davies (1976) and refined by Yakimiw and Robert (1999). The subgrid-scale parameterization package is mostly based on the Canadian GCM Version III (CGCM3.1), except for the moist convective adjustment scheme that follows Bechtold-Kain-Fritsch's parameterization (Bechtold et al., 2001). The land surface scheme is the Canadian LAnd Surface Scheme (CLASS), version 2.7 (Versegny, 1991, 1996). This version of CLASS uses three soil layers, 0.1 m, 0.25 m and 3.75 m thick, corresponding approximately to the depth influenced by the diurnal cycle, the rooting zone and the annual variations of temperature, respectively. CLASS includes prognostic equations for energy and water conservation for the three soil layers and a thermally and hydrologically distinct snowpack where applicable (treated as a fourth variable-depth layer). The thermal budget is performed over the three soil layers, but the hydrological budget is done only for layers above the bedrock. Vegetation canopy in CLASS is treated explicitly with properties based on four vegetation types: coniferous trees, deciduous trees, crops and grass. Vegetation canopy can intercept rain and snow precipitation and has its own energy and water treatment with prognostic variables for canopy temperature, water storage

and mass. CLASS adopts a pseudo-mosaic approach and divides each grid-cell into a maximum of four sub-areas: bare soil, vegetation, snow over bare soil and snow with vegetation. The energy and water budget equations are first solved for each sub-area separately and then averaged over the grid-cell.

As already mentioned, a 10-member CRCM ensemble is considered in this study. Of the 10 members, five correspond to the current 1970–1999 period while the other five are the matching pairs of simulations for the future 2041–2070 period. Five different members of a CGCM initial condition ensemble were used to drive the five CRCM current and future simulations: It should be noted that the future climate simulations correspond to IPCC’s SRES A2 scenario (high population, low economy and low technology) and current climate simulations correspond to the twentieth-century climate (20C3M) scenario. The above current and future CRCM simulations will be referred to as C1–C5 and F1–F5, respectively. In addition, another CRCM simulation driven by the ECMWF’s Re-Analysis (ERA40; Uppala et al., 2005) is also considered. This simulation will be referred to as ‘control simulation’ hereafter. As suggested by IPCC (2001), the study of RCM simulations nested by analysis of observations or so-called ‘perfect’ boundary conditions such as ERA40 can reveal RCM ‘performance errors’. Therefore, the streamflows from the control simulation are compared to those observed to assess the CRCM’s performance. The inset of Fig. 1.1 shows the CRCM simulation domain, which consists of a 200×192 points grid covering all of North America and adjoining oceans, with a horizontal grid-point spacing of 45 km. It should be noted that the current study focuses only on the 21 watersheds located in the northeastern part of the simulation domain (Fig. 1.1).

Streamflow is generated from CRCM simulated runoff using a modified version of the routing model WATROUTE (Soulis et al., 2000). The routing scheme solves the water balance equation at each grid-cell, and relates the water storage to outflow from the grid-cell, using Manning’s equation. The modified scheme includes a groundwater reservoir, which is modelled as a linear reservoir as proposed in Lucas-Picher et al. (2003) and Sushama et al. (2004). Flow directions, channel lengths and slopes required by the routing scheme were derived from the HydroSHEDS database (Lehner et al., 2008), available at 30-second resolution on a

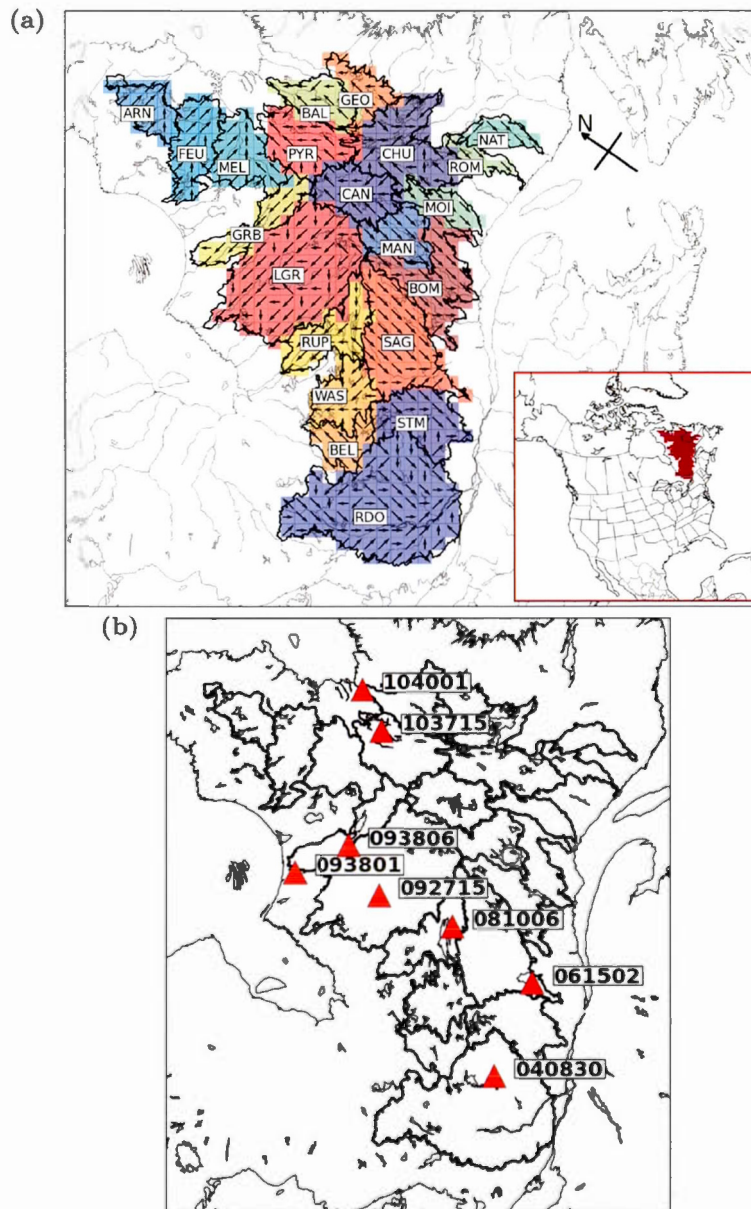


Figure 1.1: (a) Study domain with its 21 watersheds along with the flow directions. Watersheds are marked using their abbreviated names (Table 1.1). Simulation domain of the CRCM is shown in the inset. (b) Location of the gauging stations (red triangles) used in the evaluation of CRCM simulated streamflow characteristics. Station identification numbers assigned by CEHQ are also shown.

latitude-longitude grid. These data were up-scaled and projected to the model's grid and resolution. The up-scaling algorithm is based on the one developed by Döll and Lehner (2002). The flow directions thus derived are also shown in Fig. 1.1.

1.3 Methodology

Verification of CRCM-simulated mean hydrological regime and characteristics of extreme flow events, i.e. timing and return levels of selected return periods, and their projected changes in future climate are considered in this study. For verification purposes, model-simulated streamflow characteristics from the control simulation are compared to those observed, derived from the daily streamflow dataset from CEHQ (Centre d'expertise hydrique du Québec; <http://www.cehq.gouv.qc.ca/>) at selected gauging stations. The location of the gauging stations considered in the study is shown in Fig. 1.1b. The duration of the data available at these gauging stations, within the period of interest, i.e. 1970–1999, varies from 10 to 20 years. Nash-Sutcliffe (ns) index (Nash and Sutcliffe, 1970) and correlation coefficient (r) (Walpole and Myers, 1985) are used to compare the observed and modelled daily mean hydrographs at these stations. In addition, biases in the timing and magnitude of peak flows are explored and connections established with those in temperature and snow water equivalent (SWE) where applicable.

The Generalized Extreme Value (GEV) distribution is used to compute return levels of extreme (high and low) flow events. A high (low) flow event is defined as the maximum (minimum) 1-day (15-day) flow occurring over the March to July (January to May) period. Ten- and 30-year return periods are considered for high flows, while 2- and 5-year return periods are considered for low flows. The choice of smaller return periods for low flows is based on the fact that a hydrological drought of 2-year return period is catastrophic enough to have an adverse impact not only on the hydropower sector, but also on the ecosystem, particularly the aquatic life (Smakhtin, 2001). The cumulative distribution function of the GEV distribution is given by:

$$G(z) = \text{Probability}(Z \leq z) = \exp \left\{ -[1 + \xi(z - \mu)/\sigma]^{-1/\xi} \right\} \quad (1.1)$$

where the extreme flow z is such that $1 + \xi(z - \mu)/\sigma > 0$, and μ , σ and ξ are respectively the location, scale and shape parameters.

Full range of properties and some common applications of the GEV distribution are described in Coles (2001). There are several methods that are often used for parameter estimation of this distribution: Probability Weighted Moments (PWM) (Hosking et al., 1985), L-moments (Hosking, 1990), Maximum Likelihood (ML), Generalized Maximum Likelihood (GML) (Martins and Stedinger, 2000) and mixed methods (Ailliot et al., 2011). One of the advantages of the GML and ML is that the fitted data automatically belong to the domain of definition of the obtained probability density function, which is not guaranteed by other methods. However, the ML method performs poorly for small samples (Stedinger et al., 1993).

To estimate parameters μ , σ and ξ of the GEV distribution, the GML approach proposed by Martins and Stedinger (2000), but using a uniform prior distribution for the shape parameter ξ as in Ailliot et al. (2011), is used. Knowing the parameters of the GEV distribution, low-flow return level for a given return period T (in years) is estimated using the relationship $G(z)T = 1$, as

$$z(T, \mu, \sigma, \xi) = \frac{\sigma}{\xi} \left[(\ln T)^{-\xi} - 1 \right] + \mu \quad (1.2)$$

For high flows, a return level is estimated using the relationship $[1 - G(z)]T = 1$, as

$$z(T, \mu, \sigma, \xi) = \frac{\sigma}{\xi} \left[\left(\ln \frac{T}{T-1} \right)^{-\xi} - 1 \right] + \mu \quad (1.3)$$

Projected changes to mean annual, seasonal and extreme flows are assessed for the 2041–2070 period with respect to the current 1970–1999 period. This is achieved by comparing statistics of interest derived from the F1–F5 simulations with the corresponding statistics derived from the C1–C5 simulations. Projected changes to seasonal streamflows are linked with projected changes in seasonal temperature, precipitation and SWE, where possible. In the assessment of projected changes to mean, seasonal and extreme flows, two approaches are adopted. In

the first approach, projected changes based on each pair of the five CRCM current and future simulations are estimated, which are then averaged to obtain the ensemble-averaged projected change. In the second approach, based on the statistical evidence provided by the multiple comparison tests, i.e. the Kruskal-Wallis test (Walpole and Myers, 1985) and ranksum test (Walpole and Myers, 1985) combined with the False Discovery Rate (FDR) approach of Benjamini and Hochberg (1995), the five simulations for the current climate are merged to create a longer sample for each grid-cell. The same procedure is followed for the future climate. The projected changes are then assessed from the merged current and future period longer samples. Similar approaches have been used in May (2008) to assess projected changes to extreme precipitation events and characteristics of wet and dry spells over Europe. The advantage of this second approach over the first one is reduced uncertainty associated with extreme flow return levels due to larger sample size. Uncertainties due to smaller sample sizes could be substantial for extreme flow return levels (Stedinger et al., 1993).

Statistical significance of projected changes to mean annual and seasonal flows and selected return levels of extreme (high and low) flows are assessed using the nonparametric vector bootstrap resampling method (Efron and Tibshirani, 1993; GREHYS, 1996; Khaliq et al., 2009) to estimate standard errors and assuming normality of these statistics to develop confidence intervals (Hall et al., 2004; Mladjic et al., 2011), as discussed below. For a given sample of flows at a grid-cell, the 95% confidence interval for a statistic (i.e. mean annual and seasonal flow or a return level) is calculated as: $R0 \pm 1.96SE$, where $R0$ is the sample statistic and SE is the standard error of the statistic estimated using 1000 bootstrap resamples. Such confidence intervals for selected return levels and mean annual and seasonal flows are calculated for each grid-point for both future and current climates. The statistical significance of the difference between the future and current period values is assessed using these confidence intervals. The change (positive/negative) is considered significant if, for a given case, these confidence intervals do not overlap. The Student's t-test (Walpole and Myers, 1985) is also used to test the statistical significance of the difference between the current and future period mean annual and seasonal flows. For the case of ensemble averaged statistics, ensemble averaged standard errors are used to develop confidence intervals.

Confidence in the CRCM projections is assessed on the basis of the spread of projected changes obtained with the five pairs of current/future simulations, represented here by the coefficient of variation (CV), defined as the ratio of the standard deviation to the ensemble-mean change based on the five pairs of CRCM simulations. Small (large) values of CV are suggestive of high (low) confidence level in the CRCM projections. Given the nature of the CRCM ensemble, the spread in the CRCM projected changes computed as discussed above will reflect the part of the uncertainty associated with the natural variability of the CGCM3.1 and CRCM's own internal variability.

1.4 Results

1.4.1 Model verification

The observed and modelled hydrographs (mean daily streamflows) are compared at selected stations in Fig. 1.2. Modelled hydrographs are derived from the CRCM's control simulation. For some basins, important differences can be noted both in the magnitude and timing of peak flows, which are reflected in the ns and r values shown in Fig. 1.2. These differences can be partly explained by the biases associated with the temperature and precipitation and therefore in the snow water equivalent (SWE) in the CRCM control simulation (Fig. 1.3). The biases in the winter (DJF) SWE are estimated by comparing climatologic winter SWE from CRCM's control simulation with that from the gridded North American SWE data from Brown et al. (2003). The observational dataset (Brown et al., 2003) was produced by applying the snow depth analysis scheme developed by Brasnett (1999) to generate a 0.3° latitude/longitude grid of daily and monthly mean snow depth and corresponding estimated water equivalent for North America. This observational dataset was produced for the 1979–97 period and therefore Fig. 1.3a presents validation of climatologic SWE for the 1979–97 DJF period, common to both simulated and observed datasets. The spring (MAM) temperature biases presented in Fig. 1.3b are estimated by comparing 1970–1999 MAM temperature climatology from CRCM control simulation with that from the gridded Climatic Research Unit (CRU2; Mitchell and Jones, 2005) analyzed data.

For the northernmost gauging stations 103715 (Swampy Bay, at the outlet of the lake Patu) and 093801 (Grande Rivière de la Baleine, around 30 km upstream of the river Denys), magnitude of peak flows is overestimated, while they are reasonably well simulated for stations 104001 (Baleine River, 40 km from the outlet) and 093806 (Grande Rivière de la Baleine, 13 km downstream of the lake Bienville). Careful examination of the biases in SWE (Fig. 1.3a; see Fig. 1.1a for flow directions) suggests that the overestimation of peak magnitudes for the two stations is associated with the positive biases in SWE for the region upstream of the stations. However, for the gauging stations located in the central to southern watersheds, i.e. 092715, 081006 and 061502, an underestimation of peak magnitudes is noted. This is due to the underestimation of SWE for the regions upstream of these stations, which contribute to the streamflows at the stations (Fig. 1.3). In general, for all basins, the simulated peaks occur earlier than observed, and is believed to be due to the positive temperature bias (Fig. 1.3b) during spring (MAM). It should be noted though that the model underestimates temperature for the other seasons (figure not shown).

Characteristics of low and high flows are also validated by performing a comparison between modelled return levels and those obtained from observations. As reported in Sushama et al. (2006) and Khaliq et al. (2008), low-flow events can occur in late winter or early spring due to prolonged cold periods, or can occur in late fall mainly associated with increased evapotranspiration. The low-flow events considered in this study are for the January–May period, i.e. those associated with longer cold periods, while the high-flow events considered are for the March–July snowmelt dominated period.

Comparison of observed and modelled return levels (Fig. 1.4) at the same gauging stations shown in Fig. 1.1 suggests that the model is able to capture the high flow magnitudes reasonably well. However, the errors associated with the low flows are large, particularly for the northern watersheds. This is primarily due to the coarse resolution of the soil dataset and therefore values of depth to bedrock used in the model and the drainage formulation used in the model. For the northernmost watersheds, depth to bedrock is mostly 0.1 m, i.e. only the top 0.1 m of the soil column is hydrologically active. Besides, according to the drainage

formulation used in CLASS, the depth to bedrock must be deeper than 0.35 m to have any drainage. Therefore in winter months, for these regions with depth to bedrock in the 0.1–0.35 m range, drainage is zero in the model and therefore the ground water contribution is very much reduced. A new formulation for drainage is currently being implemented in the new version of CRCM, which may help eliminate some of these discrepancies. The underestimation of low flows, particularly for the northern watersheds, can also be partly attributed to the overestimation of snow and the underestimation of total precipitation at the end of fall, which both tend to decrease the winter flow. In the absence of an alternative, we will henceforth assume that the errors in low flows related to the soil dataset and drainage formulation will remain the same in the future climate, and therefore will not affect the climate-change signal.

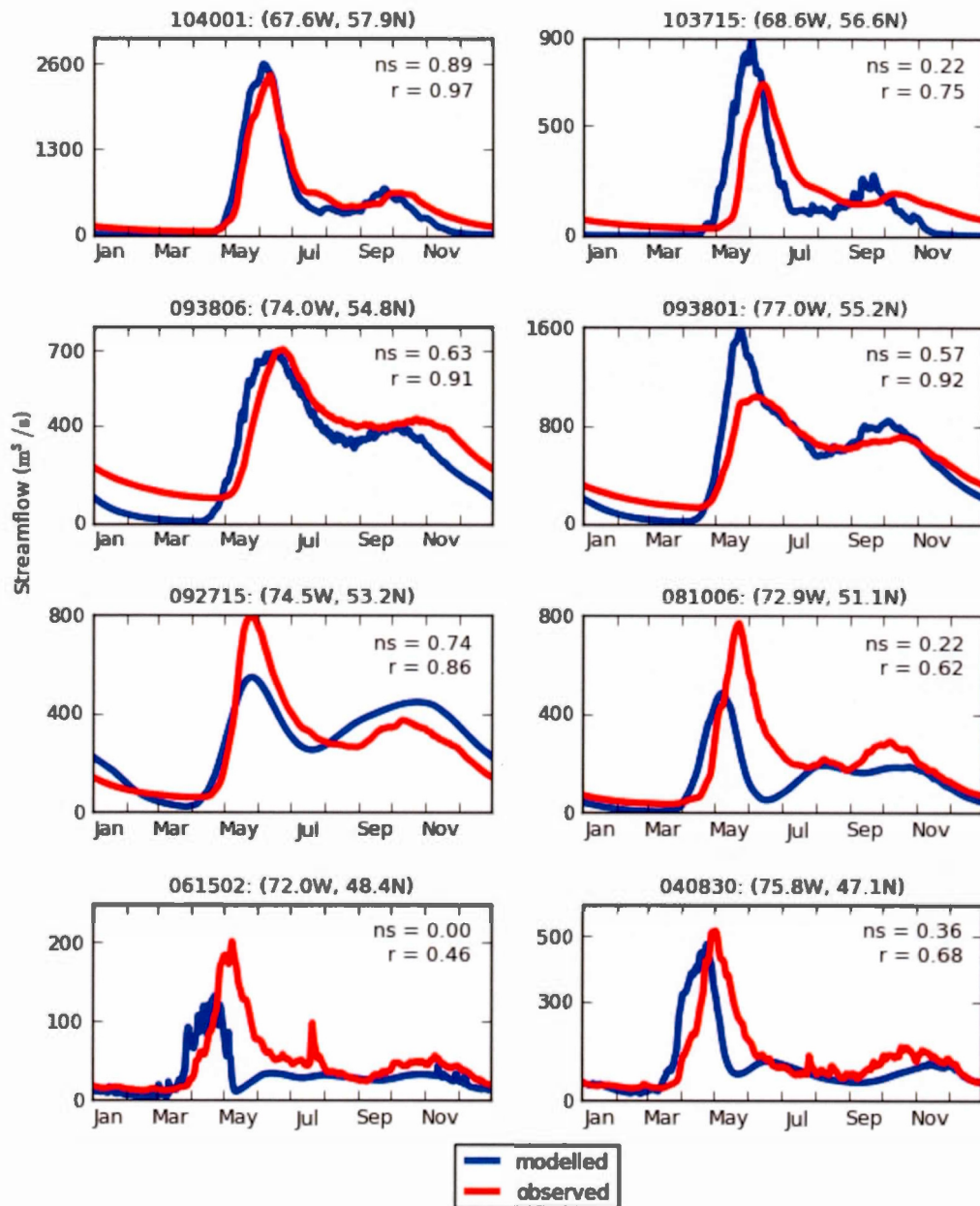


Figure 1.2: Comparison of observed and modelled hydrographs (mean daily streamflows). The length of the observed record varies from 10–20 years within the 1970 to 1999 period. The values of the Nash-Sutcliffe (ns) index and correlation coefficient (r) based on mean daily streamflow comparisons, station identification number and longitude-latitude values of station location are also shown.

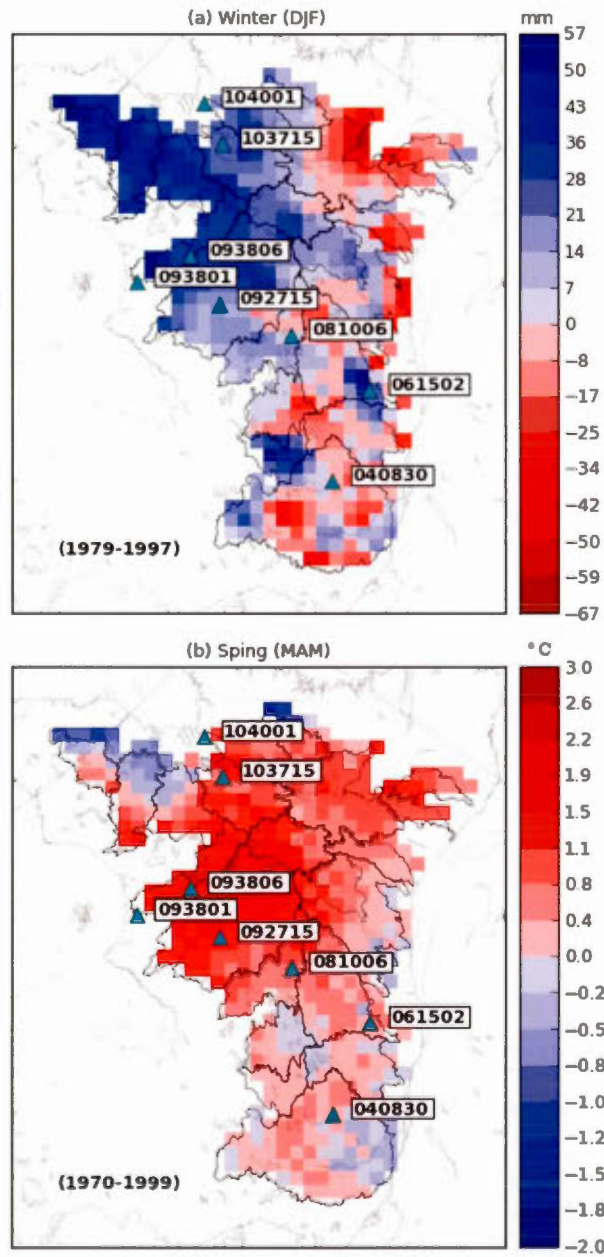


Figure 1.3: Biases in the (a) mean winter (DJF) snow water equivalent (in mm) and (b) mean spring (MAM) 2-m temperature (in °C).

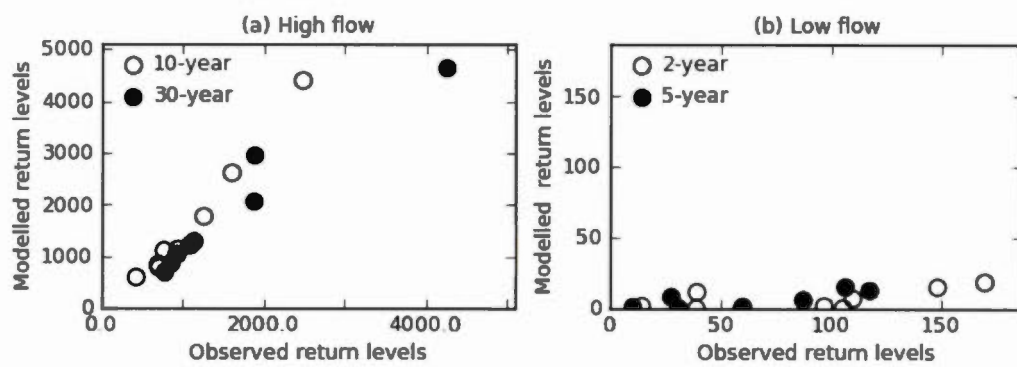


Figure 1.4: Scatter plots of selected observed and modelled (a) high and (b) low flow return levels (in m^3/s).

1.4.2 Projected changes based on ensemble averaging approach

Mean annual and seasonal flows

Ensemble averaged projected changes to the mean annual streamflow for the future 2041–2070 period, with respect to the current 1970–1999 period, are shown in Fig. 1.5a. Statistical significance of the projected changes, at the 5% significance level, is assessed using the vector bootstrap-based test discussed in the methodology section. The mean annual flow is projected to increase from current to future and the changes are statistically significant for a majority of the watersheds, except the RDO, BEL, STM, southern parts of WAS and SAG, and some parts of NAT, ROM, MOI and BOM watersheds. The magnitude of percentage changes to mean annual flows is larger for northern compared to other watersheds.

The ensemble-averaged projected changes to the seasonal (DJF, MAM, JJA, and SON) flows are shown in Figs. 1.5b–e. From the seasonal plots, the changes for the northern part of the domain are consistently positive throughout the year, except for some non-significant decreases in summer (JJA). For the southern regions however increases can be noted during the winter (DJF) and spring (MAM) seasons, while decreasing streamflows are projected for the summer (JJA) and fall (SON) seasons, resulting in the non-significant or smaller projected changes to mean annual streamflow for this region. Furthermore, t-test is also applied to individual pairs of current and future period simulations and the p values of the t-test also suggest significant changes for most of the studied watersheds during winter, while for the other seasons, regions with non-significant changes were noted (figure not shown), as is the case for the ensemble averaged changes shown in Figs. 1.5b–e.

The above noted projected changes in seasonal streamflows are associated with changes in temperature and precipitation and therefore SWE, which are shown in Figs. 1.6 and 1.7, for various seasons. The vector bootstrap-based test, discussed earlier, has been used to assess significance of projected changes, at 5% significance level, for temperature, precipitation and SWE shown in Figs. 1.6 and 1.7. Figure 1.6 suggests that the ensemble averaged projected increases in temperature are significant for all watersheds, for all seasons. Projected changes to

temperature are maximum for winter, and are generally in the 3.5 to 6 °C, for the entire studied region. The ensemble averaged projected changes to precipitation (Fig. 1.7a–d) suggest significant increases almost everywhere for winter and spring, while the changes are not significant for the southern watersheds during summer and fall.

The significant increase in winter streamflows (Fig. 1.5b) discussed earlier can be partly attributed to the significant increase in temperature during fall and winter, which delays the freezing of soil, thus increasing drainage in the central to southern watersheds where the depth to bedrock is deeper than 0.35 m. In addition, significant increase in precipitation and increased fraction of winter precipitation falling as rain instead of snow, due to warmer temperatures, also contribute to increased streamflows during the winter period. The spring flows for all studied watersheds, as already discussed, are related to snowmelt. As can be seen from Fig. 1.7e, the majority of the watersheds show no significant changes to SWE during DJF. However, the increased temperatures during MAM (Fig. 1.6b) cause earlier snowmelt, which is responsible for the noted significant increase in spring streamflows.

During summer, though precipitation increases are significant for the northern regions (Fig. 1.7c), streamflows show no significant changes due to increased evaporation associated with warmer temperatures in summer (Fig. 1.6c). The northern regions show some increases in streamflows during fall, which could be attributed to the increased precipitation and temperature in a future climate; it should be noted that since the soil in the northernmost regions, in the current climate, start freezing up in late fall, the warmer temperatures in the future climate delay this, leading to increased streamflows.

High- and low-flow extremes

Prior to looking at projected changes to return levels of high and low flows, it is useful to see if the selected periods (i.e. March–July for high flows and January–May for low flows) would be suitable for future climate as well. Figures 1.8 and 1.9 show ensemble averaged annual frequency of occurrence of high and low flow events, respectively, for current and future climates, for northern, central

and southern watersheds. The frequencies are normalized by the number of years (30 in the present case) and the number of grid cells in a given watershed. High flows from snowmelt mostly occur during the March to July period as expected (Fig. 1.8) – high flows associated with the majority of the southern watersheds occur as early as April, while for northern watersheds they occur somewhere between May and June. From the insets of Fig. 1.8, one can see that the high flow events occur earlier in the future climate for most of the watersheds, with the high flows still concentrated over the March–July period. Therefore, the choice of the March–July period to study high-flows is satisfactory for both current and future climates.

From Fig. 1.9, it can be seen that the low-flow events, in both current and future climates, caused by prolonged winter periods, occur during the January–May period, with low flows occurring earlier within this period for southern and central watersheds and towards the middle of the period for northern watersheds. The majority of the low-flow events occur at the end of winter or at the beginning of the spring season. For some southern watersheds, low-flow events are projected to occur more in fall in the future climate compared to current climate. For example for RDO watershed (index 18), most of the low-flow events in a future climate are projected to occur during the September–October period. BEL and STM watersheds also show similar trends, though less pronounced. In a future climate, early occurrence of low flows in the January–May period is clearly seen from the insets of Fig. 1.9. Despite this shift, the January–May period is still satisfactory for the study of low flows.

Projected changes to 10- and 30-year return levels of high flows, for the five pairs of current and future simulations, are shown in Figs. 1.10 and 1.11, respectively. The results for three of the five pairs suggest increases over most part of the domain for both 10- and 30-year return levels, with the remaining two suggesting primarily negative changes mixed with positive changes at scattered grid cells. Important differences are seen between the projections based on the five pairs of CRCM simulations. An investigation of the spread among the five current and five future simulations based on the CV measure indicate that, the spread among the future members is large compared to the current members, particularly for central and

southern watersheds. A preliminary investigation suggests that this could partly be due to the increased differences between the sea surface temperatures (SSTs) and sea ice cover (SIC) in the five future CRCM simulations compared to the five current climate simulations, particularly in the Hudson Bay region, which is located to the west of the study domain. An in-depth analysis is required to identify other contributing factors and is not attempted here as it is outside the scope of this article. Although ensemble-averaged projected changes to 10- and 30-year return levels are positive for most parts, significant changes are found only for a few grid cells located mainly in the northern watersheds (Fig. 1.10f and Fig. 1.11f). This is due to the low level of agreement between the results of individual members in the sign of change for high-flow return levels.

Changes to 2- and 5-year low-flow return levels (Figs. 1.12 and 1.13) exhibit strong agreement across members, showing increases all over the study domain (there is only a single grid-cell in the RDO watershed where a negative change is found – Figs. 1.12a and 1.13a). Although the relative changes to low flows are high, the absolute changes are indeed small. Overall, there are only slight differences for the southern and northern parts of the domain. This agreement is expected, since the low flow is influenced by the averaged effect of spring, summer and autumn precipitation events and thereby shows less variability, whereas high flows depend on spring precipitation and melting processes and their relative timings. Compared to low-flow return levels, considerable variability in spring high flows also could explain the lack of significant changes in high-flow return levels. All the five members suggest significant changes to low-flow return levels for the entire region except a few grid cells located mainly in the RDO and northern watersheds where the number of members suggesting significant changes varies between one and four. Because of the good agreement between individual members, ensemble-averaged changes are also found statistically significant at the 5% level for the entire study domain, except a few grid cells located in the RDO watershed (Fig. 1.12f and Fig. 1.13f).

The CV plots for projected changes to high- and low-flow return levels shown in Fig. 1.14 indicate that greater confidence can be attributed to the changes in low-flow return levels since CV values are much smaller than one over most of

the domain. More specifically, in the case of high flows, smaller values of CV are found for northern (ARN, FEU, MEL, PYR and BAL) watersheds.

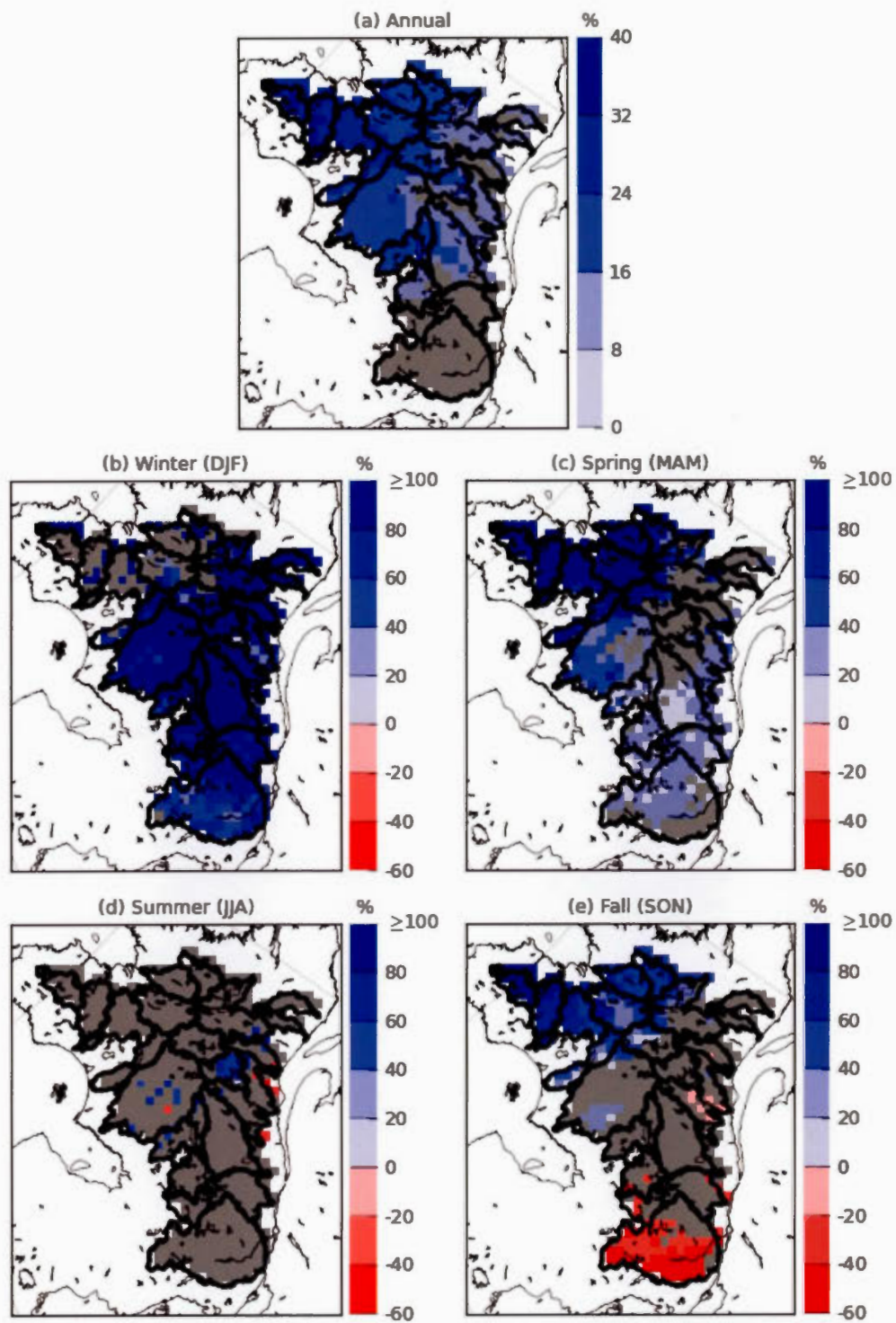


Figure 1.5: Ensemble averaged projected changes to mean **a** annual and **b-e** seasonal streamflow. Grid cells where the changes are not significant at the 5 % significance level are masked in grey.

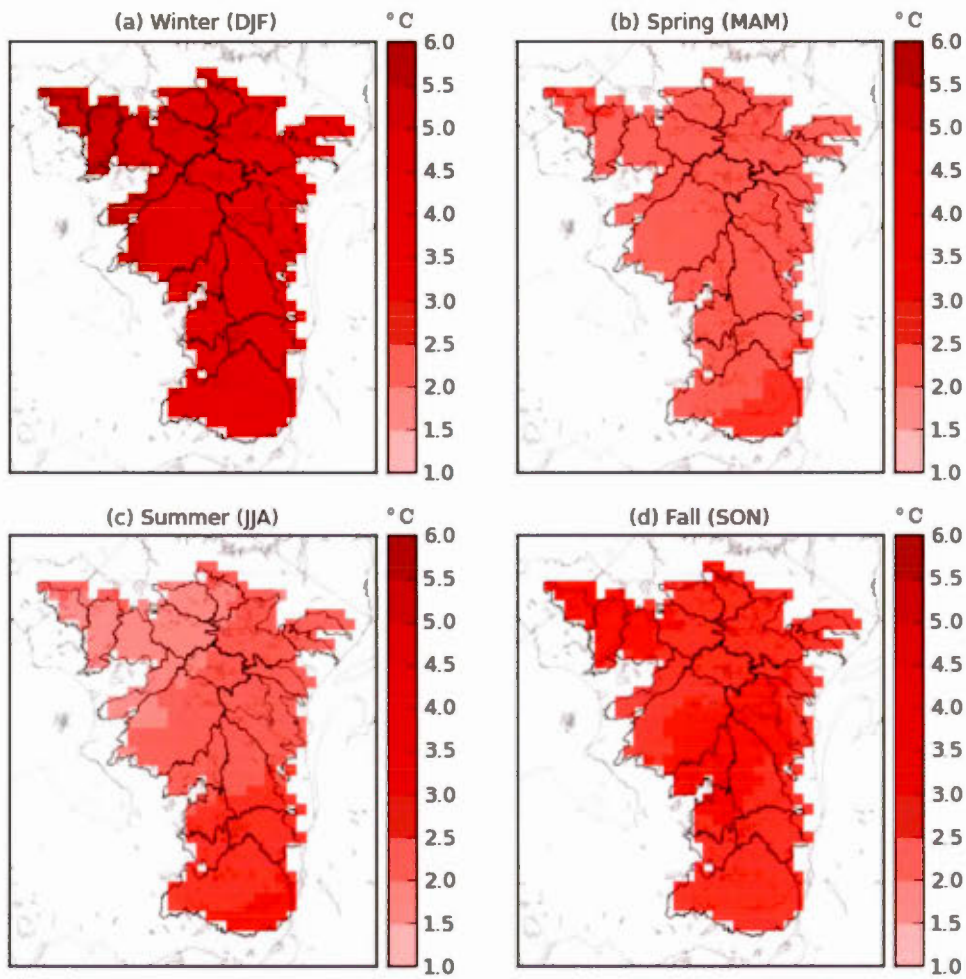


Figure 1.6: Ensemble averaged projected changes to mean **a–d** seasonal 2-m temperature. Grid cells where the changes are not significant at the 5 % significance level are masked in grey.

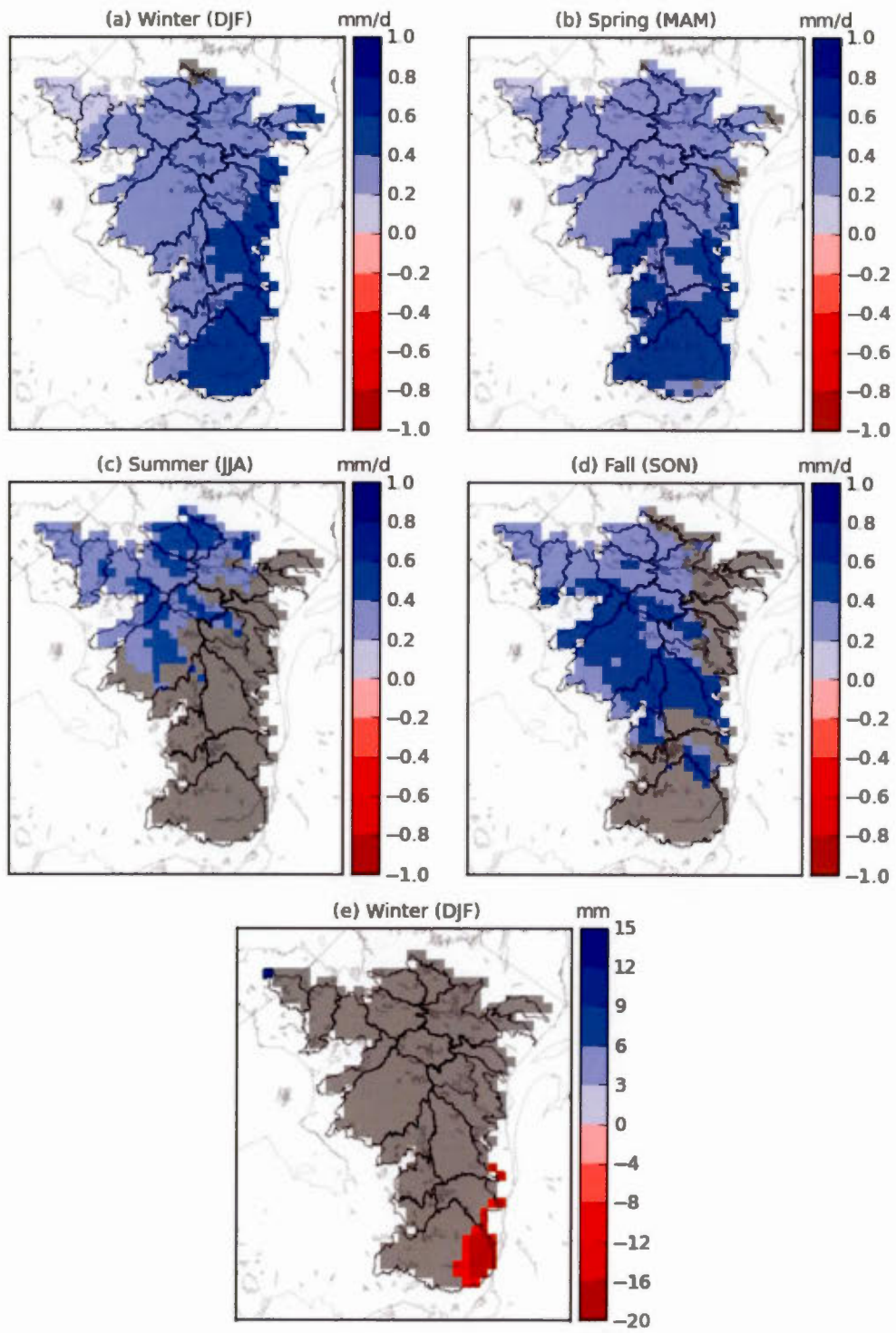


Figure 1.7: Ensemble averaged projected changes to mean a–d seasonal precipitation (in mm/day), and e winter (DJF) SWE (in mm). Grid cells where the changes are not significant at the 5 % significance level are masked in grey.

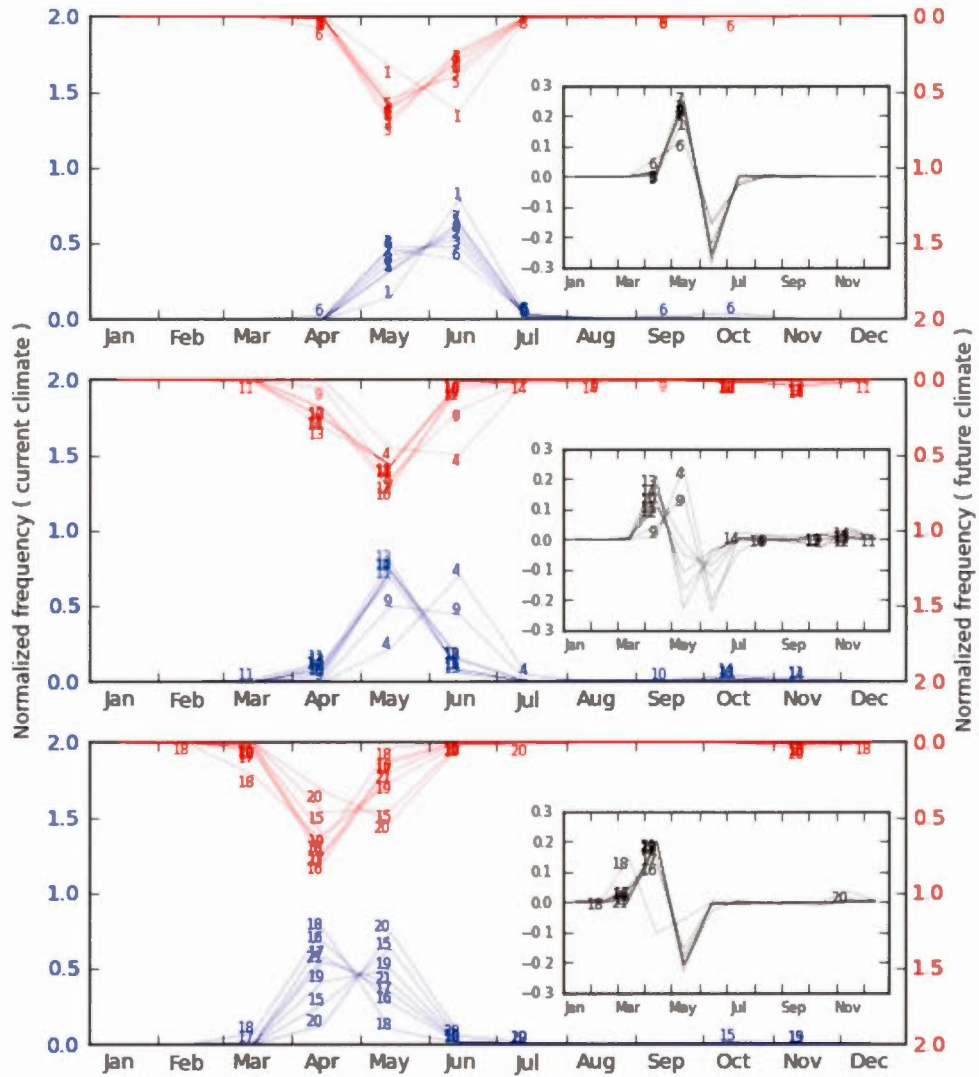


Figure 1.8: Ensemble averaged normalized frequency of occurrence of 1-day high flow events for current 1970–1999 (left y-axis) and future 2041–2070 (right y-axis) period for northern (top panel), central (middle panel) and southern (bottom panel) watersheds. The numbers correspond to watershed indices given in Table 1.1. Inset shows changes to normalized frequency of occurrence from current to future climate.

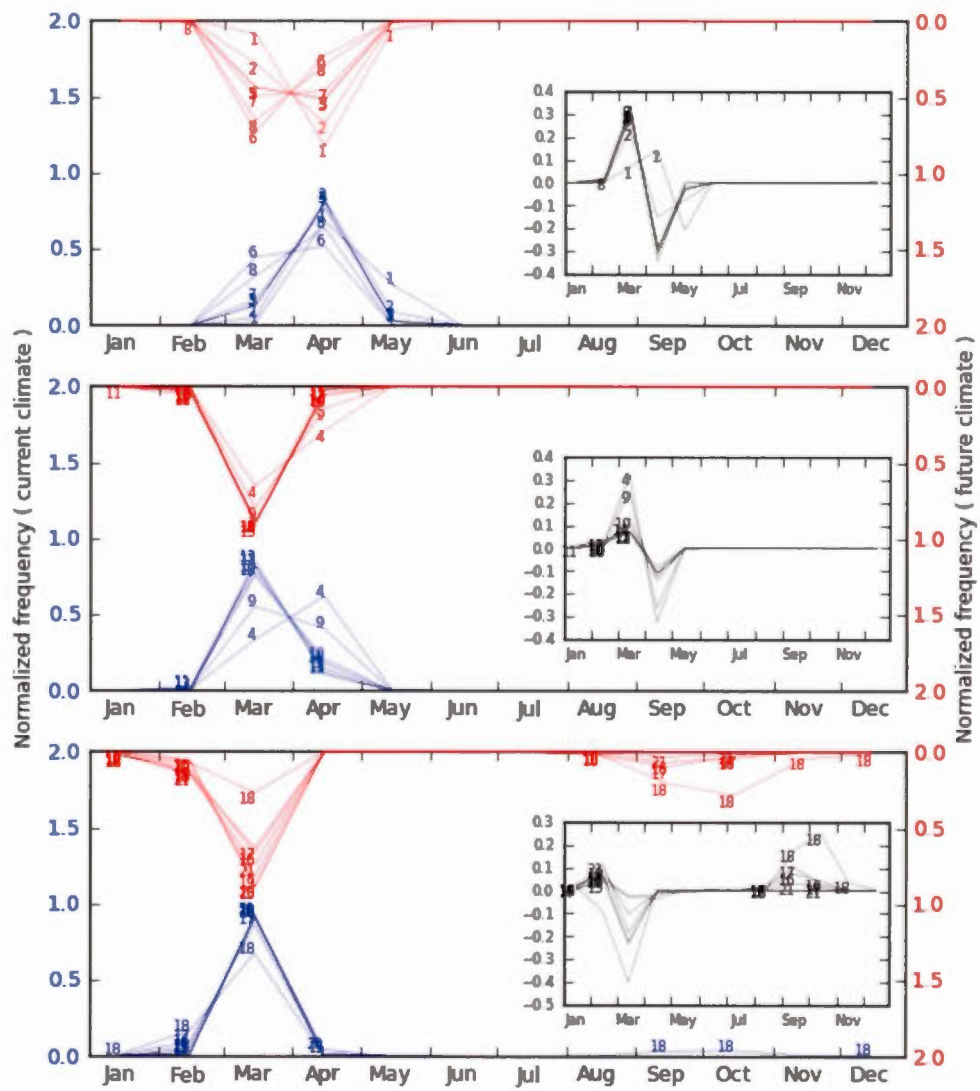


Figure 1.9: Same as in Fig. 1.8 but for low flow events.

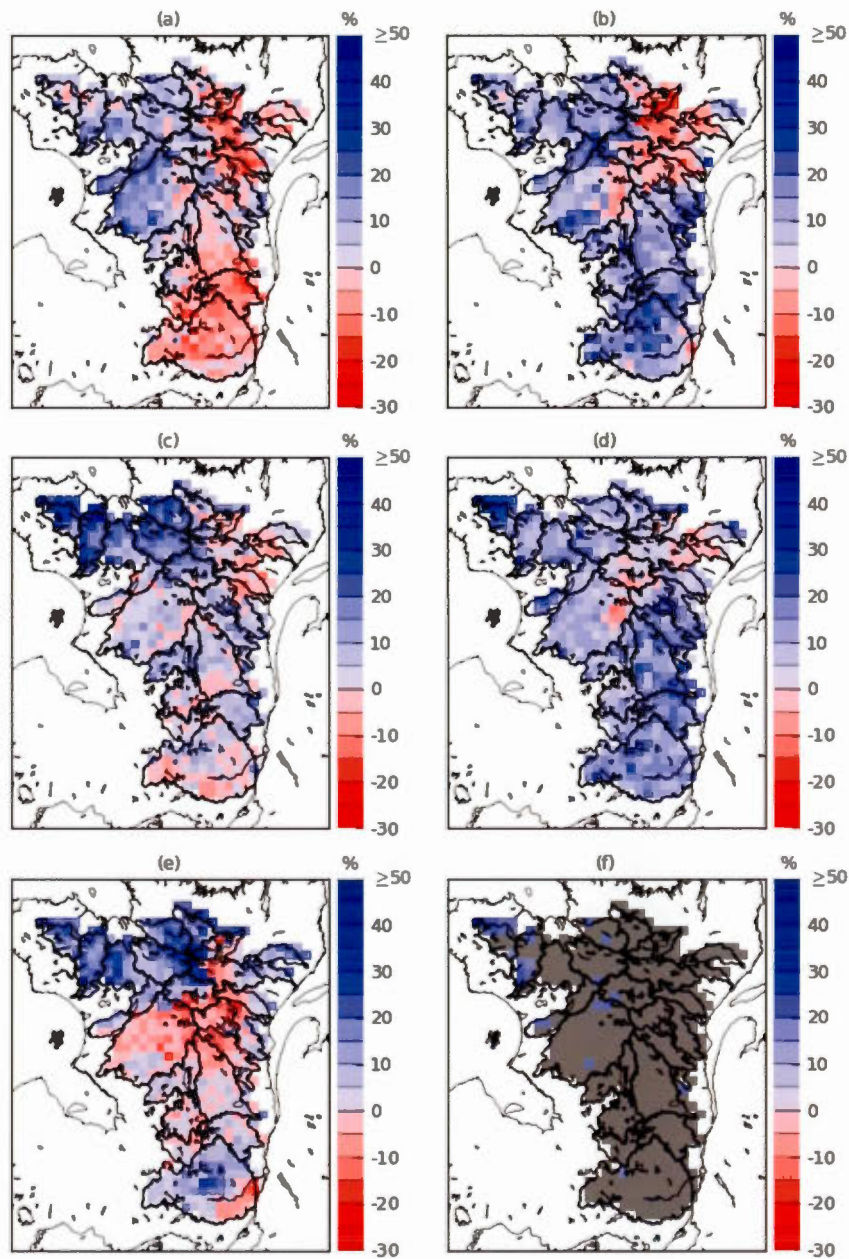


Figure 1.10: a–e Projected changes (in %) to 10-year return levels of 1-day high flows derived from five future and current period simulation pairs (F1–C1, F2–C2, ..., F5–C5). f Ensemble averaged changes to 10-year return levels of high flows. Grid cells where the changes are not significant at the 5 % significance level are shown in grey.

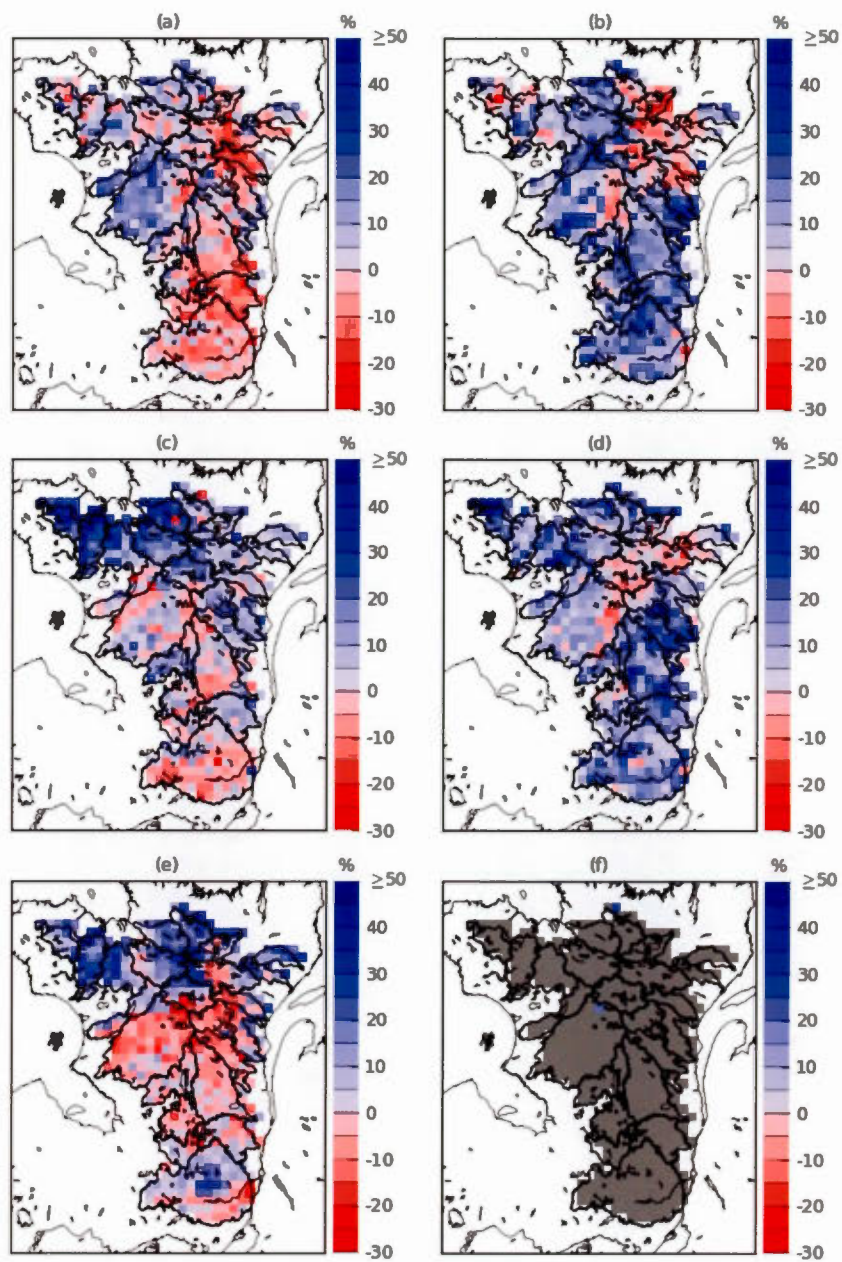


Figure 1.11: Same as in Fig. 1.10 but for 30-year return levels of high flows.

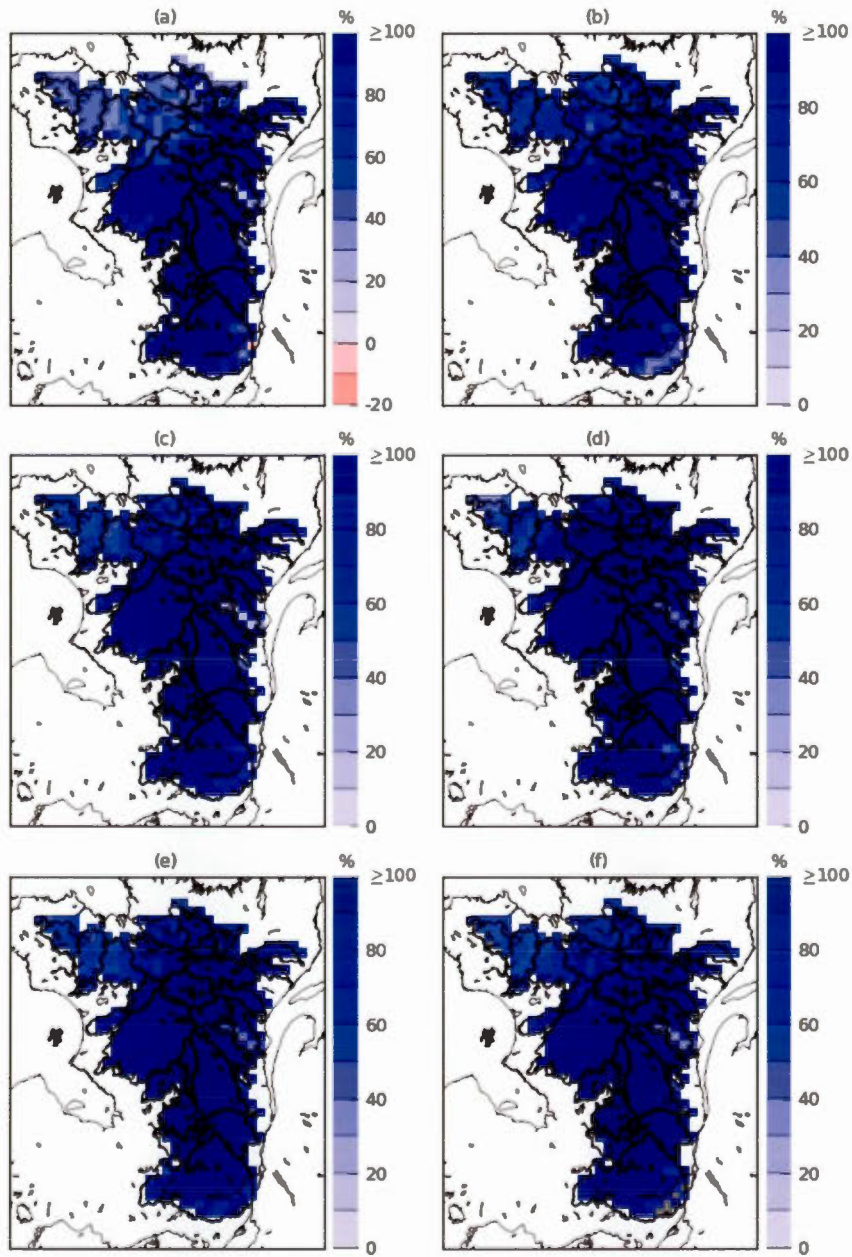


Figure 1.12: **a–e** Projected changes (in %) to 2-year return levels of 15-day low flows derived from five future and current period simulation pairs (F1–C1, F2–C2, ..., F5–C5). **f** Ensemble averaged changes to 2-year return levels of low flows. Grid cells where the changes are not significant at the 5 % significance level are shown in grey.

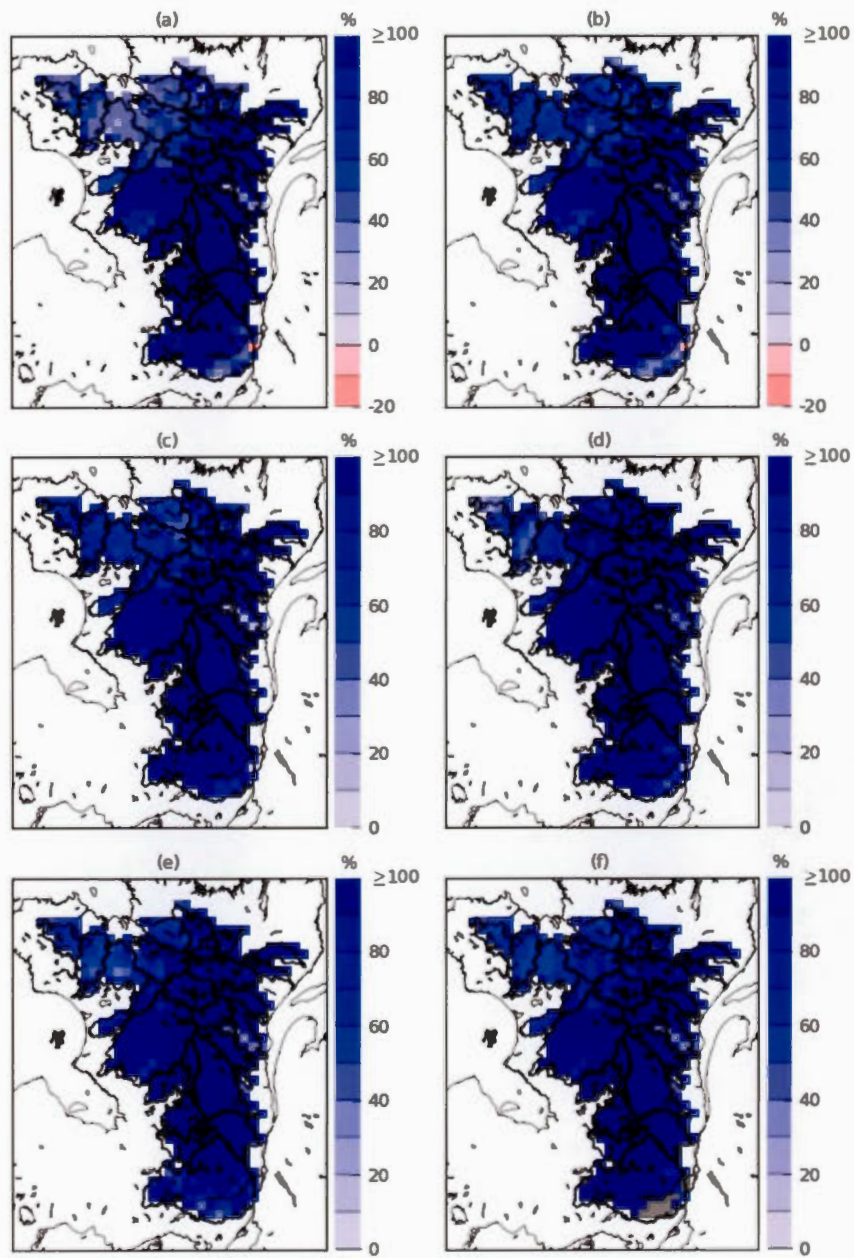


Figure 1.13: Same as in Fig. 1.12 but for 5-year return levels of low flows.

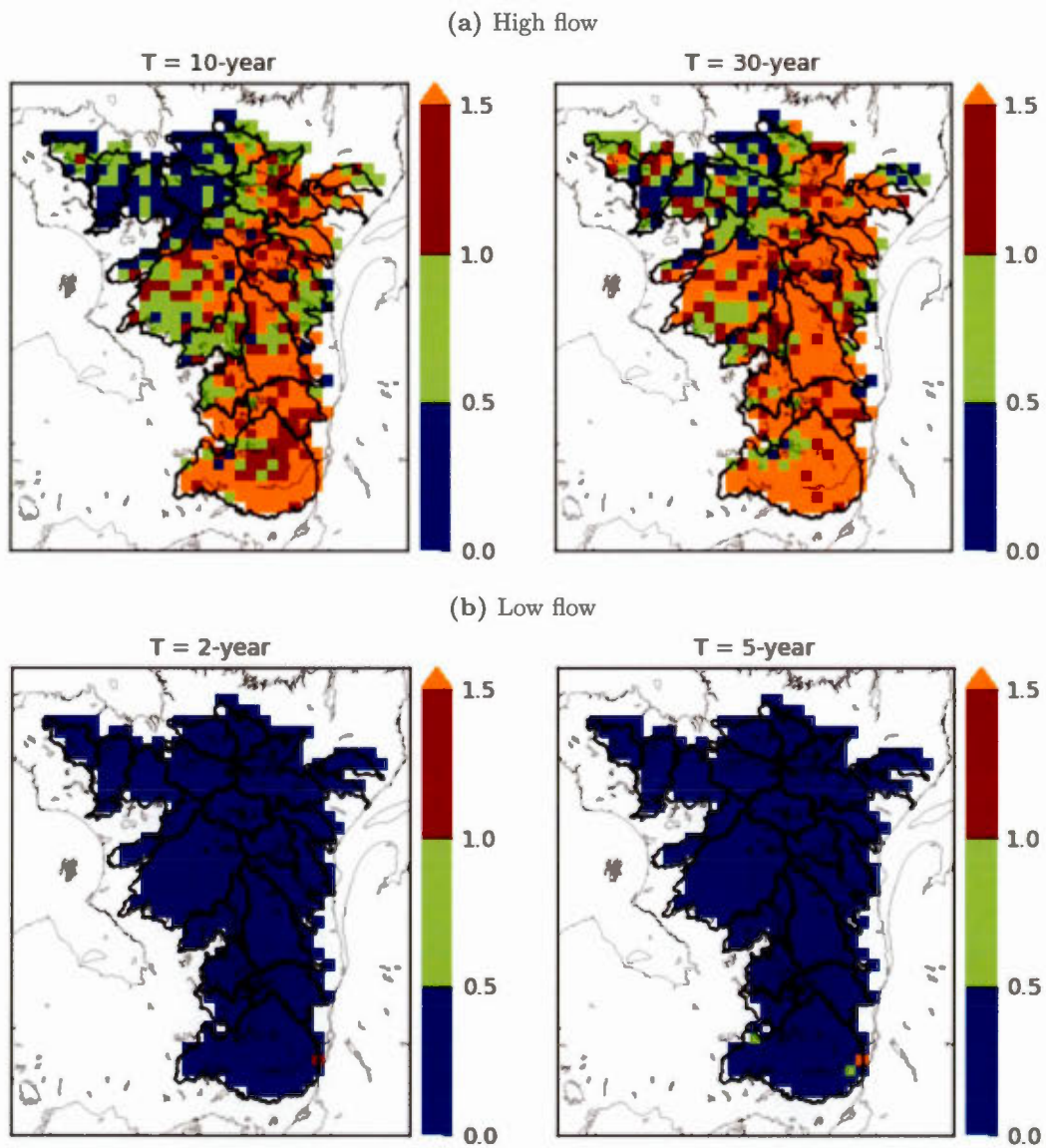


Figure 1.14: Coefficient of variation (ratio of standard deviation to the mean absolute value based on the five ensemble members) of projected changes to selected return levels of high and low flows.

1.4.3 Projected changes based on merged longer samples

To decrease the uncertainties associated with the small sample size, we tested separately for current and future climates the hypothesis that the samples of mean annual streamflows from the five ensemble members originate from the same distribution using two multiple comparison tests discussed in the methodology, i.e. the Kruskal-Wallis test and the ranksum test combined with the FDR approach. The same analysis is performed separately for the samples of high- and low-flow extremes. The results of both tests were similar and therefore only those corresponding to the former test are shown in Fig. 1.15. The p values of the Kruskal-Wallis test plotted in Fig. 1.15a suggest that the null hypothesis that the five samples of mean annual flows originate from the same distribution cannot be rejected at the 5% level for majority of the grid cells. The same is the case for low- and high-flow samples. However, compared to the case of mean annual and low flows, there are more grid cells, located mainly in the central and southern parts of the study domain, where the null hypothesis does not seem to hold for high flows. Since for majority of the grid cells the null hypothesis does seem to hold for both current and future climates, projected changes in mean annual and seasonal flows and return levels of low- and high-flows are assessed using longer samples consisting of 150 values obtained by merging the 5 current simulations and similarly the 5 future simulations for each grid-cell. The results of this analysis are summarized below as for the first method.

The projected changes to mean annual and seasonal flows are shown in Fig. 1.16. The changes to mean annual flows are found significant at the 5% level for the entire study domain, except a few grid cells located in southernmost parts of the RDO watershed. The spatial pattern of changes to winter flows is very similar to that of the mean annual flows. Compared to the results for the ensemble mean shown in Fig. 1.5, significant reduction to flows is more widespread over the southern watersheds in fall as well as in summer. For spring flows, the smaller positive increases for southern parts of the domain, which were not significant earlier, are now found significant at the 5% level. Similar patterns of spatial changes to annual and seasonal flows were noticed using the t-test.

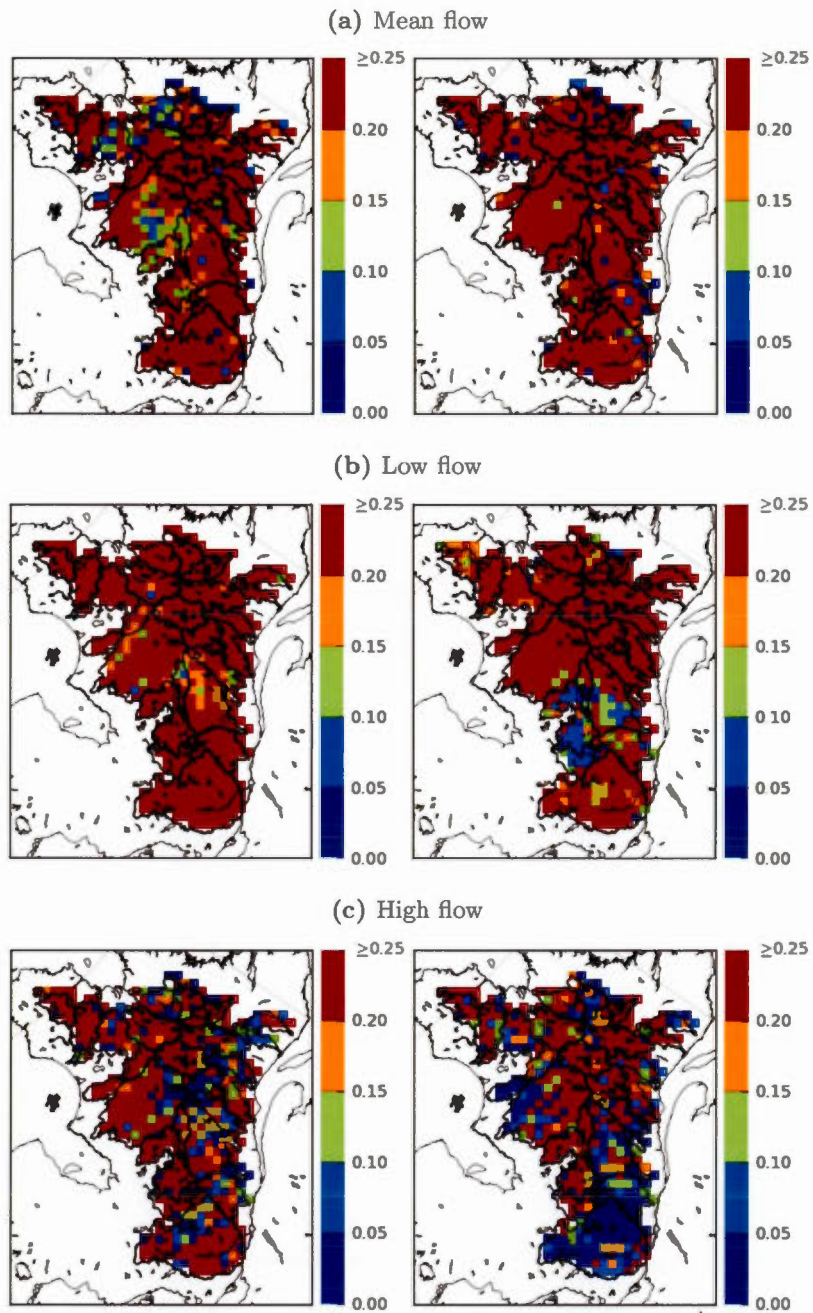


Figure 1.15: p values of the Kruskal–Wallis test for **a** mean annual flows, **b** 15-day low flows, and **c** 1-day high flows for current (left column) and future (right column) climates.

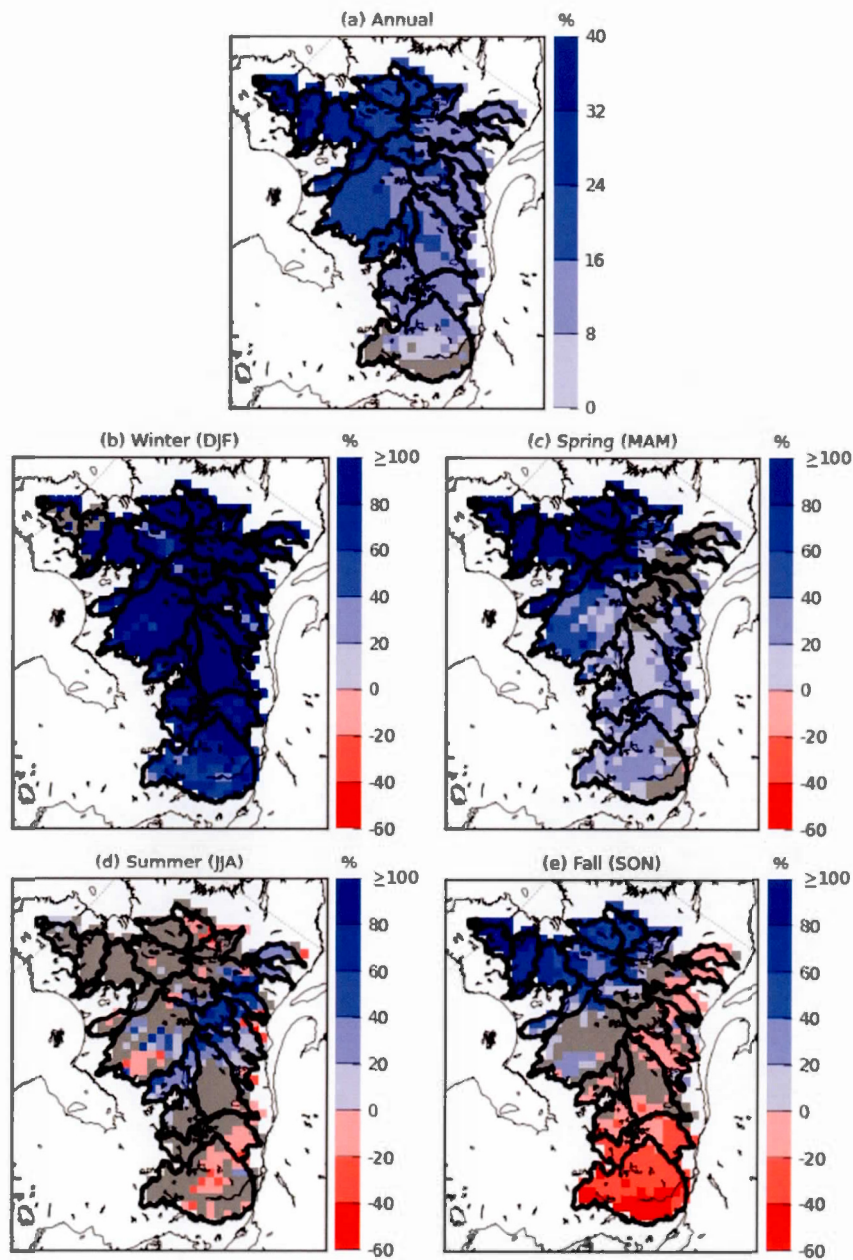


Figure 1.16: Projected changes (in %) to mean (a) annual and (b–e) seasonal streamflows. Grid cells where the changes are not significant at the 5% significance level are shown in grey.

Spatial patterns of projected changes to selected return levels of high and low flows are shown in Fig. 1.17. Compared to the results shown in Figs. 1.10f and 1.11f, there are a larger number of grid cells where the increases to 10- and 30-year return levels of high flows are now found significant at the 5% level. This is clearly the

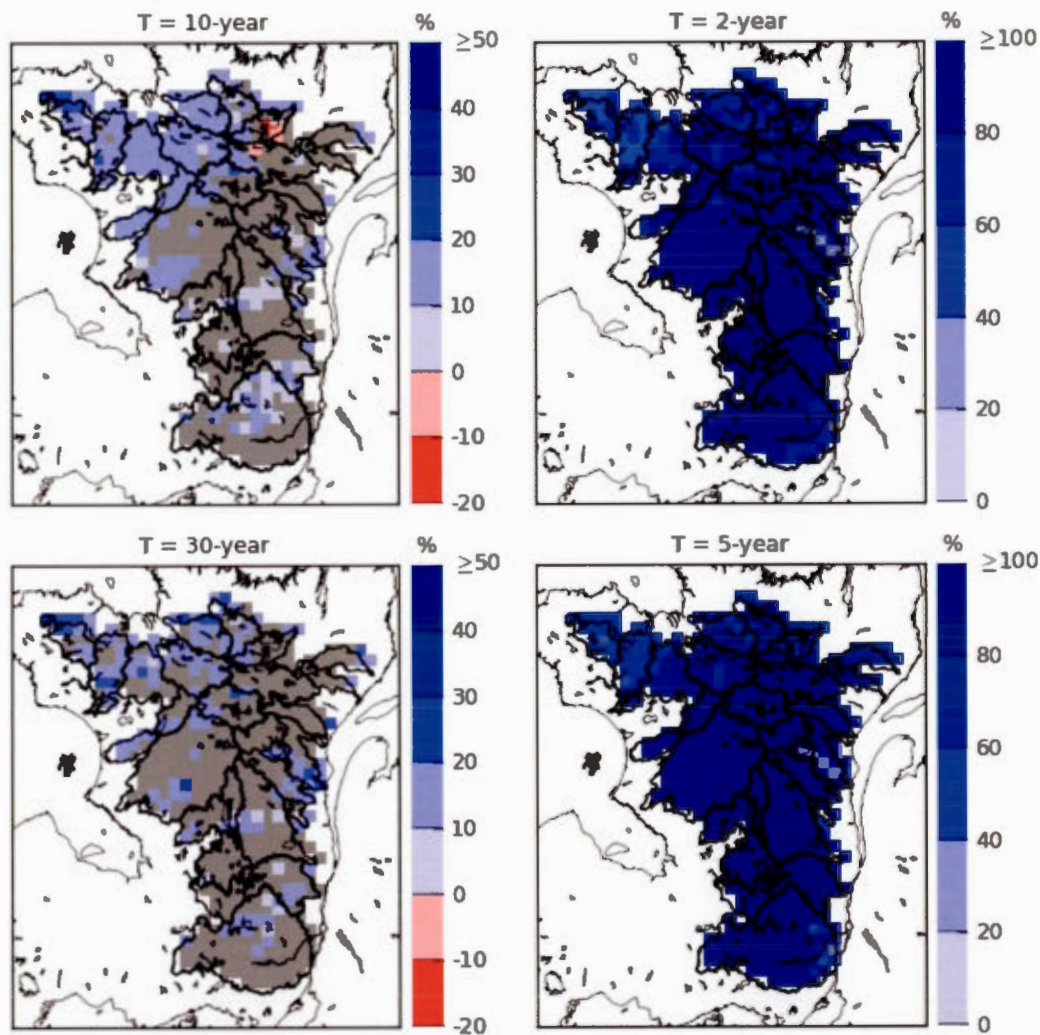


Figure 1.17: Projected changes (in %) to 10- and 30-year return levels of high flows (left column) and 2- and 5-year return levels of low flows (right column) derived using longer samples (consisting of 150 values) for each grid-cell both for current and future climates. Grid cells where the changes are not significant at the 5% significance level are shown in grey.

case for the northern watersheds: ARN, FEU, MEL, PYR, BAL and GRB. The increases to 2- and 5-year low-flow return levels are significant all over the study domain. Thus, this approach based on longer samples results in an increase in the number of grid cells with significant changes.

These results strongly suggest that the uncertainties due to small sample sizes could be substantial. Therefore, longer simulations appear to be much valuable to derive a robust climate change signal, not only for extreme flows but also for annual and seasonal means. In our case, the increase of the sample size from 30 to 150 seems appropriate to discriminate the climate-change signal from the noise due to smaller sample size, in addition to other factors.

1.5 Discussion and conclusions

According to the 4th Assessment Report of the IPCC (IPCC, 2007), increase in precipitation for some regions around the world, including the northern mid- to high- latitudes, is expected in future climate. This can directly influence characteristics of streamflows. The northeast Canadian watersheds considered in this study are particularly vulnerable to changes in streamflow patterns since 96% of consumed electricity in the region is hydro-based. In the northern part of Quebec, which is also the focus of future development, storage power stations represent 95% of installed capacity, while run-of-river power stations account for 95% of the installed capacity in the southern parts of Quebec. Therefore, assessment of projected changes to streamflow characteristics is important to aid decision-making and identification of appropriate measures for adaptation of hydroelectric storage reservoirs in this economically important region of Canada.

This paper presents an evaluation of the CRCM-simulated streamflow characteristics (mean annual and seasonal streamflows and selected return levels of high- and low-flow events) over 21 Northeastern Canadian watersheds. High flows, defined as 1-day maximum flows occurring over the March to July period (commonly known as spring floods) and low flows, defined as 15-day minimum flows occurring over the January to May period, are derived from daily streamflow values, which in turn are obtained by routing CRCM-generated runoff using a modified WATROUTE scheme (Soulis et al., 2000; Poitras et al., 2011). Projected changes

to streamflow characteristics are derived using an ensemble of ten CRCM simulations, five corresponding to the current 1970–1999 period and five to the future 2041–2070 period under the A2 SRES scenario. Two methods, one based on the ensemble-averaging approach and the other based on merged samples of five current and five future simulations following multiple comparison tests, are used to develop projected changes. From the set of analyses performed in this study, the following conclusions were drawn.

A comparison of mean daily streamflow hydrographs derived from the CRCM simulation when it was driven by ERA40 data (Uppala et al., 2005) at its boundaries and those derived from observed data at selected stations shows that the shapes of the hydrographs agree overall. However some differences are noted both in the magnitude and timing of peak flows. Overall, the model simulates reasonably well the magnitude of high-flow events, but it performs poorly in simulating the magnitude of low-flow events. The low-flow discrepancies are attributed primarily to the coarse resolution of the soil dataset and the drainage criterion used in the model.

Future climate change projections suggest significant increases in mean annual river flows with maximum changes occurring over the northern part of the study domain. Significant decreases in fall seasonal flows are projected for southern parts of the studied region and almost same is the case for summer seasonal flows. Changes to winter flows follow closely the pattern of mean annual flows. Although increases in spring seasonal flows are also significant over most part of the domain, they are more widespread for northern compared to southern watersheds.

The magnitude of low-flow extremes is projected to increase significantly nearly for all watersheds, though the change in absolute terms is small. Compared to the case of low-flow extremes where the changes are mostly significant, changes to high-flow extremes are not generally found significant based on the ensemble-averaged approach. However, when small sample uncertainties are addressed by using merged longer samples, a number of grid cells with significant increases in high-flow return levels emerged for northern watersheds: ARN, FEU, MEL, PYR, BAL and GRB. In general, the return levels corresponding to short return periods are found significant more often compared to those corresponding to longer return

periods.

From the analysis performed in this study, it can be concluded that larger number of ensemble members and/or longer simulations seems to be indispensable for deriving a robust climate-change signal as was concluded by Kendon et al. (2008), from their analysis of a 3-member Hadley Centre RCM. In the use of a parametric approach for analysis of changes to return levels of extremes, as is the case of the current study, longer simulation periods could also decrease the uncertainties associated with the estimation of extreme value distribution parameters. In this study, the increase of the sample size from 30 to 150 values seems appropriate to discriminate the climate change signal from the noise, since the study is based on a single RCM.

To improve the confidence in projected changes to streamflows, model improvements are necessary. The land surface scheme in the CRCM simulations considered in this study used a 3-layer configuration, with a very thick third layer. To improve further the realism of the simulated soil thermal and hydrologic cycle, and therefore the simulated streamflows, it is preferable to have higher resolution for soil layers. Another aspect that can be further improved is the frozen soil formulation in the model. For example, Niu et al. (2007), obtained important improvements with simulated streamflows for cold regions, particularly with respect to the timing and magnitude of peak streamflow, in their study using the Community Land Model (CLM), by introducing supercooled soil water by implementing a freezing-point depression equation and by relaxing the dependence of the hydraulic properties on soil ice content by incorporating the concept of fractional impermeable area, which enhanced the permeability of frozen ground. In addition, Yuan and Liang (2011) in their study using a Conjunctive Surface-Subsurface Process model, with an explicit treatment of surface-subsurface flow interaction with the bedrock treated as an unconfined aquifer, showed improved simulation of seasonal-interannual runoff and streamflow variations and extreme events. It is expected that similar improvements to the CRCM could further improve the quality of the simulated streamflows.

Since one of the main aims of the current article had been to demonstrate the need for longer simulations by considering two approaches, which included merging of

samples from the same RCM, we have not considered multi-RCM ensembles in this study. However, future analysis will take into account multi-RCM ensembles, driven by multi-GCMs, to quantify various sources of uncertainties such as structural uncertainty, and those associated with the use of different GCMs as the driving data at the lateral boundaries using the NARCCAP simulations (Mearns et al., 2009). Such assessments are crucial to enable a risk-based approach to decision making (Kay et al., 2009). There is also a need for high-resolution simulations of the order of at least 10 km to better capture the surface heterogeneity and thus to better simulate streamflows to provide information required for many impact and adaptation studies. It is expected that such simulations will be available in the near future.

Acknowledgements

This research was carried out within a Collaborative Research and Development (CRD) project funded by the Natural Sciences and Engineering Research Council (NSERC) of Canada, with Hydro-Quebec/Ouranos as industrial partner. The authors would like to thank the Climate Simulations Team of Ouranos Consortium for providing the CRCM runoff data used in the study and two anonymous referees and the Editor Prof. E. K. Schneider for their helpful comments.

CHAPTER II

IMPACT OF LAKE-RIVER CONNECTIVITY AND INTERFLOW ON THE CANADIAN RCM SIMULATED REGIONAL CLIMATE AND HYDROLOGY FOR NORTHEAST CANADA

This chapter is presented in the format of a scientific article that has been submitted to the peer-reviewed journal *Climate Dynamics*. The design of experiments and methods, as well as the analysis of data and preparation of the article were entirely carried out by myself, with Dr. Sushama involved in the supervision of all these tasks. The detailed reference is:

Huziy, O. and Sushama, L. (2015). Impact of lake-river connectivity and interflow on the Canadian RCM simulated regional climate and hydrology for northeast Canada.

Abstract

Lakes and rivers are important components of the climate system. Lakes affect regional climate by modulating surface albedo, surface energy and moisture budgets. This is especially important for regions such as Northeastern Canada with approximately 10% of the landmass covered by lakes, wetlands and rivers. From the regional hydrology perspective, interactions between lakes and rivers are important as streamflow patterns can be significantly modified by lake storage, and similarly lake levels can be modified by streamflows. In this study, using a suite of experiments performed with the fifth generation Canadian Regional Climate Model (CRCM5) driven by the European Centre for Medium-range Weather Forecasting ERA40 reanalysis data at the lateral boundaries for the 1979–2010 period, lake-river-atmosphere interactions and their impact on the regional climate/hydrology of northeastern Canada are assessed. In these CRCM5 simulations a one-dimensional lake model represents lakes, while the rivers are modeled using a distributed routing scheme, and one of the simulations includes interflow, i.e. lateral flow of water in the soil layers. Comparison of CRCM5 simulations with and without lakes suggests significant differences in winter/summer precipitation and winter temperature for the study region. CRCM5 simulations performed with and without lake-river interactions suggest improved representation of streamflows when lake storage and routing are taken into account. Adding the interflow process leads to increased streamflows during summer and fall seasons for the majority of the rivers, causing modest changes to land-atmosphere interactions via modified soil moisture. The impact of interflow on streamflow, obtained in this study, is comparable to the impact of lake-atmosphere interactions on streamflows. This study clearly demonstrates the need for realistic representation of lake-river interactions in regional climate models for realistic simulation of regional hydrology, particularly streamflows.

2.1 Introduction

Climate change will have significant impacts on water resources around the world due to the close connection between climate and the hydrologic cycle. Scientists agree on some of the important broad-scale features of the expected hydrologic

changes, the most likely of which will be an intensification of the global hydrologic cycle, with an increase in the global average precipitation and evaporation as a direct consequence of warmer temperatures. However, there will be important regional differences in precipitation, runoff and recharge that are important to understand. This has led to an increased interest in assessing projected changes to hydrologic characteristics, including river flow regimes, at regional scale (Hurkmans et al., 2010; Monk et al., 2011; Poitras et al., 2011; Forzieri et al., 2014). The conventional approach to study projected changes to streamflow is based on hydrologic models driven by outputs (precipitation and temperature) from transient climate change simulations performed with global climate models and regional climate models (GCMs and RCMs). Studies based on streamflow directly from both GCMs (Falloon et al., 2011; Weiland et al., 2012) and RCMs (Poitras et al., 2011; Huziy et al., 2013) are on the rise though. RCMs and GCMs, with their complete closed water budget including the atmospheric and land surface branches, are ideal tools to understand better the linkages and feedbacks between climate and hydrologic systems and to evaluate the impact of climate change on streamflows. Currently, RCMs offer higher spatial resolution than GCMs, allowing for greater topographic complexity and finer-scale atmospheric dynamics to be simulated and thereby representing a more adequate tool for generating the information required for regional impact studies. In a number of recent studies, RCMs have been used to study projected changes to various components of the hydrologic cycle (Jha et al., 2004; Wood et al., 2004; Kay et al., 2006b,a; Sushama et al., 2006; Graham et al., 2007a,b; Mladjic et al., 2011; Monk et al., 2011; Poitras et al., 2011). Therefore, to improve confidence in similar future work, this study focuses on improving the realism of RCM-simulated climate and hydrology, particularly streamflow, by introducing lake-river interactions and interflow (i.e. lateral flow of water in the upper soil layers along the topographic slopes) in the regional climate model.

The role of lakes in modulating regional climate, through bigger thermal inertia, smaller roughness and smaller albedo (when not frozen) in comparison with the surrounding land areas, is well known (Samuelsson et al., 2010; Martynov et al., 2012; Notaro et al., 2013a). Lakes also influence significantly the regional hydrology. For instance, Bowling and Lettenmaier (2010) demonstrated, for the case of the northern coast of Alaska, that up to 80% of the snowmelt water could

go to lake storage and thus does not contribute to the spring peak flow. Therefore, modelling lakes in climate models is important for better representation of streamflows.

Other processes that are important for realistic simulation of streamflows include interflow, surface-groundwater interactions, land use changes, urbanization, irrigation etc., which are not usually represented in many climate models, including the fifth generation Canadian Regional Climate Model (CRCM5). Although interflow might be an important component, it has been neglected so far in climate models that did include simulation of runoff. This was a reasonable assumption at coarse resolutions, given that interflow depends on many parameters, such as horizontal hydraulic conductivity of soil, drainage density, for which the representativeness of up-scaled values might be questionable. At high resolutions it could be beneficial to parameterize interflow in RCMs (Soulis et al., 2000). For example, during intense precipitation events, lateral flow could significantly increase the peak streamflow values in places where water impeding soil layers are near the surface (Chanasyk and Verschuren, 1983). Soulis et al. (2000) and Wen et al. (2007) studied the impact of interflow and baseflow on streamflows using offline land surface scheme simulations. Although they obtained improvements in streamflows after modifying the land surface scheme, the effect of interflow alone was not clearly demonstrated. Furthermore, Wen et al. (2007), in their simulations, did not notice any significant changes to soil moisture with interflow and groundwater modifications in the land surface scheme, which might be the reason for the weak response of streamflow to interflow in their study.

The main objectives of this study are therefore to improve the CRCM5 by modelling additional processes, i.e. lake-river interactions and interflow, to study lake-atmosphere and lake-river interactions, and their influence on regional climate and hydrology, particularly streamflows, for selected northeast Canadian watersheds spread mainly across the province of Quebec and parts of Ontario, Newfoundland and Labrador provinces. This region is selected because of the importance of rivers in the economic activities (notably hydropower generation) and the presence of large number of small lakes for which the use of a 1D column lake model is appropriate. Although previous studies have looked at the impact

of lakes on regional climate, to the best of our knowledge, no studies have looked at the impact of lakes on the regional hydrology, particularly streamflow, in the context of a regional climate modelling system.

The article is organized as follows. Section 2 describes models used in the study, i.e. the regional climate model, lake model and river routing approach and observation datasets used for validation purposes. The methodology, more specifically the design and purpose of the conducted experiments, is presented in section 3. Results are presented in section 4, followed by a summary and conclusions in section 5.

2.2 Models, experimental configuration and data

The regional climate model used in this study CRCM5 is based on a limited-area version of the Global Environmental Multiscale (GEM) model used for numerical weather prediction at Environment Canada (Côté et al., 1998). GEM employs semi-Lagrangian transport and a (quasi) fully implicit stepping scheme. In its fully elastic non-hydrostatic formulation (Yeh et al., 2002), GEM uses a vertical coordinate based on hydrostatic pressure (Laprise, 1992). The following physical parameterizations, inherited from GEM, are used in CRCM5: deep convection (Kain and Fritsch, 1990), shallow convection (Kuo, 1965), large-scale condensation (Sundqvist et al., 1989), correlated-K solar and terrestrial radiations (Li and Barker, 2005), subgrid-scale orographic gravity-wave drag (McFarlane, 1987), low-level orographic blocking parameterization (Zadra et al., 2003, 2012) and planetary boundary layer parameterization (Benoit et al., 1989; Delage and Girard, 1992; Delage, 1997; Zadra et al., 2012).

The Canadian land-surface scheme CLASS version 3.5 (Verseghy, 1991, 2009), which allows a flexible number of soil layers and depth, is used in CRCM5. A detailed description of the CRCM5 can be found in Martynov et al. (2012). Resolved and sub-grid lakes are represented in CRCM5 using the one-dimensional lake model developed by Hostetler (Martynov et al., 2012), where the vertical heat transfer is simulated by eddy conductivity and convective mixing (Hostetler et al., 1993). Lake water balance is activated in the current study by taking into account all lake inflows and outflows, i.e. precipitation and evaporation, ice thaw

and freeze as well as river flows. The influence of lake level variation on lake temperature profile is neglected in this study.

2.2.1 River-lake routing model

The river routing scheme WATROUTE (Soulis et al., 2000), modified to include ground water reservoir (Poitras et al., 2011), is used to simulate streamflows from runoff in CRCM5. The routing scheme solves the water balance equation at each grid cell, and relates the water storage to streamflow using Manning's equation (Te Chow, 1959).

Two types of lakes are distinguished for lake routing, local and global (Fig. 2.1). A gridcell is considered to have a local lake, when the total lake fractional area of all lakes that fall within the cell is less than 0.6. A global lake on the other hand is spread over several grid cells and receives inflow from upstream cells. However,

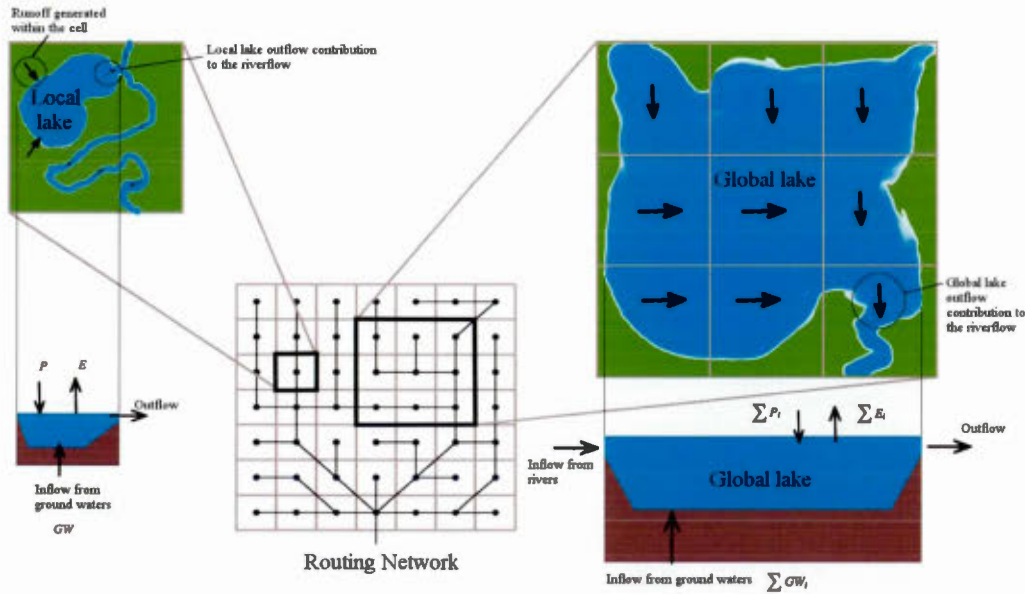


Figure 2.1: Representation of local and global lakes in the lake-river routing scheme.

local lakes do not receive flow from upstream cells as it is assumed here that main streams usually do not flow through smaller local lakes. The only runoff contribution to the local lakes is from runoff generated within the same grid cell and the groundwater contribution of the same cell. However, the outflow from local lakes contributes to the river flow in the cell. The outflow from both local and global lakes is modelled using the storage-discharge function proposed by Döll et al. (2003):

$$Q(S) = k_r S \left(\frac{S}{S_{\max}} \right)^{1.5}, \quad (2.1)$$

where S is the active storage [m^3]; S_{\max} is the maximum active storage [m^3] and is computed as $S_{\max} = H \cdot A_{\text{lake}}$, where H is the maximum active storage depth [m], which is taken as 5 m, A_{lake} is the area of the lake; k_r is the outflow coefficient [d^{-1}] (0.01 d^{-1}). This relation, when applied for observed lake sites over the study domain, where lake levels and streamflows are available, gives satisfactory results. In addition, it also compares well with the equation proposed by Bowling and Lettenmaier (2010). In this study the function from Döll et al. (2003) is used as it involves less parameters, and provides reasonable results.

For local and global lakes, the change in lake level is calculated from the change in the lake storage as:

$$\Delta h = \frac{\Delta S}{A_{\text{lake}}}, \quad (2.2)$$

where Δh is the change in the lake level, ΔS is the change in lake storage during the time step, and A_{lake} is the lake area.

2.2.2 Experimental configuration and observation data

The integration domain of CRCM5 covers northeastern Canada and is shown in Fig. 2.2a. Simulations are performed at 0.1° horizontal resolution. The grid is uniform in the rotated latitude-longitude projection, with 56 hybrid vertical levels. For the land surface scheme CLASS, a 26-layer soil configuration reaching 60 m is used. Such a deep CLASS configuration is chosen to better represent near-surface permafrost in the northern parts of the simulation domain (Paquin and Sushama, 2015).

The land surface scheme recognizes four broad categories of vegetation, i.e. needle-leaf, broadleaf, crops and grass. These are specified in the model using multiple high-resolution datasets (i.e. USGS-GLCC, GlobCover, GLC2000, LCC2000-V etc.). The depth to bedrock, sand and clay fields needed for the soil model are specified from the 1° resolution datasets provided by Webb et al. (1993). These fields for the study domain are shown in Fig. 2.2c-e. Initial conditions for the soil temperature and soil liquid and frozen water contents are obtained by running CLASS offline for 300 years using atmospheric forcing for the 1961–1970 period from the European Centre for Medium-range Weather Forecasting (ECMWF) ERA40 reanalysis data (Uppala et al., 2005), recursively; these data are available at 2.5° resolution. The depth of the modelled soil column justifies this long spinup period.

The lake fractions (Fig. 2.2b) over the domain are based on the Global Land Cover Characteristics (GLCC) dataset. According to this dataset, lakes cover 8% of the landmass within the integration domain. Nine percent of the grid cells with nonzero lake fraction have at least 60% of a grid cell area covered by lakes, i.e. the cells that are classified as global lake cells in this study. The flow directions, river lengths and slopes required by the routing scheme are derived from the HydroSHEDS database (Lehner et al., 2008), available at 30-second resolution on a latitude-longitude grid. Sea surface temperature and sea ice cover in the CRCM5 simulations are prescribed from ERA-Interim (ECMWF) reanalysis, available at 1.5° resolution (Dee et al., 2011).

For validation of simulated temperature and precipitation fields, daily analysis from Hopkinson et al. (2011) is used. These data are available at 10 km resolution over the study region south of 60°N, for the 1970–2010 period. Snow water equivalent (SWE) simulated by the model is validated using daily gridded SWE dataset developed by Brown et al. (2003), which is available for the period 1980–1996 over North America at 0.25° resolution. Simulated streamflow characteristics and lake levels are validated against those from the Centre d’expertise Hydrique du Québec (CEHQ; <http://www.cehq.gouv.qc.ca/>). Six unregulated streamflow gauging stations, with lakes upstream, are selected for validation of the simulated streamflow. Three additional gauging stations with lake levels are

also selected for validation purposes.

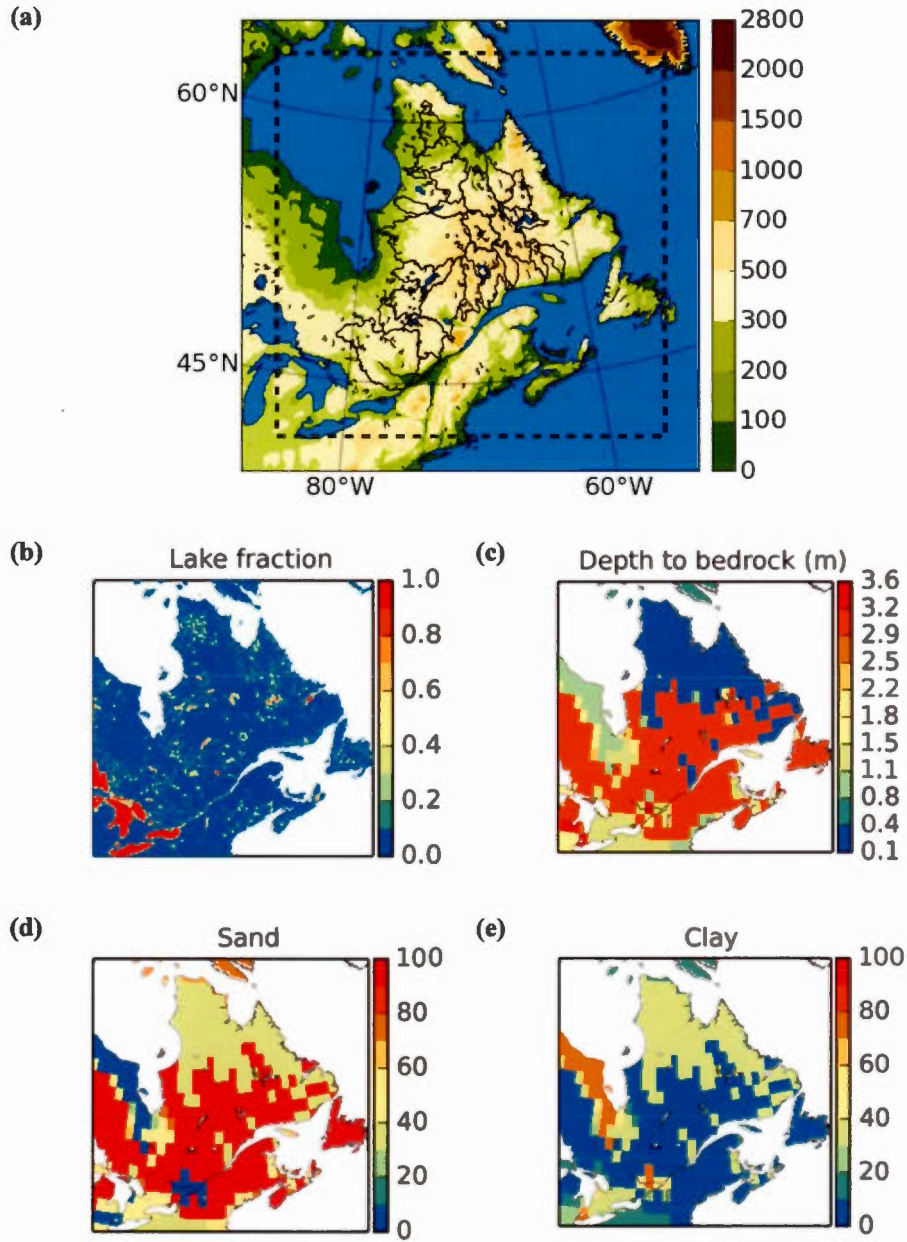


Figure 2.2: (a) Simulation domain; the dashed line separates the blending and free zones. The colours correspond to topography (m). Ocean and inland water bodies are shown in blue. Geophysical fields used in the simulations: (b) lake fraction, (c) depth to bedrock, (d) percentage of sand and (e) percentage of clay.

2.3 Methodology

As mentioned earlier, the objectives of this study are to improve CRCM5 by including additional processes, i.e. lake-river connectivity and interflow, and to study lake-atmosphere and lake-river interactions and its impact on regional climate and hydrology. To this end, four CRCM5 simulations (Table 2.1), as discussed below, driven by ERA-Interim, are performed for the 1979–2010 period. The analysis is performed for the 1991–2010 period, as the first thirteen years of the simulation are considered as spin-up.

Simulation CRCM5-NL, without lakes, is the reference simulation and spans the 1979–2010 period. Lakes are replaced with bare soil in this simulation. The second simulation, CRCM5-L1, considers lakes, but lake routing is not considered. Lakes are represented in this simulation using the Hostetler model (Hostetler et al., 1993). The influence of lakes on routing is only through the modification of atmospheric conditions by lakes. Comparison of this simulation with CRCM5-NL

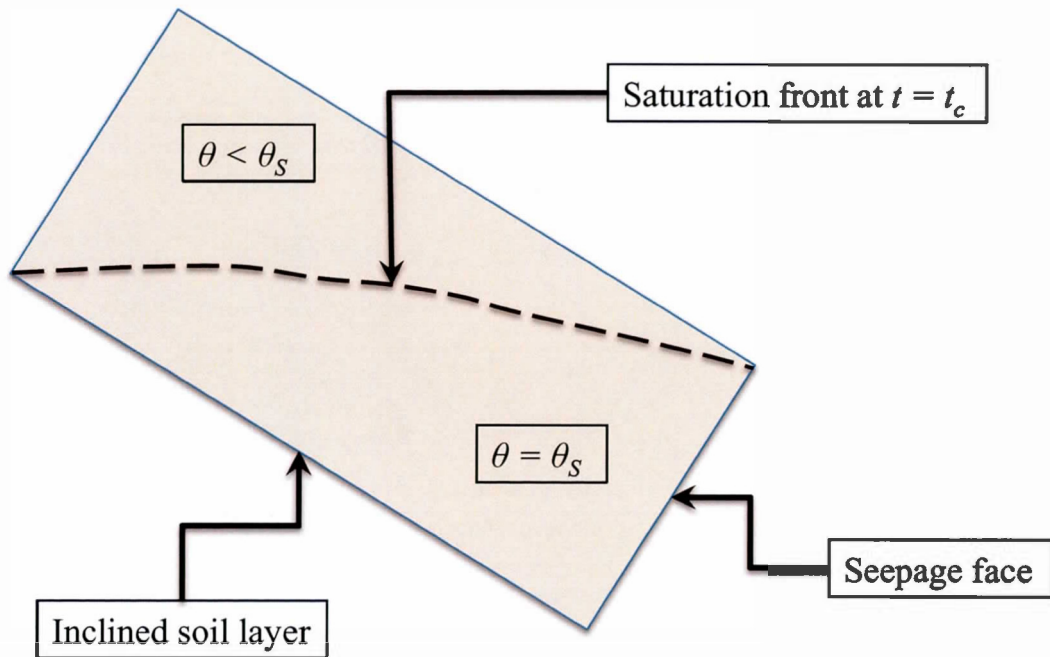


Figure 2.3: Inclined soil layer and saturation front at the critical time ($t = t_c$) when the interflow regime changes from linear to exponential function of time.

Station ID	Simulation Period	Analysis period	Description
CRCM5-NL	1979–2010	1991–2010	Lakes replaced by bare soil
CRCM5-L1	1979–2010	1991–2010	Lakes, simulated by Hostetler model, no lake routing
CRCM5-L2	1979–2010	1991–2010	CRCM5-L1 + lake routing
CRCM5-L2I	1979–2010	1991–2010	CRCM5-L2 + interflow, interflow slope as for routing

Table 2.1: List of simulations used in the current study.

will help to quantify the effect of lake-atmosphere interactions on the regional climate (e.g. temperature, precipitation, latent and sensible heat fluxes) and its indirect effect on streamflow. The third simulation CRCM5-L2 is similar to CRCM5-L1, but includes lake routing. It is used to study the direct influence of lakes on streamflow, i.e. to quantify the lag and damping effect of lakes on peak flows. Since this simulation accounts for both direct and indirect influence of lakes on rivers and the simulation CRCM5-L1 contains only the indirect link through modified atmospheric conditions, the effect of direct lake-river interactions can be evaluated by comparing CRCM5-L2 with CRCM5-L1.

The fourth experiment CRCM5-L2I is similar to CRCM5-L2, but considers interflow. Interflow is mostly driven by gravity, and the interflow formulation, used in this study, follows Soulis et al. (2000) and Mekonnen et al. (2012). According to this formulation, water movement is assumed to occur only along topographic slopes and the influence of moisture gradients is neglected. The interflow rate I (m/s) can then be derived, using the continuity and Darcian equations, as an explicit function of time (t) elapsed since complete saturation of a soil layer:

$$I = \frac{SR(t) - SR(t + \Delta t)}{\Delta t} H \theta_s, \quad (2.3)$$

where Δt is the model time step [s], and H is the depth of the soil layer [m]. $SR(t)$ in the above equation is the liquid saturation ratio, i.e. the ratio of the current

soil liquid water content θ to the maximum possible liquid soil water content θ_S . It is a prognostic variable, calculated by the interflow model using the following expression:

$$SR(t) = \begin{cases} 1 - \frac{t}{c \cdot t_c}, & t \leq t_c \\ \frac{c-1}{c} \left(\frac{t_c}{t} \right)^{1/(c-1)}, & t > t_c \end{cases}, \quad (2.4)$$

where t is the time elapsed [s] since total saturation of the soil layer; t_c is the critical time [s], i.e. the time it takes for the saturation front to reach the seepage face of the soil layer (Fig. 2.3). In equation (2.4), $c = 2b + 3$, where b is a soil texture parameter presented in Clapp and Hornberger (1978).

Critical time is a function of drainage density, slope, horizontal hydraulic conductivity of soil and θ_S (Mekonnen et al., 2012). Drainage density, i.e. river network length per square kilometre of a watershed, is calculated from HydroSHEDS (Lehner et al., 2008). The river network for North America was available only to the south of 60°N in HydroSHEDS when this work was carried out. Therefore, grid cells not covered by the HydroSHEDS dataset are assigned mean values of the drainage density for the study domain. The horizontal hydraulic conductivity is assumed to decrease exponentially with depth. To derive the maximum value of the horizontal hydraulic conductivity, i.e. the value for the first soil layer, the vertical hydraulic conductivity of soil and anisotropy ratio (β) of the layer are used. The anisotropy ratio is calculated based on the soil texture using the table values of the anisotropy ratio from Fan et al. (2007) for the sand ($\beta = 2$), clay ($\beta = 48$) and silt ($\beta = 10$).

2.4 Results

2.4.1 Impact of lakes on regional climate and hydrology

As was stated in the methodology section, the effect of lake-atmosphere interactions on regional climate and streamflow is studied by comparing simulations with and without lakes, i.e. CRCM5-L1 and CRCM5-NL, respectively.

As expected, warmer temperatures are obtained with CRCM5-L1 compared to

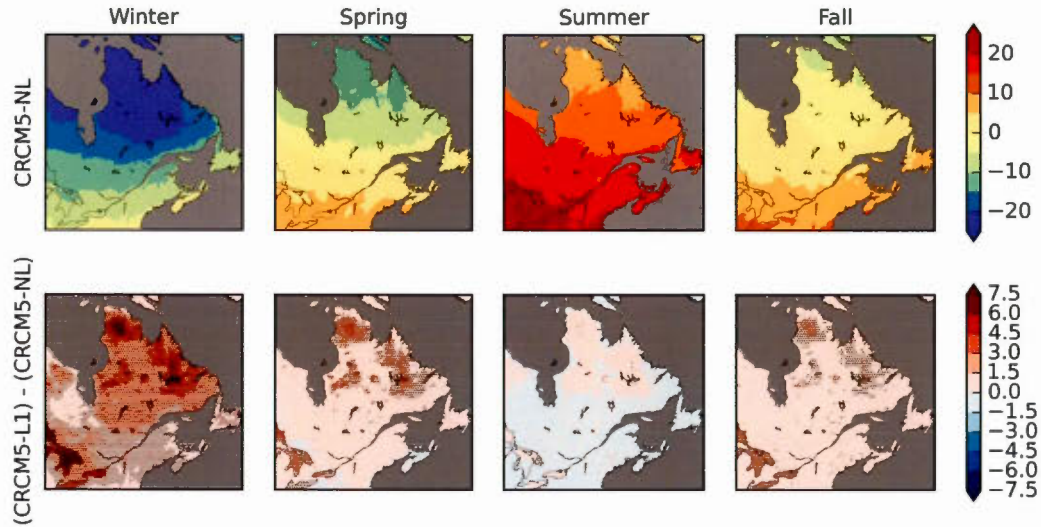


Figure 2.4: Upper row: CRCM5-NL simulated seasonal mean 2-m air temperatures (°C), for the 1991–2010 period. Lower row: difference between CRCM5-L1 and CRCM5-NL simulated mean seasonal 2-m air temperature. Black dots are used to show grid points where the differences are statistically significant at 10% significance level.

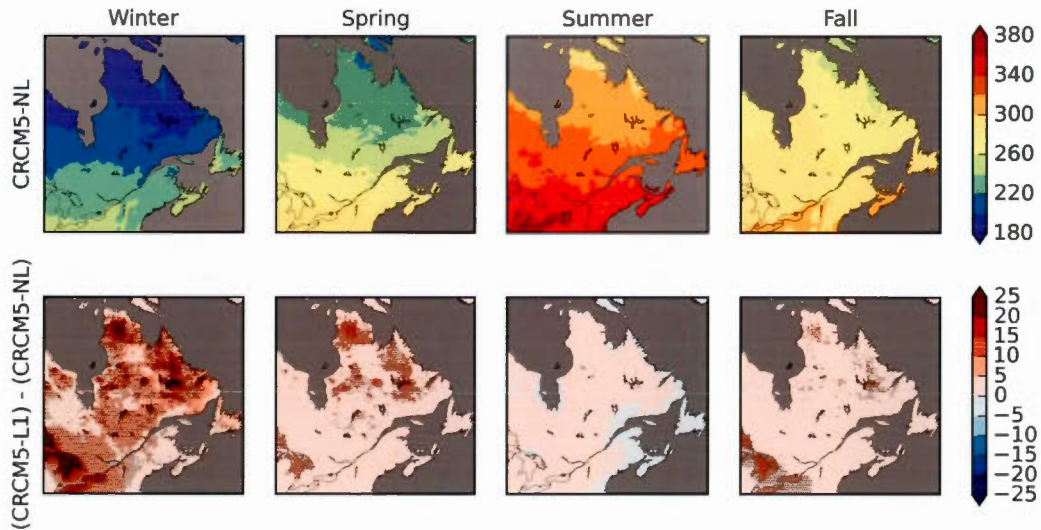


Figure 2.5: Same as Fig. 2.4 but for down-welling long-wave radiation at the surface in W/m².

CRCM5-NL, particularly for winter, while a slight cooling is obtained in the southern part of the study domain during summer (Fig. 2.4). The warming effect of lake in winter is as high as 6°C, which is around 2° warmer than the maximum winter warming reported by Martynov et al. (2012) for the same region, using

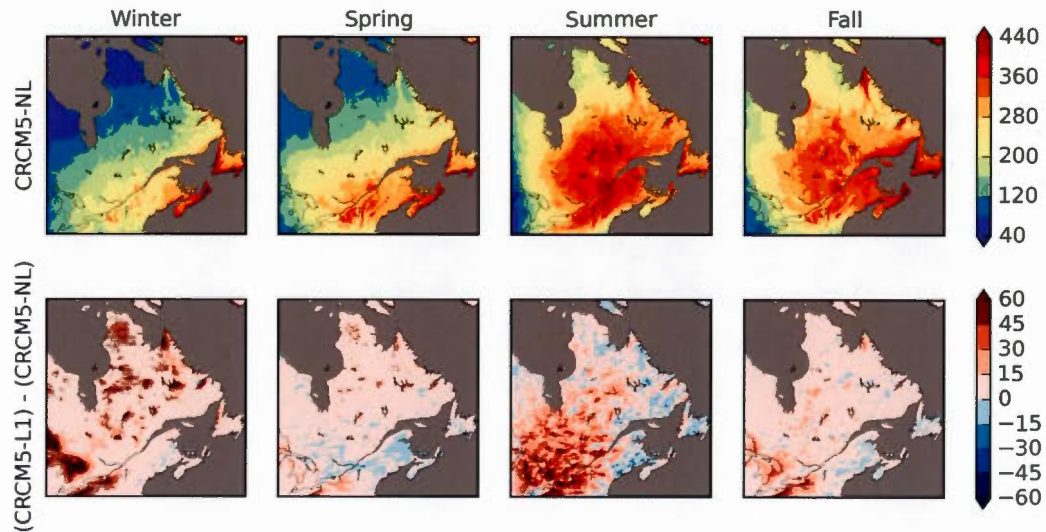


Figure 2.6: Same as Fig. 2.4 but for total precipitation (mm/season).

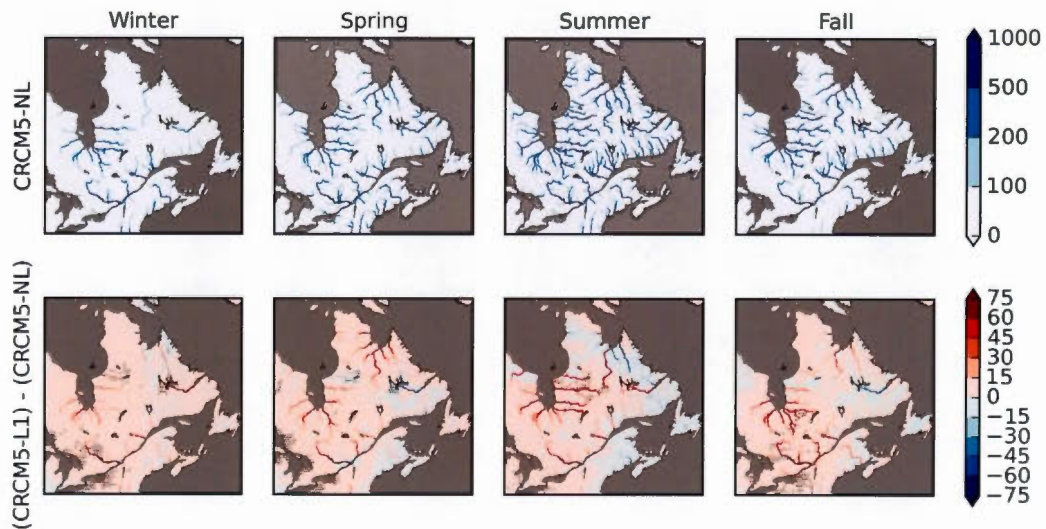


Figure 2.7: Same as Fig. 2.4 but for streamflow (m³/s).

CRCM5 at a coarser resolution. The cooling effect in spring is smaller and almost not visible after averaging over the March to May months. The summer cooling, associated with evaporative cooling, is more widespread, with cooling directly over lakes mostly visible during the June-July months (monthly figures are not shown). Although increased cloud cover can also contribute to this summer cooling, the very low non-significant differences in downwelling long-wave radiation (Fig. 2.5) between the two simulations suggest no significant impact of cloud cover.

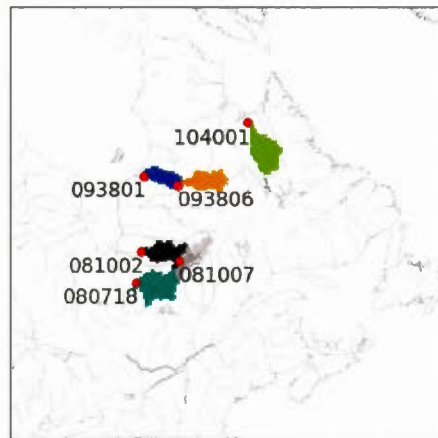
Impact of lakes on the seasonal mean precipitation field is shown in Fig. 2.6. The simulation with lakes CRCM5-L1 has more precipitation compared to the simulation without lakes CRCMR-NL, for all seasons. Maximum differences of up to 60 mm in the total winter precipitation are noted. For summer, higher precipitation differences are generally located to the east of the Great Lakes. Samuelsson et al. (2010), in their study over Europe, showed that the effect of lakes could lead to both increases or decreases in total precipitation (PR) during summer season. They reported an increase in precipitation in the case of shallow lakes and a decrease in the case of deep lakes. The decrease in precipitation for deep lakes in their study is probably due to the effect of cooler temperatures at depth compensating the destabilization caused by additional moisture in the air (Lofgren, 1997).

Accounting lake contributions in the energy and humidity exchanges between the surface and atmosphere is expected to have an impact on streamflow mostly due to changes in precipitation. Fig. 2.7 shows generally higher streamflows in CRCM5-L1 compared to CRCM5-NL, which is generally in agreement with the differences in precipitation between the two simulations (Fig. 2.6). There are some regions, where streamflow values are lower in CRCM5-L1, particularly where there are sub-grid lakes, and this could be due to reduced runoff-contributing area due to the presence of lakes instead of bare soil.

To validate the simulated streamflows, six gauging stations are selected. The locations of these stations and their corresponding upstream areas, as seen by the model, are shown in Fig. 2.8a. The observed and modelled streamflows shown in Fig. 2.9 indicate an overestimation of spring peak flows by both CRCM5-NL and CRCM5-L1 for all stations. This overestimation is primarily due to the

absence of lakes in CRCM5-NL, and absence of lake routing in CRCM5-L1. The overestimations for the northern stations (104001, 093801, 093806) are also related to the overestimation of winter SWE for the northern regions in both CRCM5-NL and CRCM5-L1 (Fig. 2.8b). The winter SWE is relatively better represented for the southern region in CRCM5-L1 and CRCM5-NL. Generally, in CRCM-L1, where lake-atmosphere interactions are included, the volume of water flowing yearly through the selected gauging stations is higher than that for CRCM-NL and also the summer streamflows are slightly higher, due to higher precipitation in CRCM5-L1 compared to CRCM5-NL. However, the errors in the timing and magnitude of spring peak flows remain in both simulations, as lake routing and other processes are not considered in these two experiments. The impacts of lake routing and interflow are discussed below.

(a)



(b)

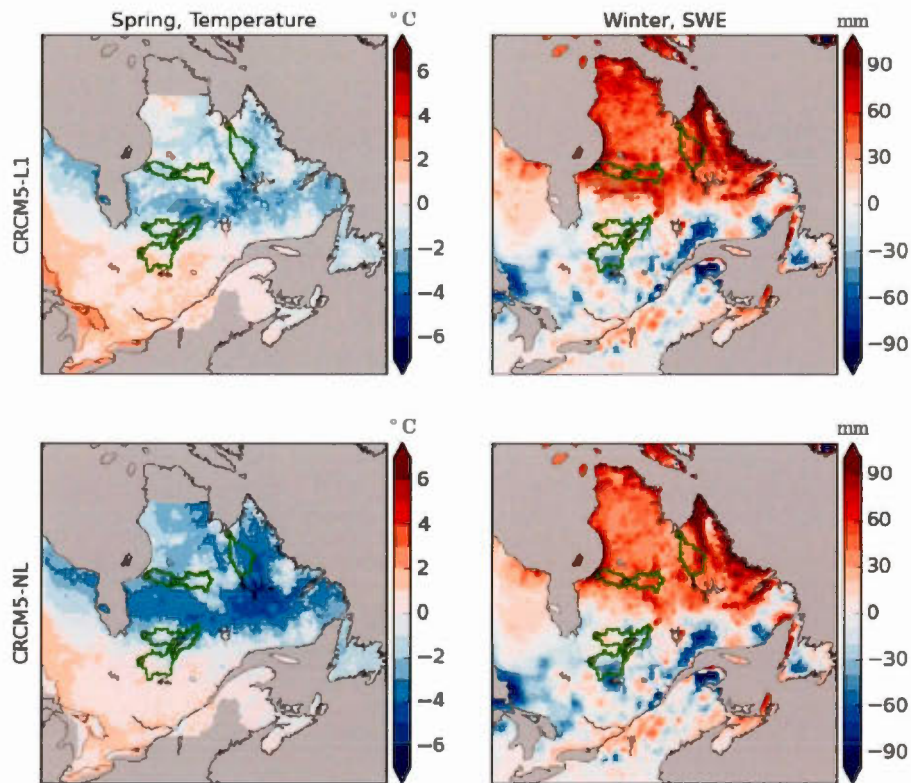


Figure 2.8: (a) Locations of streamflow gauging stations (red dots) and their corresponding upstream areas. (b) Differences between modelled (CRCM5-L1 and CRCM5-NL simulations) and observed (Brown et al., 2003) SWE (mm) for winter (DJF) and for spring 2-m temperature.

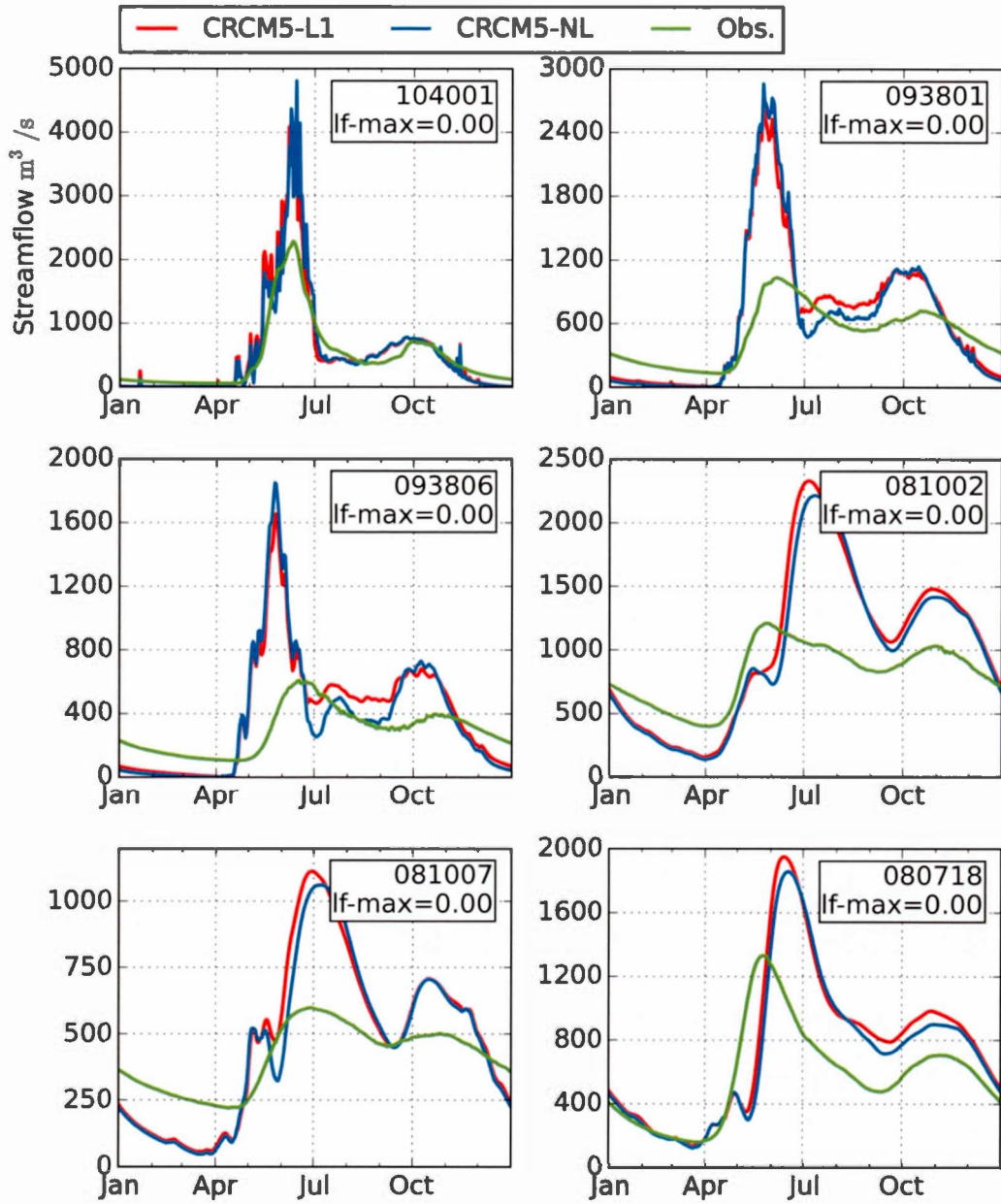


Figure 2.9: Comparison of the climatologic streamflow from experiments CRCM5-NL, CRCM5-L1 and observations at selected gauging stations. The panels are sorted according to the station latitude, i.e. the northernmost (southernmost) stations are shown in the top (bottom) panels.

2.4.2 Direct impact of lakes on streamflow

Direct impact of lakes on streamflow is studied in this section by comparing simulations with (CRCM5-L2) and without (CRCM5-L1) lake routing. Lakes retain snowmelt water and precipitation, acting as sinks/reservoirs in spring and summer. After summer they revert to supply water to rivers during autumn and winter seasons. Lakes are very important sources of water in winter. This is clearly visible in Fig. 2.10, which shows the spatial distribution of the effect of lake routing on seasonal mean streamflows. Fall and winter streamflows are clearly higher in CRCM5-L2, with winter differences statistically significant for most of the northern land regions. Spring flows are clearly reduced in CRCM5-L2 as lakes store part of the snowmelt.

Lake routing leads to better representation of spring peak flows in CRCM5-L2 (Fig. 2.11a), when upstream surface runoff dominates (093801), compared to the cases where subsurface runoff has greater influence on streamflow (081002). Nevertheless the improvement due to lake routing is robust and the comparison of

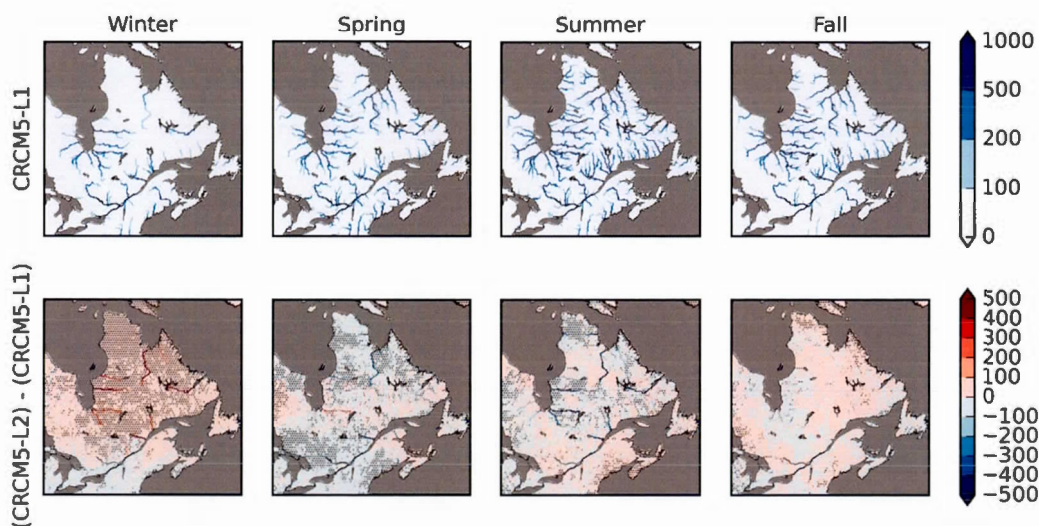


Figure 2.10: Mean seasonal streamflow (upper row, for simulation CRCM5-L1) and changes to the mean streamflow due to lake routing (bottom row, i.e. CRCM5-L2 minus CRCM5-L1). All values are in m^3/s . Dots show grid cells where the differences are statistically significant at 10% significance level.

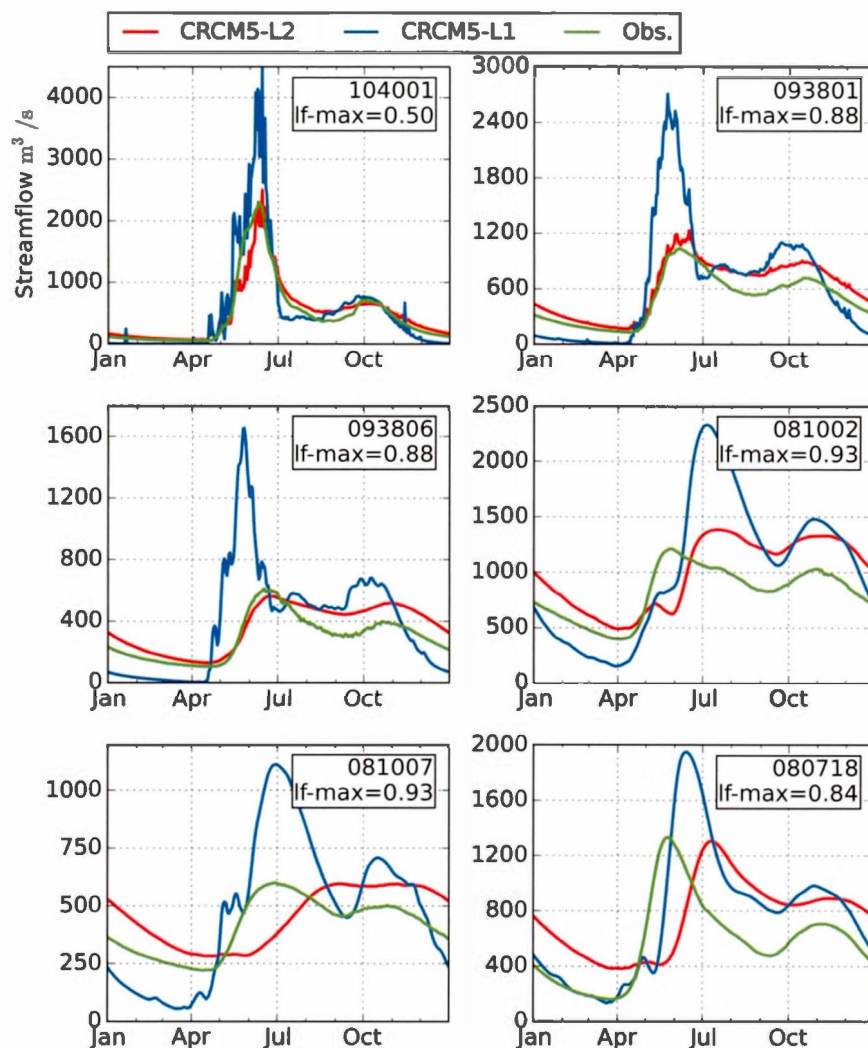
modelled and observed hydrographs confirm this at other stations (Fig. 2.11a). The winter flow increases in CRCM5-L2 and is closer to observations in the majority of the cases, especially for the northern stations. In these regions, the contribution of groundwater to streamflow during winter is almost negligible, due to the small soil moisture storage capacity of the thin soil layer, which is related to the proximity of bedrock to the surface. During fall, streamflow is overestimated at all gauging stations. The overestimation can be partly explained by the overestimation of fall precipitation (figure not shown). The higher streamflow overestimation for the stations in regions with deeper bedrock (i.e., the southern stations) might be caused by uncertainties in soil parameters used to estimate infiltration, which then leads to the overestimation of drainage in spring, which is released into rivers later during fall season.

Fig. 2.11b shows scatter plots of the observed and modelled 10th and 90th percentiles (i.e. Q10 and Q90) of daily climatological streamflows. Lake routing improves model's ability in reproducing these characteristics. The 90th percentile, which is overestimated in CRCM5-L1 due to the lack of lake storage during snowmelt, is improved for all stations when lake routing is considered. The 10th percentile, which is underestimated in CRCM5-L1, is improved through lake contribution to streamflows and is now closer to the observed values for the majority of the selected gauging stations, except for 080718. This is reflected in the R^2 values shown in Fig. 2.11b where it increases from 0.66 to 0.83.

Lake-river connectivity, as discussed above, is important to improve streamflows and similarly it is important for lakes as streamflow entering lakes can change the lake water budget and therefore lake levels. The observed and CRCM5-L2 modelled mean annual cycle of lake level variation are shown in Fig. 2.12 for three lake level gauging stations (093807, 011502 and 040408). Good agreement between modelled and observed variability is evident from this figure. To further demonstrate the importance of lake-river connectivity in determining lake levels and its variability, lake level variability is determined for CRCM5-L2 at the same three gauging stations, considering only precipitation and evaporation, i.e., the streamflow contributions to lake water budget is neglected. This new lake level variability, named CRCM5-L2(P-E) is also plotted in Fig. 2.12. Clearly, the lake

level variability obtained by neglecting streamflow contribution to lakes fails to capture the timing and magnitude of observed lake level variability at all three gauging stations, suggesting the importance of lake-river connectivity on lake level variability.

(a)



(b)

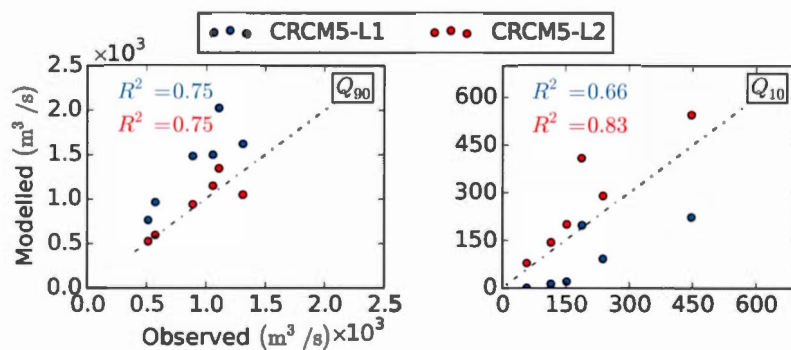


Figure 2.11: (a) Same as Fig. 2.9 but for simulations CRCM5-L1 and CRCM5-L2, (b) Scatter plots of 90th (left) and 10th percentiles (right) of the daily mean climatologic streamflows derived from observed and modelled (CRCM5-L1 and CRCM5-L2) streamflows.

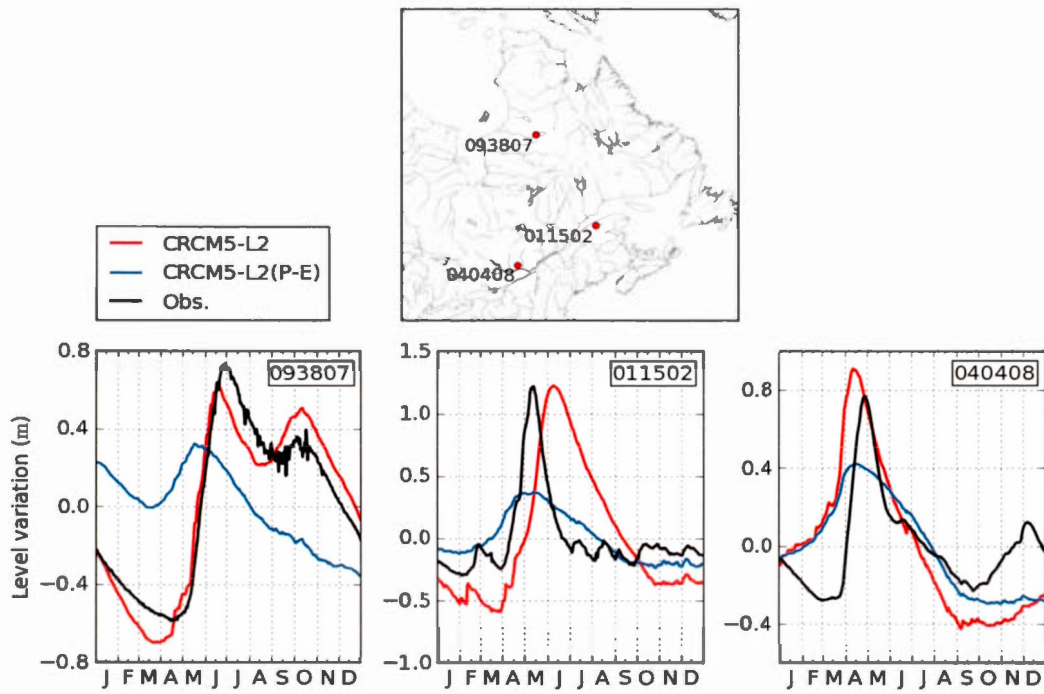


Figure 2.12: (a) Locations and identification numbers of lake level gauging stations. (b) Mean seasonal cycle of observed and simulated lake level variability. CRCM5-L2 (red), CRCM5-L2(P-E) (blue), and observed (black, taken from CEHQ dataset).

2.4.3 Impact of interflow

As discussed earlier, the interflow process is considered in CRCM5-L2I simulation. The simulated zonally averaged mean interflow rate for the 1991–2010 period is shown in Fig. 2.13. The interflow process first starts in the southern part of the domain in March and then propagates northward following snowmelt. Interflow also occurs in summer and fall associated with precipitation events in the southern parts of the region. However, this summer interflow is modest since the precipitation events that trigger interflow increases soil moisture only for a shorter period in comparison to snowmelt where the soil stays saturated for longer periods due to continuous infiltration of snowmelt water. Interflow in winter is practically zero due to frozen conditions, except in December over the southernmost parts of the region.

To study the impact of interflow on streamflows, the differences in streamflows for CRCM5-L2I and CRCM5-L2 are shown in the top row in Fig. 14, which suggests higher streamflows in CRCM5-L2I compared with CRCM5-L2, particularly visible for the major streams. However, some decreases can also be noted. To understand these differences, the surface and subsurface runoff/drainage and soil moisture

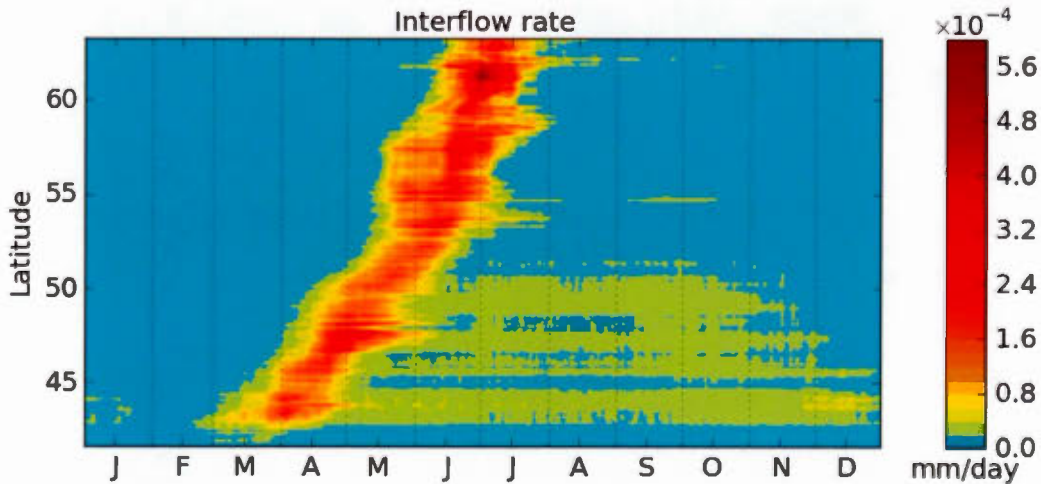


Figure 2.13: Zonally averaged mean interflow rate for the first soil layer, for the 1991–2010 period, for CRCM5-L2I.

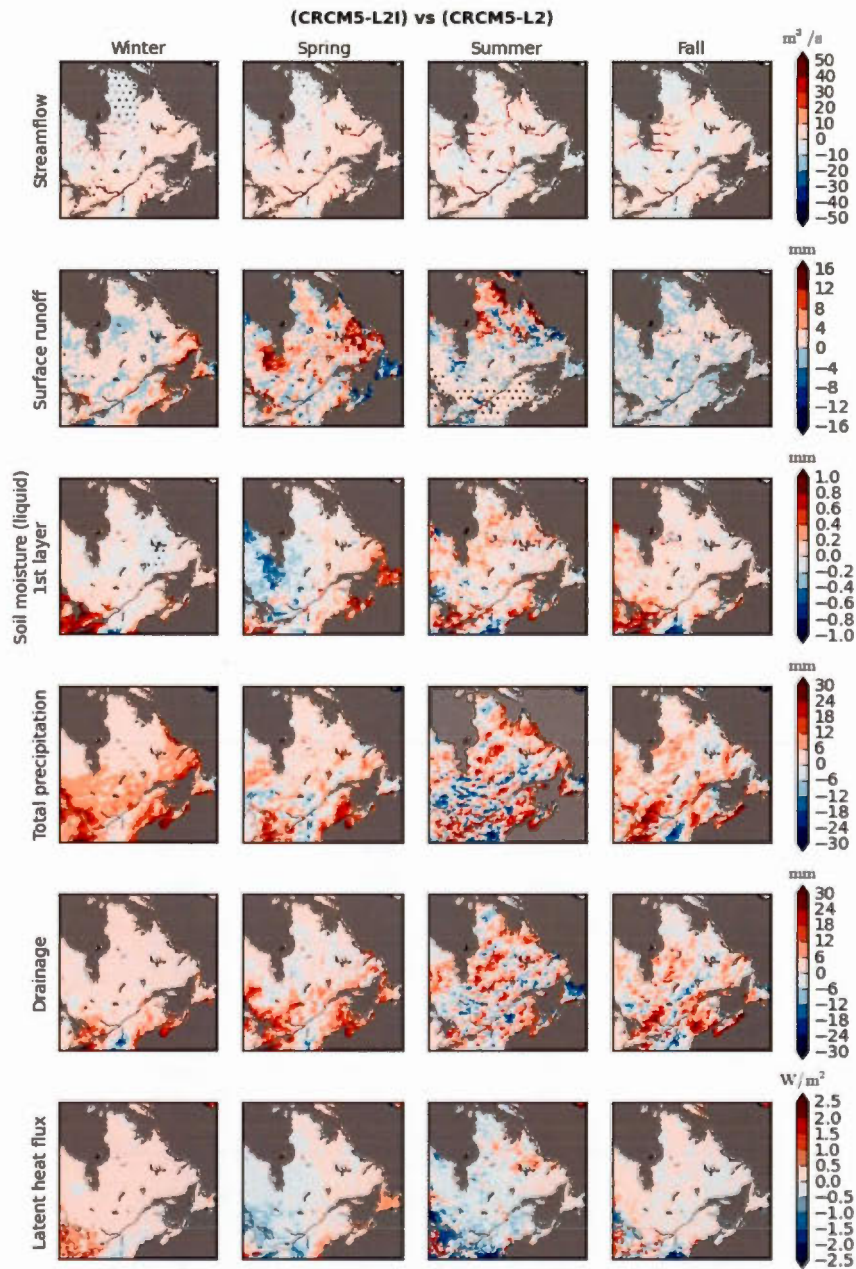


Figure 2.14: Differences between CRCM5-L2I and CRCM5-L2 simulated fields; from top to bottom are streamflow, surface runoff, moisture in the first soil layer, total precipitation, subsurface runoff and latent heat flux. Black dots indicate grid cells with statistically significant differences at 10% significance level.

fields are further analysed (Fig. 2.14). Note that the surface runoff in CRCM5-L2I includes interflow contribution.

In general, higher surface runoff is noted over southerly and central regions during spring in CRCM5-L2I compared to CRCM5-L2. This is due to spring snowmelt, which saturates the soil, thereby enhancing lateral flows. Although lateral flows can lower soil moisture, the continuous infiltration of snowmelt water helps to maintain higher soil moisture levels and therefore lateral flows during spring. Once snowmelt ceases, i.e. during summer, the southernmost region shows reduced surface runoff in CRCM5-L2I due to reduced soil moisture caused by lateral flows and due to the absence of a continuous source of infiltration as during snowmelt. Regions of higher surface runoff in CRCM5-L2I compared to CRCM5-L2 migrates further north by summer, as snowmelt continues through the early part of summer for these regions. Statistically significant differences, with higher surface runoff values in CRCM5-L2I, are noted for the southerly regions during summer, though it is not translated to significant changes in streamflows. This is due to higher interflow contribution to surface runoff associated with precipitation events. The relation between precipitation and interflow in this southern region in summer is confirmed by the positive correlation between precipitation and interflow (Fig. 2.15).

The impact of interflow on surface fluxes is now explored to see possible impacts

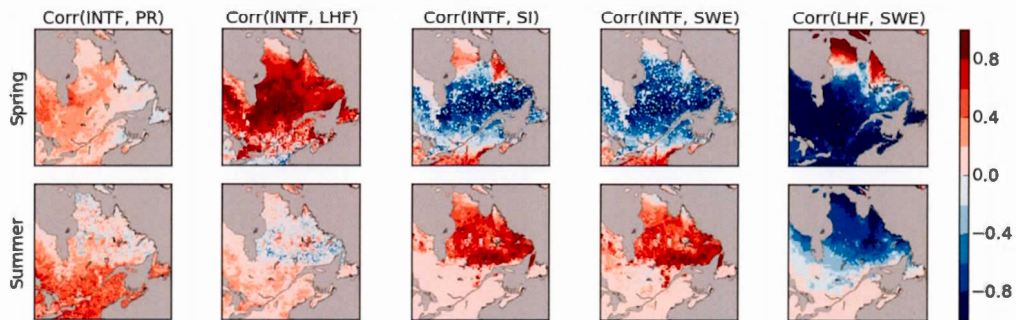


Figure 2.15: Correlations between CRCM5-L2I variables, for the 1991–2010 period (INTF – interflow rate in the top soil layer, PR – total precipitation rate, SI – soil ice fraction in the top soil layer, SWE – snow water equivalent, LHF – latent heat flux), for spring and summer seasons.

on climate. The impact of interflow on the latent and sensible heat fluxes is very modest. The lower (higher) values of latent (sensible) heat flux (figure not shown for sensible heat flux) in CRCM5-L2I for the southern part of the domain in summer could partly be due to the reduced soil moisture in this simulation due to lateral flows. To understand better the connection between various variables, correlations of different interflow-related surface variables for CRCM5-L2I are studied (Fig. 2.15). In the northern and central parts of the study domain both interflow and latent heat flux increase at the same time in spring, which is signified by the high positive correlations in Fig. 2.15. This is because snowmelt increases both evaporation and infiltration and therefore interflow in spring, as is evident from the negative correlations between SWE and interflow and also between SWE and latent heat flux. On the contrary, over a smaller southernmost part of the region, a negative correlation between latent heat flux and interflow rate is obtained in spring. This could be due to the decrease in the interflow rate caused by the decrease of soil moisture, both liquid and solid, and an increase in the evaporation caused by warmer temperatures. This region with negative correlation grows and displaces northward in summer (Fig. 2.15). The positive correlation between the interflow rate and soil ice content, as well as SWE, over the southernmost region suggests that the evaporation is enhanced at the same time as the interflow is suppressed in this part of the simulation domain during summer.

2.5 Summary and conclusions

Lakes and rivers cover approximately 10% of the northeastern Canadian landmass and therefore exert an important influence on the regional climate and hydrology. The main objective of this study was to understand lake-river connectivity and interflow processes and their impacts on regional climate and hydrology. Four CRCM5 simulations driven by ERA-Interim reanalysis at the lateral boundaries for the 1979–2010 period are presented in this paper. To begin with, the impact of lakes on the regional climate is assessed by comparing simulations with and without lakes. To study direct lake-river interactions, the simulations with and without lake routing are compared. Finally, the impact of lateral flows in the soil layers are assessed using the simulations with and without interflow.

Results based on the comparison of simulations with and without lakes show that lakes act to increase air temperature in winter and for most part of summer, with the exception of larger lakes, where summertime evaporative cooling is more important. Lakes bring more moisture to the system and generally cause precipitation increases for all seasons.

Results from the simulations with and without lake routing suggest significant improvements to the timing and magnitude of spring peak flows and winter low flows. The indirect influence of lakes on rivers, obtained in this region, is modest in comparison with lake routing, i.e. the direct effect. Impact of rivers on lakes via lake inflows is found important to capture the variability of lake level. In summary, both simulated streamflows and lake levels benefit from lake routing.

Analysis of the simulation with interflow suggests maximum interflow during snowmelt periods. This is due to the high soil moisture level during this period due to snowmelt and therefore infiltration of snowmelt water. The effect of interflow on studied surface variables and fluxes is in general modest over the study domain. The effect of interflow on streamflows is mostly positive and is comparable to the effect of lake-atmosphere interactions on streamflows.

Although the study yields encouraging results with the 1D lake model applied to the lakes of all sizes, work is under way to use a 3D-model to represent the bigger lakes in CRCM5, which could improve mixing and capture the circulation patterns in lakes and consequently fluxes of humidity and heat between the lakes and the atmosphere. Adding the energy balance equation to the routing scheme and connecting lakes and rivers thermodynamically could also lead to a more comprehensive modelling tool, though the benefits at the current model resolutions might not be very significant.

There are many sources of uncertainties remaining in the runoff parametrization, such as errors in the geophysical fields. The version of CLASS used in the current study does not take into account vegetation characteristics when computing hydraulic conductivity of the soil, which might explain the small interflow values even in the forested areas. Therefore future studies are required, to look into the sensitivity of the interflow parameterization to the soil parameters and to improve

the representation of the impacts of vegetation on the soil hydraulic properties.

Simulated runoff and streamflow could also be further improved by considering interactions with the ground water table and by improving the parameterization of the hydraulic properties of frozen soil in CLASS. It must be noted that the results presented here are based on a single simulation per configuration. To improve confidence in the results, it would be useful to perform an ensemble of simulations in the future. It would also be useful to perform climate change simulations to assess the impact of lakes, lake-river connectivity and interflow processes on projected changes to the regional climate and hydrology.

Acknowledgement

This research was carried out within the Canadian Network for Regional Climate and Weather Processes funded by the Natural Sciences and Engineering Research Council (NSERC) of Canada.

CHAPTER III

LAKE-RIVER AND LAKE-ATMOSPHERE INTERACTIONS IN A CHANGING CLIMATE OVER NORTHEAST CANADA

This chapter is presented in the format of a scientific article that has been submitted to the peer-reviewed journal *Climate Dynamics*. The design of experiments and methods, as well as the analysis of data and preparation of the article were entirely carried out by myself, with Dr. Sushama involved in the supervision of all these tasks. The detailed reference is:

Huziy, O. and Sushama, L. (2015). Lake-river and lake-atmosphere interactions in a changing climate over northeast Canada

Abstract

Lakes influence the regional climate and hydrology in a number of ways and therefore they should be represented in climate models in a realistic manner. Lack of representation of lakes in models can lead to errors in simulated energy and water fluxes, for lake-rich regions. This study focuses on the assessment of the impact of climate change on lakes and hydrology as well as on the influence of lakes on projected changes to regional climate and surface hydrology, particularly streamflows, for Northeast Canada. To this end, transient climate change simulations spanning the 1950–2100 period are performed, with and without lakes, with the fifth generation of the Canadian Regional Climate Model (CRCM5), driven by the Canadian Earth System Model (CanESM2) at the lateral boundaries for Representative Concentration Pathway 8.5. An additional CRCM5 simulation, driven by ERA-Interim reanalysis for the 1980–2010 period, is performed in order to assess performance and boundary forcing errors.

Performance errors are assessed by comparing the ERA-Interim-driven simulation with available observation datasets, for the 1980–2010 period, for selected variables: 2-m temperature, total precipitation, snow water equivalent (SWE) and streamflow. The validation results indicate reasonable model performance over the study region. Boundary forcing errors are studied by comparing ERA-Interim-driven simulation with the one driven by CanESM2 for the current 1980–2010 period, to identify regions and seasons for which projected changes should be interpreted with extra caution.

Comparison of projected changes from the CRCM5 simulations with and without lakes suggest that the presence of lakes results in a dampening of projected increases to 2-m air temperature for all seasons almost everywhere in the study domain, with maximum dampening of the order of 2 °C occurring during winter, mostly in the vicinity of the lakes. As for streamflows, projected increases to spring streamflows, based on the simulation with lakes, are found to be smaller than that without lakes and this is due to the storage effect of lakes. Similarly, lower decreases in summer streamflows in future climate are noted in the simulation with lakes due to the gradual release of snowmelt water stored in lakes. An

additional CRCM5 transient climate change simulation with lakes and interflow, i.e. lateral flow in the soil layers, is compared with the simulation with lakes, but without interflow, to assess the impact of interflow on projected changes to regional climate and hydrology. Maximum interflow is projected to shift earlier in spring and the maximum interflow rate is expected to decrease by around 25 % in future. Results suggest that the impact of interflow on projected changes to precipitation, soil moisture and humidity are modest, even though the interflow intensity is changing noticeably in future climate. The impact of the interflow on projected changes to streamflows is in the range of $\pm 50 \text{ m}^3/\text{s}$. This study thus for the first time demonstrates the impact of lakes and interflow on projected changes to the regional climate and hydrology for the study region using a single regional modelling system.

3.1 Introduction

Inland water bodies, such as lakes and rivers, are essential for human livelihood (i.e. drinking water, agriculture, hydroelectricity, transportation), and this has led to many activities around lakes and rivers, which in turn resulted in the development of expensive and important infrastructure in the proximity of such water bodies. The safety and proper functioning of these infrastructures in the context of a changing climate is a major concern. For this reason, it is important to assess projected changes to the hydrological cycle and related uncertainties.

The Fifth Assessment Report of the Intergovernmental Panel on Climate Change concluded that there will be an intensification of the hydrological cycle in the future warmer climate. It was also reported that the frequency and intensity of extreme precipitation events have likely increased over North America and Europe since around 1950 (Hartmann et al., 2013) and that it will very likely increase over most mid-latitude land-masses in future climate (Collins et al., 2013). However, there is still little evidence that the changes in hydrological floods, i.e. high river flows, are affected by anthropogenic climate change. The low confidence is due to the lack of long-term records from unmanaged catchments. Nevertheless, based on recent trends in extreme precipitation and streamflows, some regions, primarily in the northern high latitudes (Hartmann et al., 2013), show higher flooding

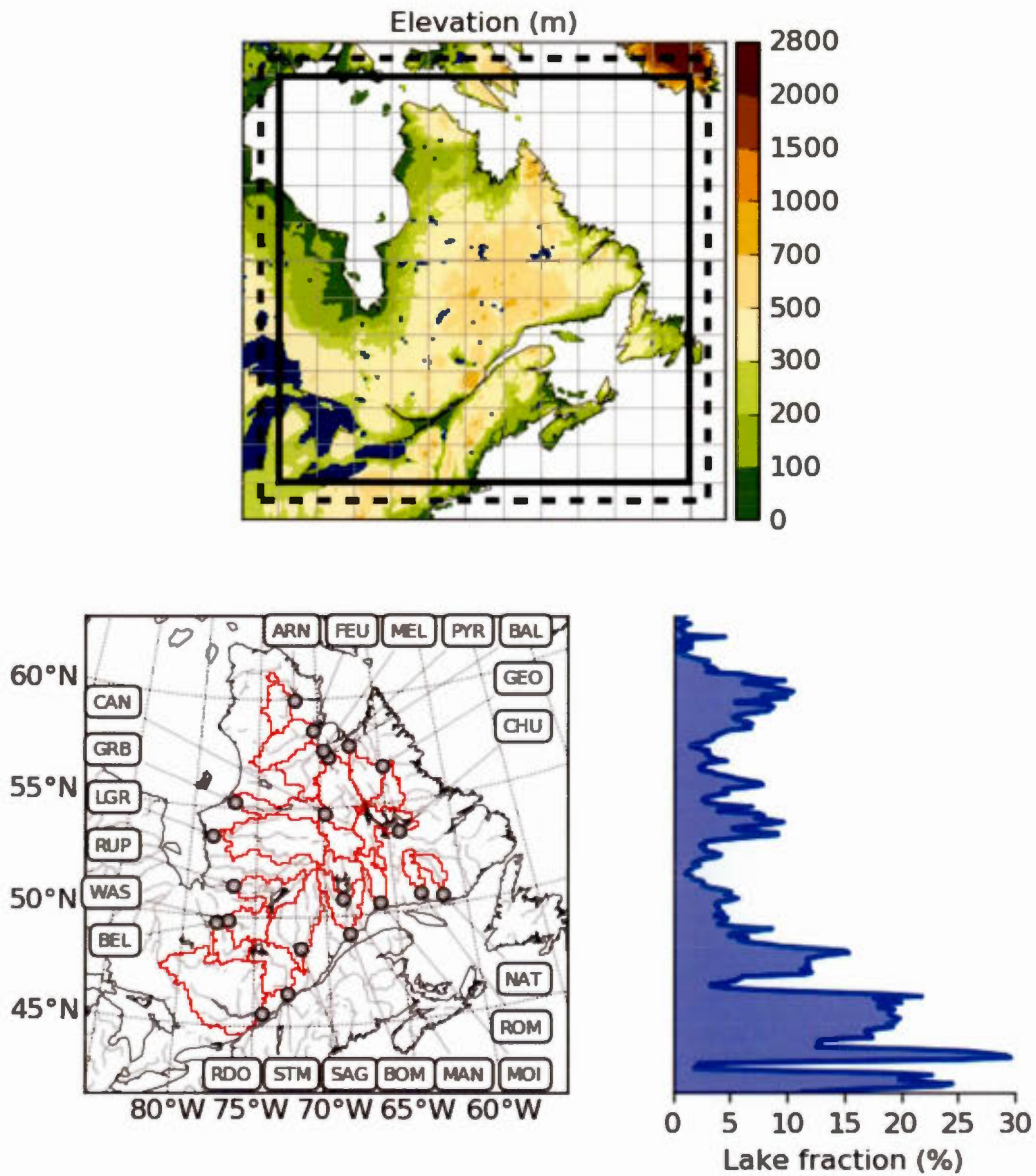


Figure 3.1: The simulation domain, with the topography shown in color. The black solid line separates the free zone from the blending zone, while the black dashed line separates the blending and outer halo zones. The grey lines show every 20th grid point. The bottom left panel shows the free domain with the basins of interest, while zonally averaged lake fractions are shown in the bottom right panel. The grey circles show basin outlets determined from the flow direction field used for streamflow simulation. Basin boundaries are shown in red.

risks. Recently, Huziy et al. (2013), using an ensemble of the fourth generation of the Canadian Regional Climate Model (CRCM4) climate change simulations, suggested significant increases to 10- and 30-year return levels of 1-day high flows for the northern part of Northeast Canada. However, the river routing scheme, used in Huziy et al. (2013), did not include lake-river interactions or interflow processes, and the CRCM4 did not represent lake-atmosphere interactions for sub-grid scale lakes. But these processes are important for the study region, abundant with lakes and rivers. Therefore, to further increase the confidence in, understanding, and correctly assessing the change in the probability of hydrological floods and droughts in future climate over such regions, a realistic representation of lakes and rivers, lake-river and lake-atmosphere interactions in climate models is important.

Lakes, due to their thermal inertia and water storage capacity, influence both regional climate and hydrology (Samuelsson et al., 2010; Martynov et al., 2012; Notaro et al., 2013b; Huziy and Sushama, 2015), leading to cooler (warmer) air temperatures in summer (fall and winter) and higher low flows in winter and attenuated spring peak flows. State-of-the-art regional climate models (RCMs) and some global climate models (GCMs) represent lakes using 1D column models (Dutra et al., 2010; Samuelsson et al., 2010; Martynov et al., 2012; Notaro et al., 2013a; Bennington et al., 2014). Two most commonly used lake models incorporated in GCMs and RCMs are FLake (Mironov et al., 2010) and Hostetler's model (Hostetler et al., 1993). The former is based on the concept of self-similarity of the vertical temperature profile below the mixed layer, while the latter, in order to establish the vertical temperature profile, solves the thermal diffusion equation and accounts for wind-driven mixing through enhanced thermal diffusion. The two models are found to perform reasonably well for shallow lakes (Martynov et al., 2012), although Martynov et al. (2012) pointed out that FLake underestimates the diurnal variability of the lake surface temperature and that Hostetler's model simulates too rapid spring warming in their study over North America. Dutra et al. (2010), based on their study at the global scale with Flake, highlighted the need for representing snow over lake ice in lake models. They suggest that snow over lake ice increases the lake ice cover duration compared to simulations without snow over lake ice, and leads to better climatology of lake ice cover duration. Furthermore, studies using the Hostetler's model for deep lakes report some

difficulties in representing vertical mixing (Gu et al., 2013; Bennington et al., 2014).

Although many climate models, particularly RCMs, include lakes, only few studies have attempted to realistically simulate the water balance of lakes, considering inflows and outflows of lakes, and the impact of lakes on streamflows. Huziy and Sushama (2015) recently implemented a river/lake routing scheme, interflow process, i.e. the lateral flow of water in the top soil layers along topographic slopes, and interactions between lakes and rivers in the fifth generation Canadian Regional Climate Model (CRCM5). By including lake routing, they noticed significant improvements to the simulated spring peak and winter low flows, which were too high and too low, respectively, without the lake-river interaction. The impacts of interflow on simulated streamflow and on the regional climate were modest according to their study. These new implementations in CRCM5 by Huziy and Sushama (2015) resulted in a more comprehensive tool for regional climate change studies that can be used to better understand interactions between atmosphere, lakes and rivers in the context of a changing climate.

This study therefore focuses on the projected changes to the regional climate and hydrology for northeastern Canada (Fig. 3.1) using CRCM5, and estimates the impacts of lake-river, lake-atmosphere interactions and of interflow on the projected changes to selected hydrologic and near-surface climate variables under the Representative Concentration Pathway 8.5 (RCP8.5). For this scenario, the concentration of greenhouse gases in the atmosphere continues to rise during the 21st century, causing an increase in the radiative forcing of 8.5 W/m^2 by 2100 with respect to the preindustrial period. The study domain (Fig. 3.1) covers 21 watersheds that are important for various economic activities (notably hydropower generation) and contain a large number of subgrid lakes for which the use of a 1D column lake model is appropriate. The zonal distribution of lakes in the region is shown in the bottom right panel of Fig. 3.1. It can be noted that mean lake fractions reach up to 20% in the southern and up to 10% in the northern regions.

The rest of the article is organized as follows. Section 2 describes models used in the study, i.e. the regional climate model, lake model and river routing approach, as well as the design and purpose of the conducted experiments. Results and

analysis are presented in section 3, followed by the summary and conclusions in section 4.

3.2 Models and methods

3.2.1 Model

The regional climate model used in this study is CRCM5, which is based on a limited-area version of the Global Environment Multiscale (GEM) model used for numerical weather prediction at Environment Canada (Côté et al., 1998). GEM employs semi-Lagrangian transport and a (quasi) fully implicit stepping scheme. In its fully elastic non-hydrostatic formulation (Yeh et al., 2002), GEM uses a vertical coordinate based on hydrostatic pressure (Laprise, 1992). The following physical parameterizations, inherited from GEM, are used in CRCM5: deep convection (Kain and Fritsch, 1990), shallow convection (Kuo, 1965), large-scale condensation (Sundqvist et al., 1989), correlated-K solar and terrestrial radiations (Li and Barker, 2005), and subgrid-scale orographic gravity-wave drag (McFarlane, 1987), low-level orographic blocking parameterization (Zadra et al., 2003, 2012) and planetary boundary layer parameterization (Benoit et al., 1989; Delage and Girard, 1992; Delage, 1997; Zadra et al., 2012).

The land surface scheme is the Canadian LAnd Surface Scheme (CLASS), version 3.5 (Versegny, 1991, 1996). This version of CLASS uses a flexible soil layering scheme, i.e. the number of soil layers and their thickness can be adjusted as required. CLASS includes prognostic equations for energy and water conservation for the three soil layers and a thermally and hydrologically distinct snowpack (treated as a variable-depth layer) where applicable. The thermal budget is performed over all soil layers, but the hydrological budget is done only for layers above the bedrock. The vegetation canopy in CLASS is treated explicitly with properties based on four vegetation types: needleleaf trees, broadleaf trees, crops and grass. CLASS adopts a pseudo-mosaic approach and divides each grid-cell into a maximum of four sub-areas: bare soil, vegetation, snow over bare soil and snow with vegetation. The energy and water budget equations are first solved for each sub-area separately and then averaged over the grid-cell. Detailed descrip-

tion of CRCM5 can be found in Martynov et al. (2013). CRCM5 has the option to use FLake or Hostetler model for lakes. In this study, lakes are represented by Hostetler's model (Hostetler et al., 1993; Martynov et al., 2012), where the vertical heat transfer is simulated by eddy conductivity and convective mixing. The lake ice and snow model is based on the modified Patterson and Hamblin (1988) formulation, and uses heat diffusion and energy balance equations to calculate snow and ice temperatures as well as ice melting and ablation (Martynov et al., 2012) (Martynov et al., 2012). Fractional ice cover is represented following Goyette et al. (2000). The Hostetler's model is selected, from the two available lake parametrizations, as it is more suited for water budget studies.

The river routing scheme, WATROUTE (Soulis et al., 2000), modified to include a ground water reservoir (Poitras et al., 2011), is used to simulate streamflows from runoff generated by CRCM5. The routing scheme solves the water balance equation at each grid cell, and relates the water storage to streamflow using Manning's equation (Te Chow, 1959). For lake routing, following Döll et al. (2003), lakes are classified into 2 types in this study: global, i.e. large lakes that occupy several grid cells, and local lakes, i.e. smaller lakes that occupy less than 60% of the grid cell area. Lake-river interaction is treated slightly differently for local and global lakes. Global lakes receive upstream river flow and runoff generated within the lake cells, while local lakes only receive runoff generated in the corresponding grid cell and influence downstream rivers, depending on how much water they store/release to the drainage network. Lake water balance is activated in the current study by taking into account precipitation and evaporation, lake ice, as well as river inflows and lake outflow. The outflow from both lake types is modelled as a function of the lake active storage. Initial lake depths are assigned from the global lake depth database developed by Kourzeneva (2010). An initial lake temperature of 4.2 °C is assumed everywhere, except for the top layer, where the initial temperature is assumed to be equal to the mean annual air temperature. The influence of lake level variation on lake temperature profile is neglected in this study. More detailed description of the river and lake routing schemes used in CRCM5 can be found in Huziy and Sushama (2015).

Interflow is represented in CLASS using Darcy's and continuity equations applied

to liquid soil moisture (Huziy and Sushama, 2015). This parameterization is activated when the volumetric fraction of liquid soil moisture exceeds the field capacity. Interflow is mostly active in spring during snowmelt and also during summer, when intense precipitation events saturate the soil.

3.2.2 Methods

Three transient climate change simulations driven by the second generation Canadian Earth System Model (CanESM2) and one simulation driven by ERA-Interim are considered in this study (Table 3.1). The ERA-Interim-driven simulation ERAI-CRCM5-L, i.e. the configuration including lakes and lake-river interactions but without interflow, is used to assess performance errors, i.e. errors due to the physics and dynamics of the model, by comparing with available observations. In this study, performance errors are assessed for mean seasonal 2-m temperature, total precipitation, snow water equivalent (SWE) fields and for climatologic hydrographs and selected high and low flow return levels at 6 gauging stations.

The Generalized Extreme Value (GEV) distribution is used to compute return levels of extreme (high and low) flow events. Following Huziy et al. (2013), the high (low) flow event is defined as the maximum (minimum) 1-day (15-day) flow occurring during the March to July (January to May) period. Ten- and 50-year return periods are considered for high flows, while 2- and 5-year return periods are considered for low flows. The choice of smaller return periods for low flows is based on the fact that a hydrological drought of 2-year return period is catastrophic enough to have an adverse impact not only on the hydropower sector, but also on the ecosystem, particularly the aquatic life (Smakhtin, 2001).

The return level, z , for a given return period T is computed using the following equations:

$$z(T, \mu, \sigma, \xi) = (\sigma/\xi) [(\ln T)^{-\xi} - 1] + \mu \quad (3.1)$$

$$z(T, \mu, \sigma, \xi) = (\sigma/\xi) \left[\left(\ln \frac{T}{T-1} \right)^{-\xi} - 1 \right] + \mu \quad (3.2)$$

where μ, σ, ξ are the parameters of the GEV distribution. Equations 3.1 and 3.2

yield the low and high flow return levels, respectively.

Performance errors associated with 2-m air temperature and total precipitation are estimated by comparing model outputs with 3 different gridded observation datasets: a) monthly UDel (Willmott and Matsuura, 1995) dataset at 0.5° resolution, available for the period 1901–2010; b) CRU TS 3.10 monthly dataset (Harris et al., 2014), with the same spatial resolution as UDel, available for the period 1900–2009 and c) 10 km resolution daily data from Hopkinson et al. (2011), available over Canada, south of 60°N , for the 1980–2010 period. The use of the three observation datasets will help assess the uncertainty associated with these observation datasets. Simulated snow water equivalent is validated using the daily analysis dataset from Brown et al. (2003), available for the period 1980–1996 at 0.25° resolution. Observed daily streamflows, used for validation, are provided by the Centre d’expertise Hydrique du Québec (CEHQ; <http://www.cehq.gouv.qc.ca>). Six unregulated gauging stations, with lakes upstream of these stations, are selected for validation of the simulated streamflow. The observed and modelled streamflows are compared over periods between 1980 and 2010 with continuous observation data.

Before looking at projected changes, boundary forcing errors, i.e. errors in the studied simulated variables due to errors in the driving data, are assessed by comparing the GCM-driven simulations in current climate with those driven by ERA-Interim. Boundary forcing errors are assessed for mean seasonal 2-m temperature, total precipitation, SWE and streamflow fields and for mean hydrographs, at selected basin outlets, by comparing CanESM2-CRCM5-L and ERAI-CRCM5-L simulations for the 1980–2010 period. Regions and seasons with large boundary forcing errors require high caution when interpreting model results, particularly projected changes.

The transient climate change simulations for the 1950–2100 period, i.e. CanESM2-CRCM5-NL, CanESM2-CRCM5-L and CanESM2-CRCM5-LI, are driven by CanESM2 at the lateral boundaries. In CanESM2-CRCM5-NL, lakes are replaced with land (bare soil), while lakes are represented by the Hostetler model in CanESM2-CRCM5-L and CanESM2-CRCM5-LI. This way the lake module is never called in CanESM2-CRCM5-NL, since all of the lake fractions are 0, and lakes do not

influence the regional climate and hydrology in this simulation. Since the routing scheme in CanESM2-CRCM5-L includes river-lake interactions, comparison of projected changes to the regional climate and hydrology based on CanESM2-CRCM5-L and CanESM2-CRCM5-NL will help assess the impact of lakes on projected changes to regional climate and hydrology, including streamflow. The third simulation CanESM2-CRCM5-LI is similar to CanESM2-CRCM5-L, and includes the interflow process parameterisation. Therefore, it is also used to study the interflow process in the current and future climates.

The analysis of projected changes is performed by comparing seasonal mean 2-m temperature, total precipitation, streamflow fields and climatologic hydrographs, at selected basin outlets for the 2070–2100 period with those for the 1980–2010 period, from the CanESM2-CRCM5-L simulation. Since the projected changes obtained with CanESM2-CRCM5-LI are very similar to that of CanESM2-CRCM5-L, only results from CanESM2-CRCM5-L are presented. Statistical significance of the projected changes is assessed using Welch’s t-test, i.e. the generalization of the Student’s t-test, which does not assume equal variances of the compared samples (Welch, 1947), at the 5% significance level. Statistical significance of the projected changes to the high and low flow return levels at the 5% significance level is determined using the non-parametric vector bootstrap resampling method (Khaliq et al., 2009).

All CRCM5 integrations are performed over a 260×260 points grid covering north-east Canada as shown in Fig. 3.1, at 0.1° horizontal resolution and with 56 hybrid vertical levels in the atmosphere. The boundaries of 21 selected watersheds that are considered in this study are also shown in this figure. More details about the watersheds are summarized in Table 3.2. All analysis, presented here, is performed for the inner free zone of 220×220 grid-points, excluding the halo and blending zones (20 points on each side). The halo zone (the outer 10 points) provides interpolated driving data for the semi-Lagrangian interpolation. The blending zone (the 10 points between the halo and the free zones) is the Davies sponge zone where the CRCM5 atmospheric fields are damped toward the driving fields. Since no additional nudging is used, the driving fields influence CRCM5 simulations only through the values in the halo and the blending zones. For the land surface

No.	Simulation	Period	Pilot data	Configuration
1	ERA1-CRCM5-L	1979–2010	ERA-Interim	With interactive lakes and lake routing
2	CanESM2-CRCM5-NL	1950–2100	CanESM2	No lakes, no lake routing
3	CanESM2-CRCM5-L	1950–2100	CanESM2	With interactive lakes and lake routing
4	CanESM2-CRCM5-LI	1950–2100	CanESM2	With interactive lakes, lake routing and interflow

Table 3.1: List of simulations used in the current study.

scheme CLASS, a 26-layer soil configuration reaching 60 m is used. The fractional areas of the four plant functional types considered in CLASS are specified using the USGS-GLCC dataset. The soil composition (sand, clay) and depth to bedrock are taken from Webb et al. (1993). Lake fractions are based on the Global Land Cover Characteristics (GLCC) dataset. Flow directions and other parameters used for routing are derived from the HydroSHEDS dataset (Lehner et al., 2008). All geophysical fields used in the study are the same as in Huziy and Sushama (2015).

Initial conditions for the soil temperature and soil water content (liquid and solid) are obtained by running CLASS offline for 300 years using atmospheric forcing from ERA40 reanalysis data (Uppala et al., 2005) for the 1961–1970 period recursively, for the ERA1-CRCM5-L simulation. For the CanESM2-driven simulations, initial conditions are obtained in a similar fashion, but using atmospheric forcing for the 1961–1970 period from a coarse resolution CRCM5 simulation driven by CanESM2. The depth of the modelled soil column justifies the long spinup period. The sea ice cover and sea surface temperatures are prescribed from ERA-Interim and CanESM2, for ERA-Interim-CRCM5-L and CanESM2-driven simulations, respectively.

No.	Name of the watershed	Abbreviation	Area (km ²)
1	Arnaud	ARN	26,712
2	Feuilles	FEU	41,078
3	Mélèzes	MEL	41,897
4	Caniapiscou	CAN	29,665
5	Caniapiscou (Pyrite)	PYR	87,290*
6	Grande rivière de la Baleine	GRB	34,451
7	Baleine	BAL	29,340
8	George	GEO	24,058
9	Churchil Falls	CHU	44,977
10	La Grande Rivière	LGR	95,914
11	Natashquan	NAT	15,456
12	Romaine	ROM	12,241
13	Moisie	MOI	18,917
14	Manicouagan	MAN	29,181
15	Rupert	RUP	39,687
16	Bell	BEL	23,700
17	Saint Maurice	STM	41,919
18	Ottawa	RDO	143,039
19	Saguenay	SAG	71,655
20	Bersimis-Outardes-Manic	BOM	64,904*
21	Waswanipi	WAS	30,267

Table 3.2: Names, abbreviations and drainage areas (km²) of the studied watersheds; the areas are calculated based on the flow direction field. The asterisk (*) indicates compound basins (PYR contains CAN and MAN is a sub-basin of BOM).

3.3 Results

3.3.1 Performance and boundary forcing errors

To assess the performance errors for 2-m air temperature and precipitation fields, simulated air temperature and precipitation are compared with gridded observation datasets for the 1980–2010 period. When comparing model outputs with the lower resolution datasets CRU and UDel, model outputs are upscaled to the same resolution. Since the performance errors obtained when comparing with CRU and UDel are very similar, only CRU comparisons are shown here. In addition, comparison with a higher resolution dataset from Hopkinson et al. (2011) is also shown (Figs. 3.2 and 3.3). Performance errors based on the higher and lower resolution datasets are in general similar, although the errors, based on Hopkinson et al. (2011), are somewhat smaller both for 2-m temperature and precipitation fields, with the exception of summer precipitation. CRCM5 overestimates winter and summer mean temperatures by about 1.6°C (1.1°C) and 0.5°C (0.8°C), respectively, compared to CRU- based (Hopkinson-based) dataset (Fig. 3.2). Neg-

ative biases appear mainly in the northern part of the domain during spring and fall, mostly due to the overestimation of snow albedo. This overestimation of snow albedo is noted when compared to that from the MODIS dataset (figure not shown). Performance errors in precipitation are mostly positive, with the exception of small regions near the western and southern boundaries of the study domain during summer and fall seasons (Fig. 3.3). Very modest negative biases in precipitation can be seen in winter as well. The area-averaged seasonal precipitation biases over the free zone, when compared to CRU, range from 0.3 mm/day

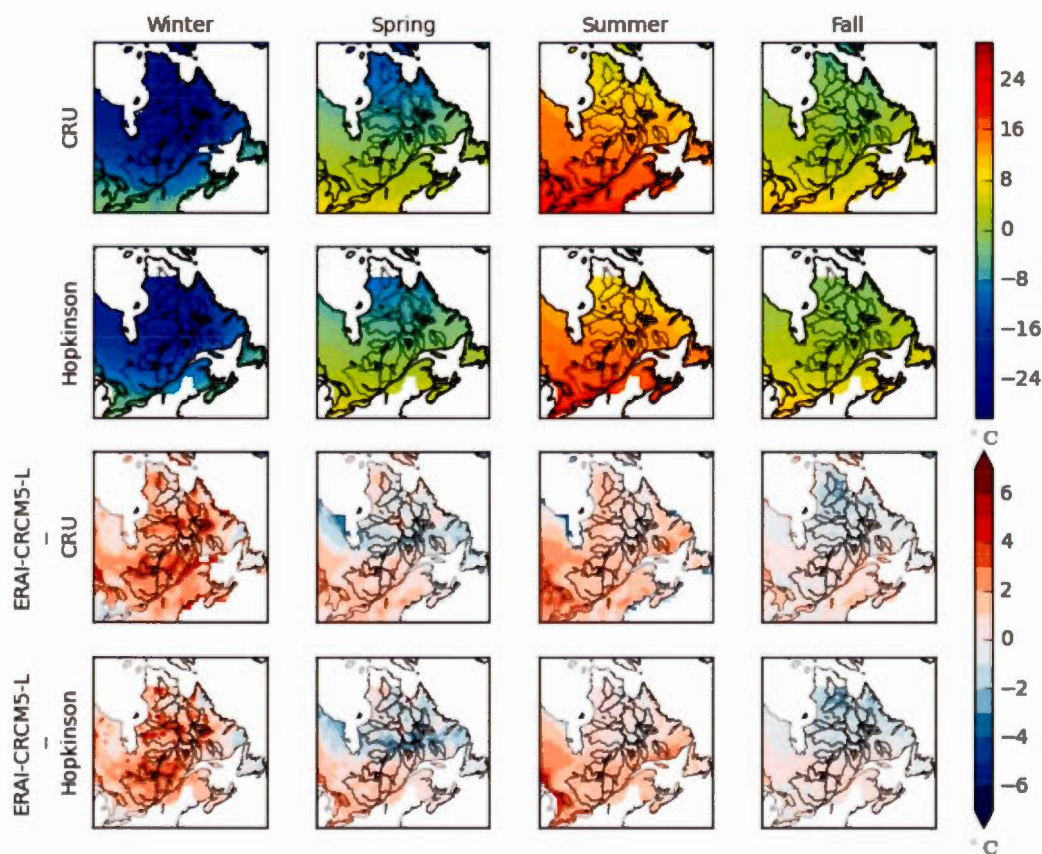


Figure 3.2: Seasonal mean 2-m air temperature [$^{\circ}\text{C}$] from CRU (first row), Hopkinson et al. (2011) (second row) and the differences between ERAI-CRCM5-L and CRU (third row) and ERAI-CRCM5-L and Hopkinson et al. (2011) (fourth row), for the 1980–2010 period. CRU values are masked over the Great Lakes, since station data from over the lakes were not used to produce this dataset.

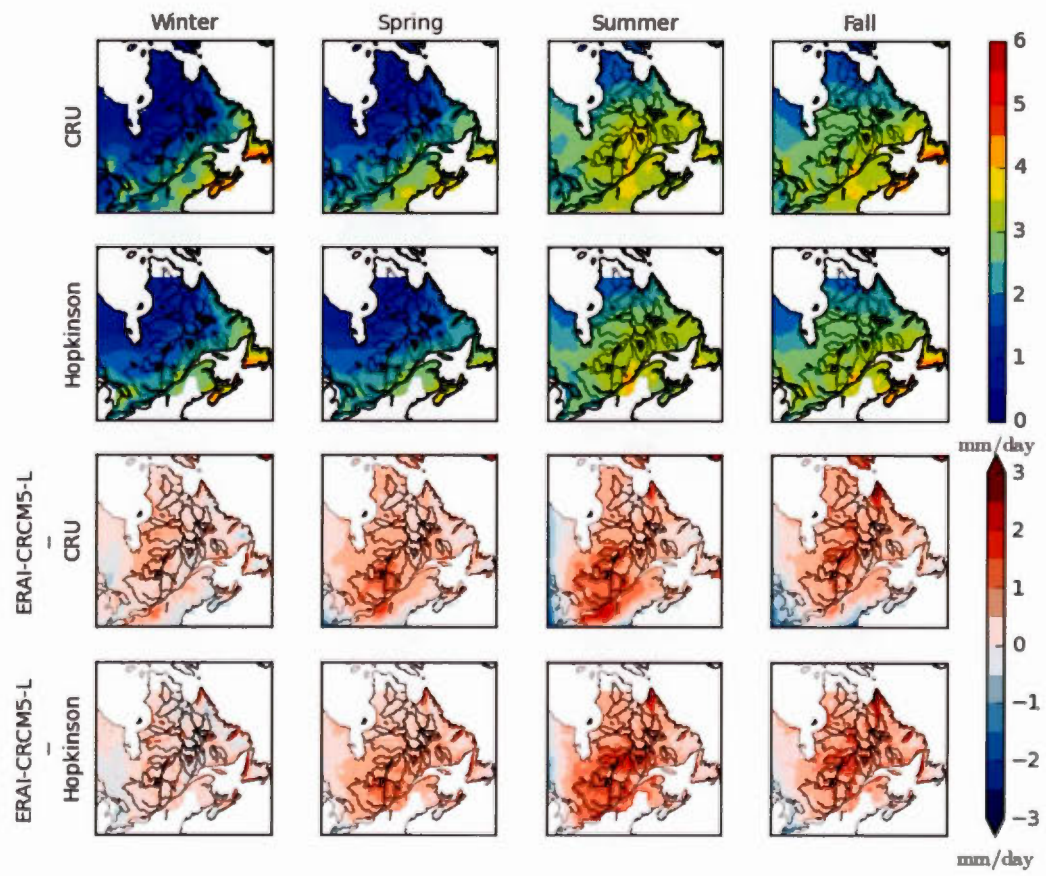


Figure 3.3: Same as in Fig. 3.2 but for the total precipitation in mm/day.

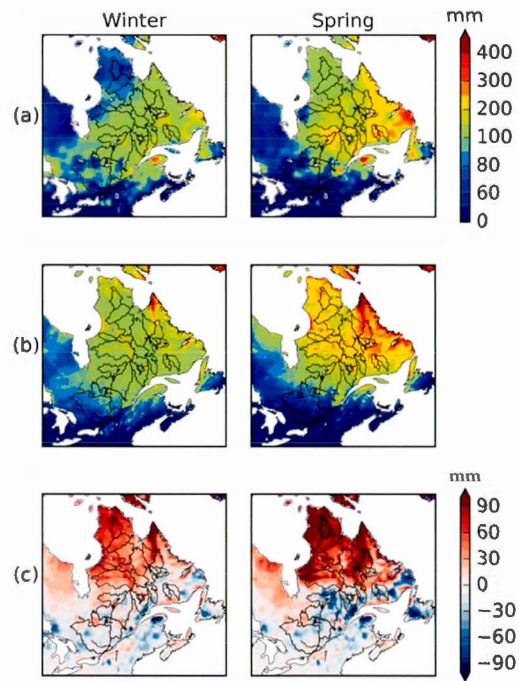
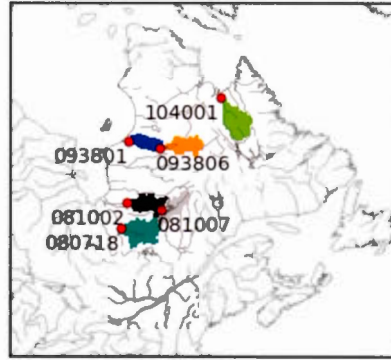


Figure 3.4: Observed (from Brown et al. (2003); top panels) and ERAI-CRCM5-L simulated (middle panels) SWE [mm] for winter and spring for the 1980–1996 period. Differences between ERAI-CRCM5-L simulated SWE and that observed are shown in the bottom panels for the same period.

(a)



(b)

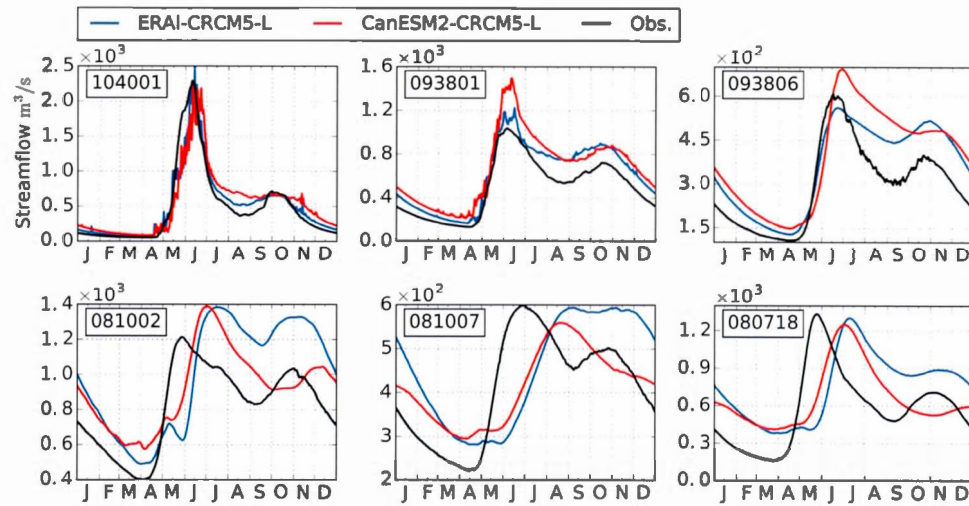


Figure 3.5: (a) Locations and identification numbers (IDs) of the gauging stations considered for validation, with their upstream areas (determined from the flow directions field) shown shaded. (b) Comparison of observed (black) and modelled (blue and red correspond to ERAI-CRCM5-L and CanESM2-CRCM5-L simulations, respectively) mean annual hydrographs [m^3/s] at selected stations. The analysed time intervals are based on the availability of observation data during the 1980–2010 period.

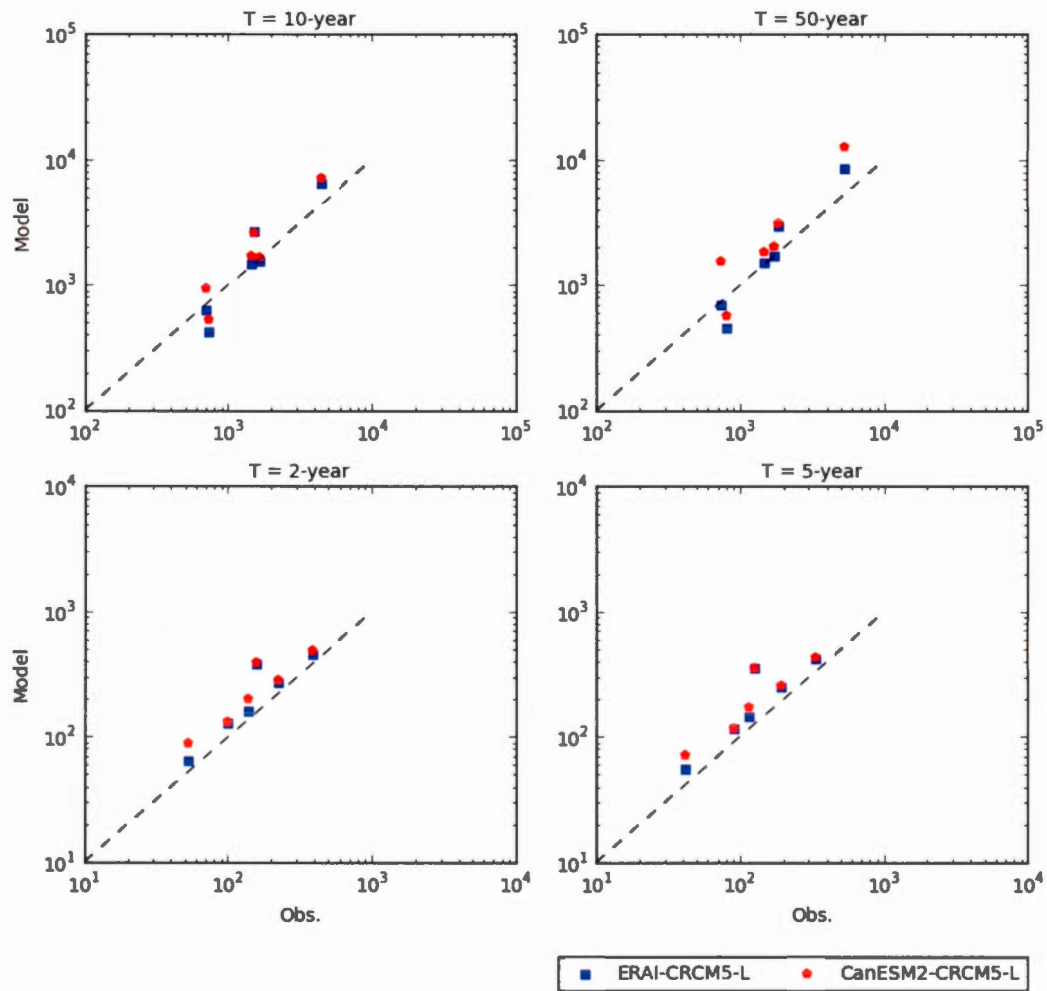


Figure 3.6: Scatter plots of 10- and 50-year observed and modelled return levels of 1-day high flow (top panels) and 2- and 5-year observed and modelled return levels of 15-day low flow, at the six selected gauging stations shown in Fig. 3.5.

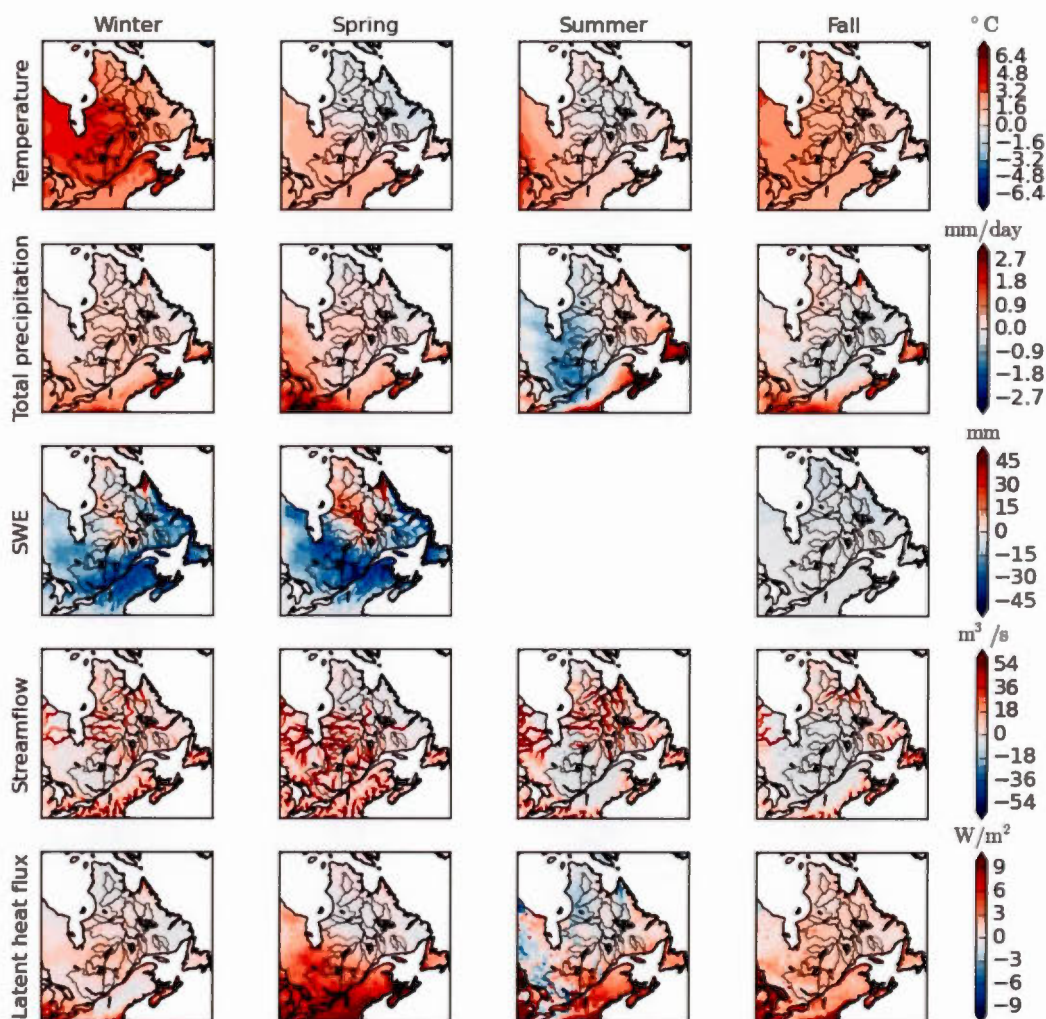


Figure 3.7: Boundary forcing errors, i.e. differences between CanESM2-CRCM5-L and ERAI-CRCM5-L simulations for the 1980–2010 period, for 2-m air temperature [°C] (first row), total precipitation [mm/day] (second row), SWE [mm] (third row) and streamflows [m³/s] (fourth row).

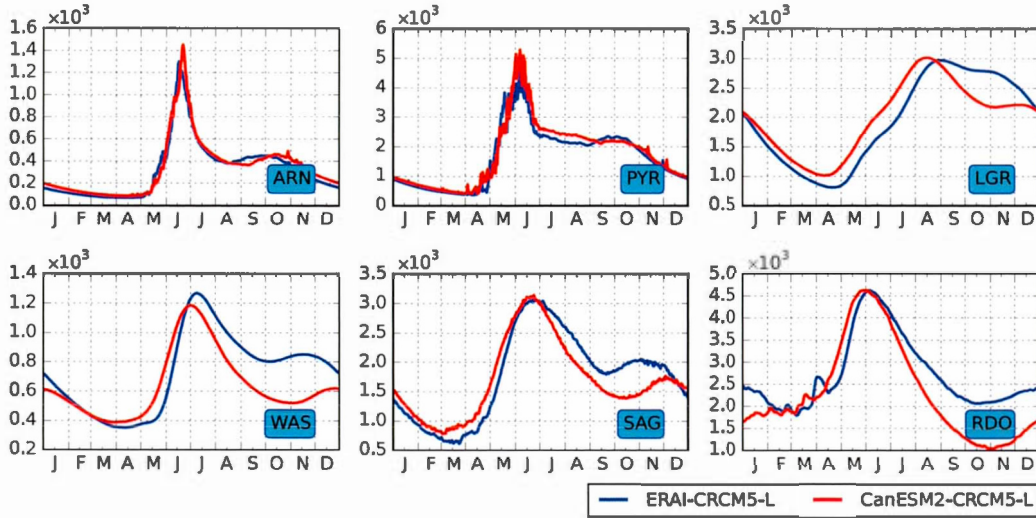


Figure 3.8: Simulated mean annual hydrographs [m³/s] for the reanalysis-driven ERAI-CRCM5-L (blue) and the GCM-driven CanESM2-CRCM5-L (red) simulations, for the period 1980–2010, at the outlets of the WAS, SAG, RDO, PYR, LGR and ARN basins.

(14%) in winter to 0.5 mm/day (17%) in summer. The area-averaged biases, based on Hopkinson et al. (2011), vary from 0.1 mm/day (6%) in winter to 0.7 mm/day (24%) in summer.

The ability of the model in capturing the inter annual variability in 2-m air temperature and precipitation fields is assessed by comparing modelled standard deviations for different seasons with those from the Hopkinson’s dataset (figure not shown) over the 1980–2010 period. The 2-m air temperature variability, over the land points where observation data are present, is underestimated in winter (by -17%), spring (-10%) and fall (-8%), and overestimated in summer (9%). The errors associated with precipitation variability are lower in winter and fall (-5% and 5% respectively) and higher in spring and summer (25% and -20% respectively).

The modelled trends are validated using temporal correlations of the observed and modelled time series for each season. The correlations of the area-averaged observed and modelled seasonal time series are very reasonable, with values in the 0.98 to 0.99 range for 2-m air temperature, and between 0.76 and 0.90 for precipitation.

The SWE errors (Fig. 3.4) exhibit a north-south dipole pattern in winter and spring, with strong positive performance errors in the northern and much weaker negative performance errors in the southern part of the domain. Winter SWE overestimation in the northern part of the domain is related to the overestimation of precipitation. The southerly biases in SWE during winter could be explained by the late onset of snow due to the temperature overestimation in the model. Similarly, spring SWE is overestimated in the north, due to precipitation overestimation and spring temperature underestimation. Negative performance errors in SWE during spring are related to the overestimation of the 2-m air temperature in the southern part of the study region in spring. These SWE errors will be reflected in the spring streamflows, which are almost entirely associated with snowmelt.

The location of the six gauging stations, selected for the assessment of performance errors associated with streamflows, along with the drainage area upstream of the gauging stations are shown in Fig. 3.5a. The performance errors can be assessed by comparing the ERAI-CRCM5-L simulated hydrographs with those observed (Fig. 3.5b). The timing of the spring peak flows of the 3 northern stations (104001, 093801, 093806) are well captured, while the peaks are delayed for the other 3 southerly stations (081002, 081007, 080718). Despite the overestimation of SWE in ERAI-CRCM5-L for the northern regions, the simulated timing and magnitude of spring peak flow agree well with that observed for the 3 northern stations. The biases are larger for the post snowmelt period. This is because the lakes store the snowmelt, which is overestimated in ERAI-CRCM5-L, and release it gradually after the snowmelt period. The precipitation overestimation (post snowmelt) also contributes to the biases during this period. The same explanation holds for the southern stations for the post-snowmelt period. A systematic delay in the timing of spring peak flows can be noted for the southern stations. This delay can be partly explained by the excessive infiltration occurring during the melting period. A summary of the annual streamflow biases and correlations with observed hydrographs is given in Table 3.3.

Finally, the ability of the model to reproduce extreme events is evaluated by comparing return levels derived from observed extreme flows and from those simulated

Station	Simulation			
	ERA-Interim-CRCM5-L		CanESM2-CRCM5-L	
	Annual bias (%)	Correlation coefficient	Annual bias (%)	Correlation coefficient
104001	5	0.96	13	0.90
093801	23	0.91	34	0.87
093806	24	0.98	36	0.98
081002	22	0.65	12	0.74
081007	10	0.47	1	0.66
080718	31	0.30	15	0.51

Table 3.3: Annual mean biases [%] and correlations for the mean hydrographs at the 6 selected stations compared to those observed. All the correlation coefficients are significant at the 1% significance level

by ERA-Interim-CRCM5-L at the same 6 gauging stations (Fig. 3.6). Although generally the return levels are well captured, similarly to mean hydrographs, the low flow return levels are overestimated for all stations and the high flow return levels are slightly underestimated for 2 of the 6 stations. The mean bias in the modelled 10- and 50-year return levels for high flows is 12%, while those associated with the 2- and 5-year low flow return levels are 42% and 53% respectively.

From the comparison of the 2-m air temperature, total precipitation and SWE fields along with streamflow from CanESM2-driven and reanalysis-driven simulations, it is possible to get some useful insights on the impact of errors in the driving data. The spatial plots of the differences between CanESM2-driven and ERA-Interim-driven simulations, i.e. boundary forcing errors, for the studied domain for the 4 seasons are shown in Fig. 3.7. From this figure, it can be noted that 2-m air temperature is associated with positive boundary forcing errors, except during spring and summer when negative boundary forcing errors are noted for the northern regions. The positive boundary forcing error in the screen level temperature is in agreement with previous studies over North America performed using CRCM5, driven by CanESM2, at a coarser resolution (Šeparović et al., 2013; Garneau and Sushama, 2015). The positive boundary forcing errors in 2-m air temperature in winter and spring (for the southern regions) leads to negative boundary forcing errors in SWE during these months. Although the boundary forcing errors in mean winter and spring SWE are negative, positive boundary forcing errors in streamflows are obtained during these seasons (Fig. 3.7), due to enhanced melting in the CanESM2-driven simulation. The earlier start of the melting season, in the CanESM2-driven simulation, results in the slightly ear-

lier occurrence of the spring peak in CanESM2-CRCM5-L simulated hydrographs (Fig. 3.8).

The spatial pattern of the boundary forcing errors of streamflow seems to follow the boundary forcing errors in total precipitation during summer and fall in the southern watersheds (Fig. 3.7). The negative boundary forcing errors during fall are more evident when comparing climatologic hydrographs at selected basin outlets for the CanESM2 and ERA-Interim driven simulations (Fig. 3.8). The positive boundary forcing errors in 2-m air temperature fields during fall could also contribute to the negative boundary forcing errors in streamflow through enhanced evaporation, which leads to smaller runoff. For example, higher temperatures and lower precipitation in the CanESM2-driven simulation in summer lead to negative boundary forcing errors in streamflow during summer and later during fall, with respect to the reanalysis-driven simulation (Fig. 3.5b). Similarly to the negative boundary forcing errors in mean hydrograph during winter and end of spring in CanESM2-CRCM5-L (Fig. 3.5b), the return levels, both of high and low flows, from the CanESM2-driven simulations show small positive boundary forcing errors with respect to ERA-Interim-driven simulation almost for all stations (Fig. 3.6).

In general, the signs of the boundary forcing (Fig. 3.7) and performance errors are the same, except for summer precipitation when boundary forcing errors are negative (Fig. 3.7) and performance errors are positive over the eastern part of the domain. This is reflected in the simulated streamflow in the CanESM2-CRCM5-L configuration. During summer and fall, streamflow from CanESM2-CRCM5-L configuration is often closer to the observations than that from the ERA-Interim-driven configuration (Fig. 3.5b), probably due to compensation of the errors.

3.3.2 Projected regional climate and streamflow changes

Projected changes based on the CanESM2-CRCM5-L transient climate change simulation are presented here for selected variables (Fig. 3.9). A comparison between future (2070–2100) and current (1980–2010) climates suggests projected increases of mostly up to 10°C for 2-m temperature in winter, and these changes are significant over the entire landmass. Summer temperatures are also projected

to increase over the entire domain generally in the 6–9°C range. The summer and fall changes are more uniform, compared to the winter period, when the northern regions are projected to have higher increases in temperature compared to the

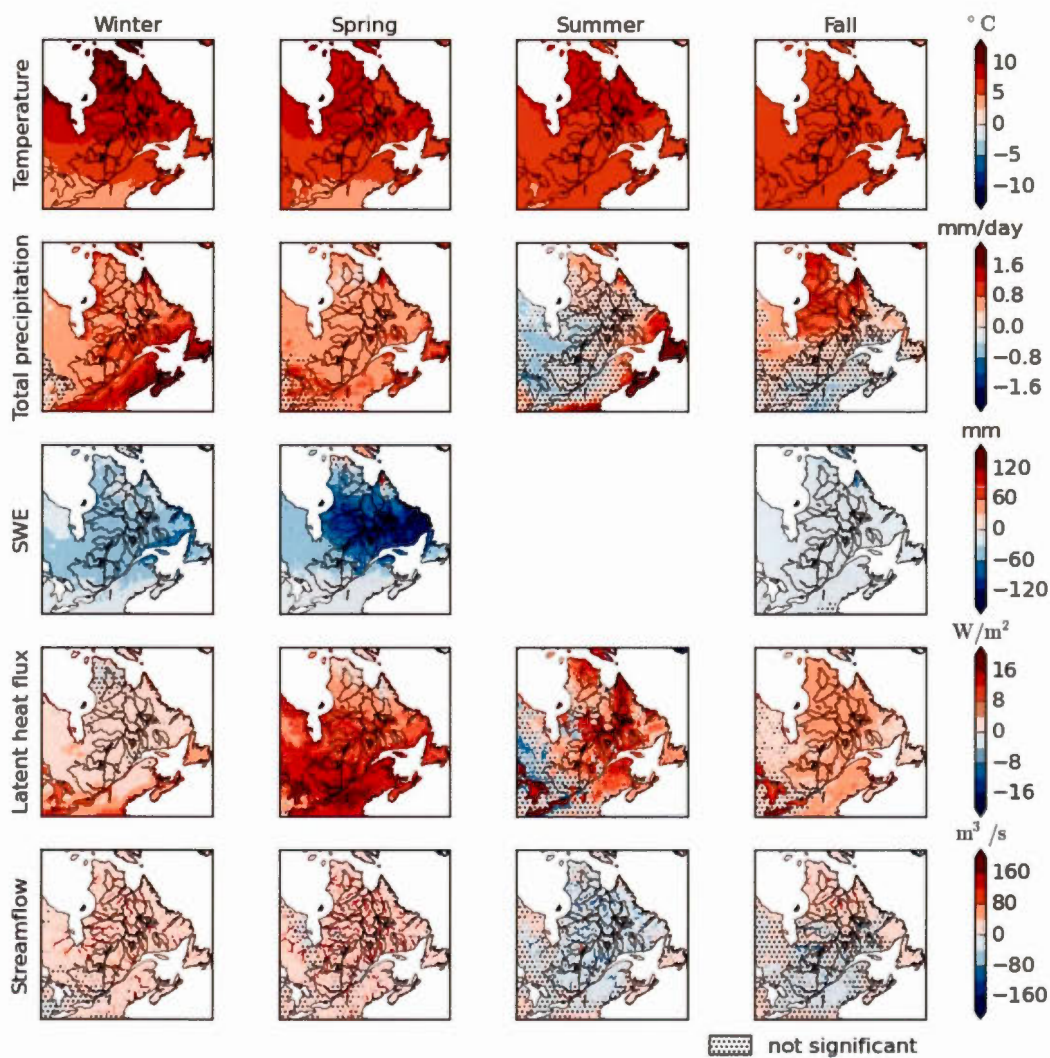


Figure 3.9: Projected changes for the 2070–2100 period with respect to the 1980–2010 period to 2-m temperature [°C], total precipitation [mm/day], SWE [mm], latent heat flux [W/m²] and streamflows [m³/s]; the grid-cells where the changes are not significant at the 5% significance level are indicated with dots. The changes are based on CanESM2-CRCM5-L simulation results between 1980–2010 and 2070–2100 periods.

southern regions. The lowest increases to 2-m air temperature are projected to occur in fall, which is around 5.8°C on average.

Winter and spring precipitation is projected to increase in future climate and the increase is significant everywhere, except for a small region to the southwest of the domain. In summer, changes to precipitation are mostly not significant, except

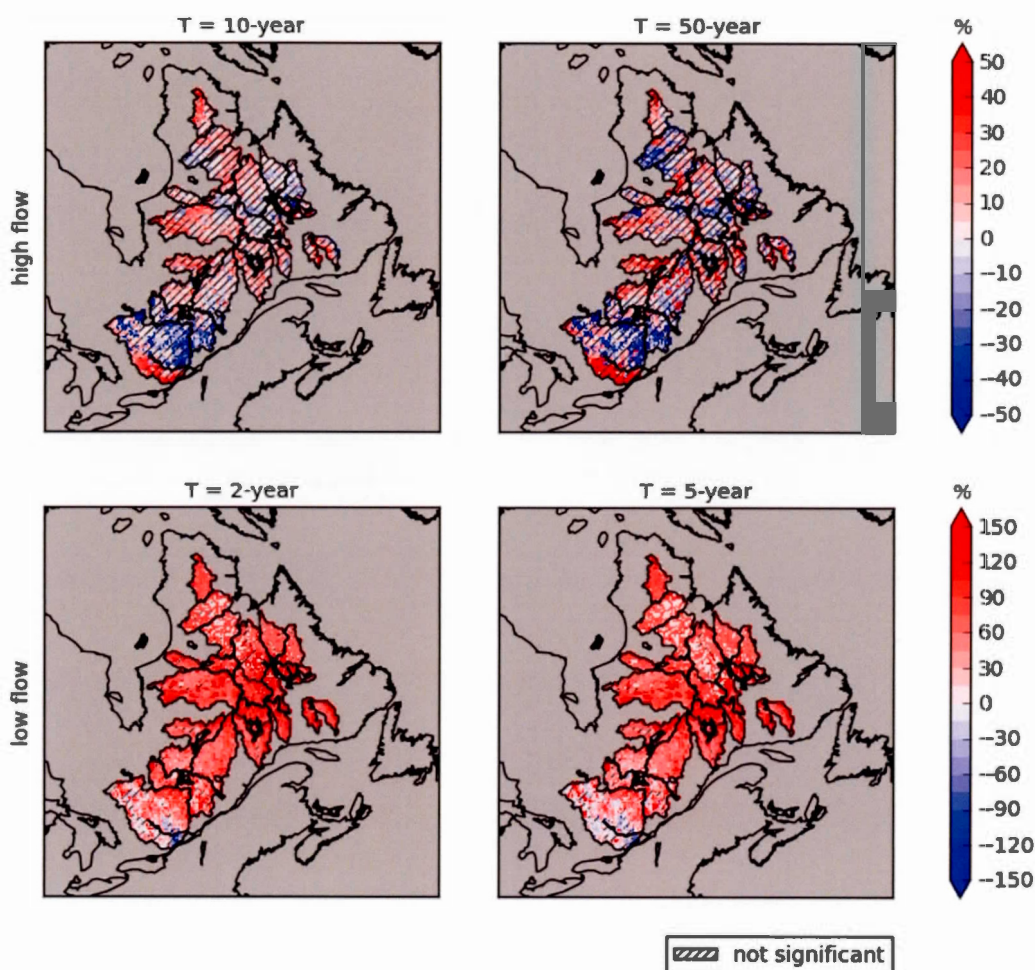


Figure 3.10: Projected changes for the 2070–2100 period with respect to the 1980–2010 period to the 10- and 50-year return levels of 1-day high flow (upper panel) and of 2- and 5-year return levels of 15-day low flow (bottom panel) for CanESM2-CRCM5-L. Changes that are not significant at the 5% significance level (evaluated using bootstrap procedure) are hatched over.

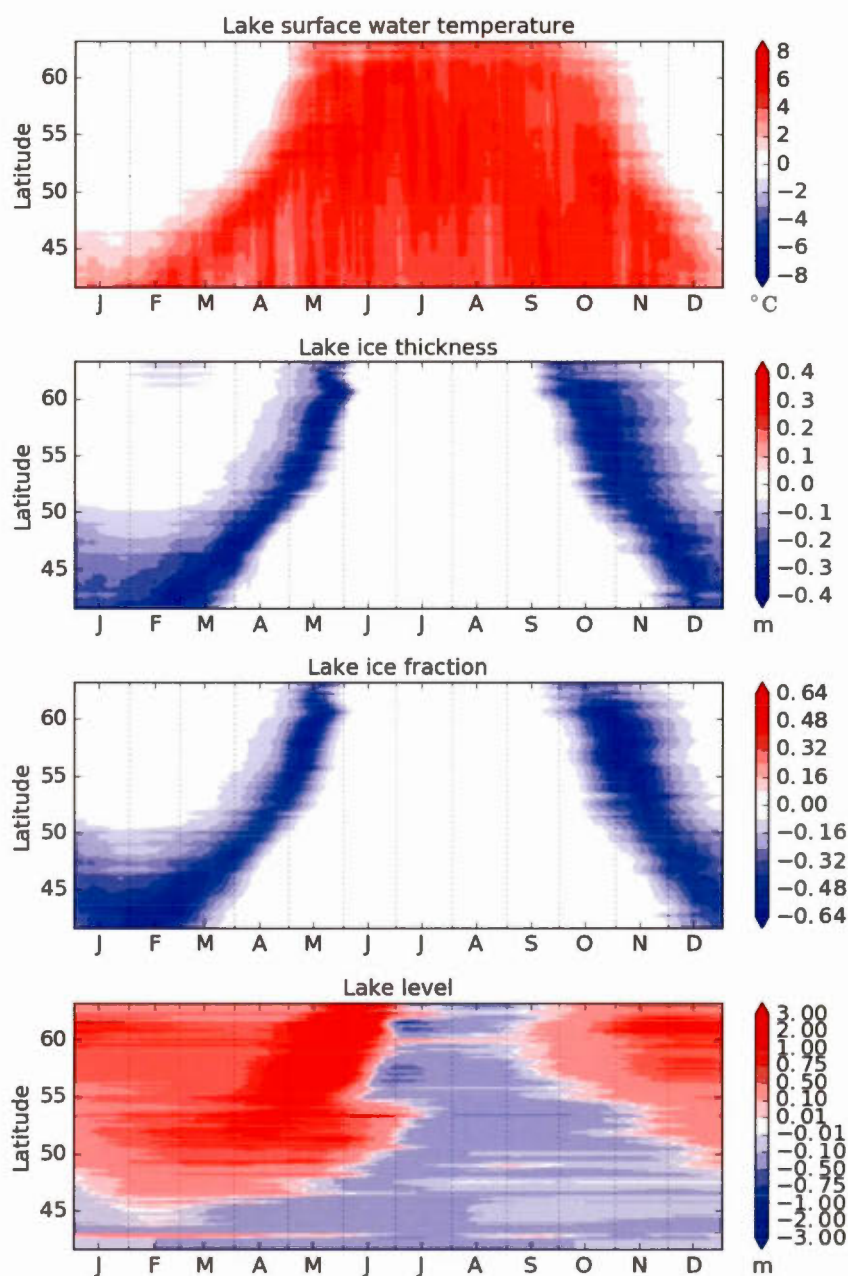


Figure 3.11: Zonally averaged projected changes to (a) lake surface water temperature, (b) lake ice thickness and (c) fraction of lake ice and (d) lake levels for the period 2070–2100 with respect to 1980–2010 from the CanESM2-CRCM5-L simulation.

over eastern Atlantic coastal regions and ARN watershed, where positive changes are obtained, and to the south of Hudson Bay, where some significant decreases in precipitation are noted. The change in fall precipitation is only significant for the northern half of the region of interest. All significant precipitation changes are positive during all seasons except summer, when positive and negative significant changes are noted. The summer decreases in precipitation are mostly due to the decreased evaporation in the southwest part of the domain.

Higher air temperatures in winter and spring in future climate lead to reduced snow cover duration, due to the late onset and early melt of snow. Though winter precipitation increases, winter SWE is projected to decrease everywhere over the study domain due to the higher rain to snow ratio during winter in the future climate. This is reflected in the projected changes to streamflows, which show increases in the future climate. Spring streamflows are also projected to increase due to increased spring precipitation and possibly due to earlier snowmelt in the future climate. Streamflows are mostly projected to decrease due to reduced precipitation, in the western and central parts of the domain, and increased evaporation, in the central and northern parts of the domain, during summer in the future climate. Projected changes to fall streamflows exhibit a dipole pattern, with increases in the northern regions and decreases in the southern regions, resembling the spatial pattern for projected changes to precipitation.

Projected changes to extreme flow characteristics, i.e. 10-year and 50-year return levels of 1-day high flows, and 2-year and 5-year return levels of 15-day low flows, simulated by CanESM2-CRCM5-L are shown in Fig. 10. Almost no significant changes to high flow return levels are detected for future climate. The changes to the low flow return levels are mostly positive and significant at the 5% significance level over all studied watersheds. The increases to the low flow return levels are mostly above 45%. However, small regions, where the changes are less than 15%, appear in the northernmost and southernmost parts of the domain. The smaller positive changes to the low flow return levels there could be explained by the smaller decreases in winter SWE and lower increases in spring precipitation (Fig. 3.9), which influence groundwater contribution to streamflow during frozen conditions, over the northernmost part of the domain. Some decreases to the

low flow return levels are noted in the southern part of the domain in CanESM2-CRCM5-L, which might indicate reduced groundwater contribution to streamflows during low flow periods at those points in future climate due to enhanced summer evaporation and reduced summer and fall precipitation. At the basin scale, mean projected changes to the 10-year and 50-year return levels of high flows range from -12% and -16% in the STM basin to 15% and 22% in the ARN and RUP basins, respectively. The basin scale mean projected changes to the 2-year and 5-year return levels of low flows range from 34% and 26% in the RDO basin to 105% and 110% in the ROM and MAN basins, respectively.

Huziy et al. (2013) also assessed projected changes to return levels of low and high flow events, using runoff from an ensemble of a previous generation of the CRCM (CRCM4) simulations over a similar region, northeast of Canada. The spatial resolution of the simulations used in that study was 45 km. The 10-year return levels of 1-day high flows were projected to increase significantly only for the northernmost part of the domain in that study. The results for the 30-year return levels of 1-day high flows were similar to those of the 10-year return levels, although the regions of significant changes were smaller. As for the return levels of 15-day low flows corresponding to 2- and 5-year return periods, the changes were greater than 80% almost everywhere except for some northern basins, and parts of RDO and BOM.

Projected changes to selected lake variables such as the zonally averaged lake water temperature, lake ice thickness and lake ice cover are discussed now (Fig. 3.11). The temperature of the surface layer in lakes is projected to increase in future climate. The mean increase is around 6°C in summer and fall and mostly less than 1°C in winter, with the exception of southern regions where the winter warming vary between 2 to 5°C. The winter lake ice cover fraction and thickness are projected to decrease on average by about 0.17 and 10 cm, respectively. These changes to the lake variables are expected to cause enhanced latent heat flux during all seasons (Fig. 3.9) in the future climate. The sensible heat flux is mostly projected to decrease over lakes, during summer (figure not shown). This decrease could be explained by the smaller increase in the lake water temperature, compared to the increase in the air temperature, which leads to lower temperature

gradients between surface and overlying air during warm seasons.

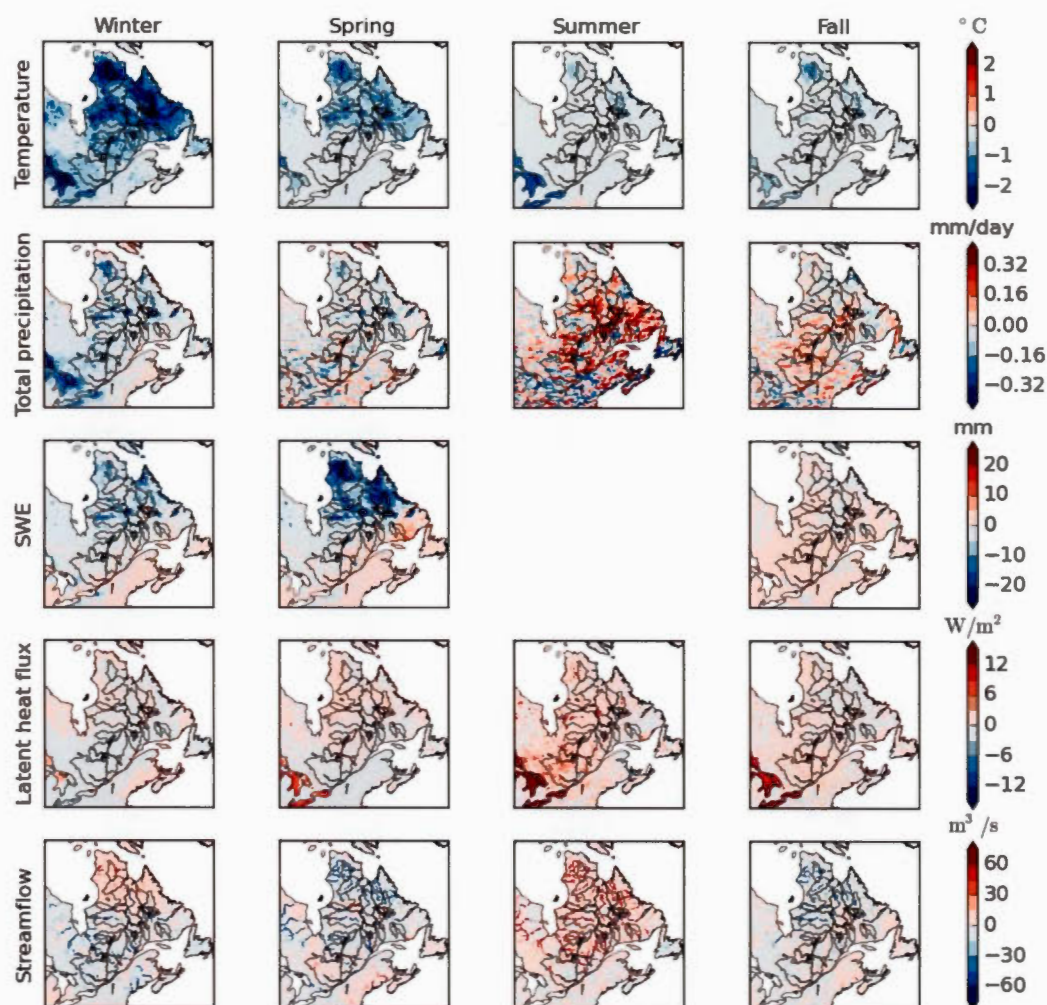


Figure 3.12: Impact of lakes on projected changes for the period 2070–2100 with respect to the period 1980–2010 (i.e. differences between projected changes based on CanESM2-CRCM5-L and CanESM2-CRCM5-NL projected changes) to seasonal mean 2-m air temperature [°C], total precipitation [mm/day], SWE [mm], latent heat flux [W/m²], streamflow[m³/s].

3.3.3 Influence of lakes on projected climate change

To study the influence of lakes on climate change simulated by CRCM5, the projected changes from CanESM2-CRCM5-L (with lakes) and CanESM2-CRCM5-NL (without lakes) are compared. It must be noted that the projected changes to the variables considered below, generally have the same sign in both CanESM2-CRCM5-L and CanESM2-CRCM5-NL. As expected, due to the high thermal inertia of lakes, an attenuation of the projected increases in 2-m temperature is noted for all seasons (Fig. 3.12), especially for the northern part of the domain during winter, where the projected increases to 2-m temperature are the highest. The area-averaged attenuation of projected increases to 2-m air temperature by lakes range from 1°C in winter to 0.2°C during fall.

The projected increases in winter precipitation are smaller in CanESM2-CRCM5-

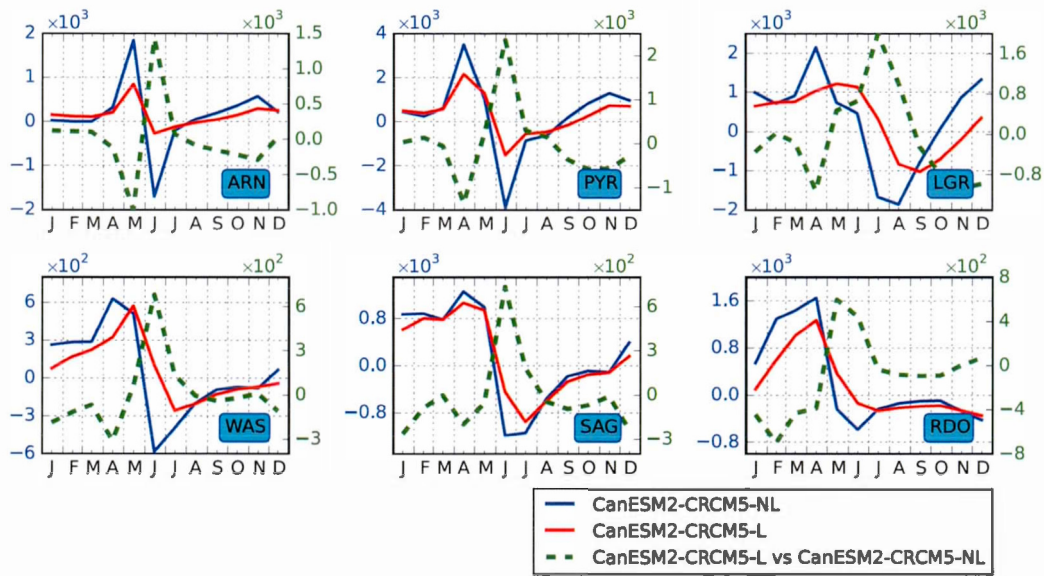


Figure 3.13: Projected changes to mean hydrographs at the outlets of the ARN, PYR, LGR, WAS, SAG, RDO basins for CanESM2-CRCM5-NL (blue) and CanESM2-CRCM5-L (red) simulations and the difference in projected changes (green). Northern (southern) basins are shown in the top (bottom) panel. All values are in m^3/s . The left axis indicates projected changes (red and blue lines) and the right axis indicates differences in projected changes.

L compared to CanESM2-CRCM5-NL. This attenuation in the projected increases in total precipitation is due to the smaller increase in temperature and therefore in evaporation in CanESM2-CRCM5-L compared to CanESM2-CRCM5-NL. The domain mean attenuation of projected increases in precipitation during winter, due to lakes, is around 0.1 mm/day, while it is almost negligible for the other seasons. The patterns for SWE changes due to lakes, in general, follow those for precipitation.

The impact of lakes on projected changes to winter streamflows exhibits a north-south dipole pattern with augmentation of the climate change signal in the northern and attenuation in the southern part of the study domain. The projected changes to winter streamflows are mostly positive in both CanESM2-CRCM5-L and CanESM2-CRCM5-NL, as discussed earlier. The attenuation in projected changes to streamflows in the southern part could be due to the attenuation in the projected changes to precipitation. It could also be due to the storage of the increased proportion of rain, as well as runoff from earlier snowmelt, in lakes, in CanESM2-CRCM5-L. Streamflow changes are augmented in CanESM2-CRCM5-L, compared to CanESM2-CRCM5-NL for the northern regions, because of the increased lake contribution to streamflows in CanESM2-CRCM5-L in the future climate. Note that snowmelt starts only in spring for these regions. In spring, these northern regions show an attenuation in the climate change signal, due to the early start of melting period and increased storage of melt water in lakes. On average, lakes tend to dampen projected increases to winter, spring and fall streamflows by 10, 15 and 7 m³/s, respectively, while the dampening of the projected decreases in summer streamflow is around 14 m³/s.

Comparison of the projected changes to 2- and 5-year 15-day low flow return levels between CanESM2-CRCM5-L and CanESM2-CRCM5-NL simulations shows a north-south dipole pattern in the differences to the projected changes (figure not shown). The dipole pattern is similar to that noted for mean winter streamflows (Fig. 3.12), i.e. positive in the north and negative in the south. The low flows occur during frozen soil conditions over the study domain and hence the mechanism of impact of lakes on the return levels is probably the same as that for the mean winter streamflows, and is based on different timings of the melting season at

different latitudes.

The effect of lakes on climate change signal thus varies with season and region considered. For example, in fall, even though the surface runoff is projected to increase, which partially goes to lake storage, the streamflow changes are dampened. In summer there is going to be a decrease in surface runoff compared to current climate (figure not shown) due to enhanced evaporation. The changes to summer evaporation are much higher than the projected increases to summer precipitation, but it is partly compensated by the lake contribution in CanESM2-CRCM5-L, which leads to positive impacts of lakes on projected changes in summer streamflows. This is also confirmed by the differences in projected changes to mean hydrographs for CanESM2-CRCM5-L and CanESM2-CRCM5-NL (Fig. 3.13). From the hydrographs it can be noted that lakes mostly attenuate the climate change signal. As for the timings of the maximum changes to the hydrographs, lakes delay them slightly, i.e. with lakes the maximum streamflow increases occur later in spring, whereas the maximum decreases occur later in summer or in fall.

The changes to lake-river interactions could be analysed using projected changes to lake levels (Fig. 3.12). The lake levels are projected to decrease in the southern part of the domain (south of 46°N) for all seasons, probably due to increased evaporation, which would cause smaller contribution of lakes to the river flow. To the north of the 46°N parallel, the lake levels are higher during winter and spring and lower during summer, which will probably lead to higher impact of lakes on the winter low flows and spring peaks, although in summer their role for river flow is projected to decrease.

3.3.4 Influence of interflow on projected climate change

A comparison of CanESM2-CRCM5-LI with CanESM2-CRCM5-L is used to study the impact of interflow process on climate change signal. The interflow process in the study region is mostly active during snowmelt periods (Fig. 3.14), which vary from March to June for southern to northern regions. During snow-free periods, interflow occurs following intense precipitation events, which lead to soil saturation, a necessary condition for triggering lateral flow. From Fig. 3.14, it can be seen that most of the precipitation related lateral flows are observed in

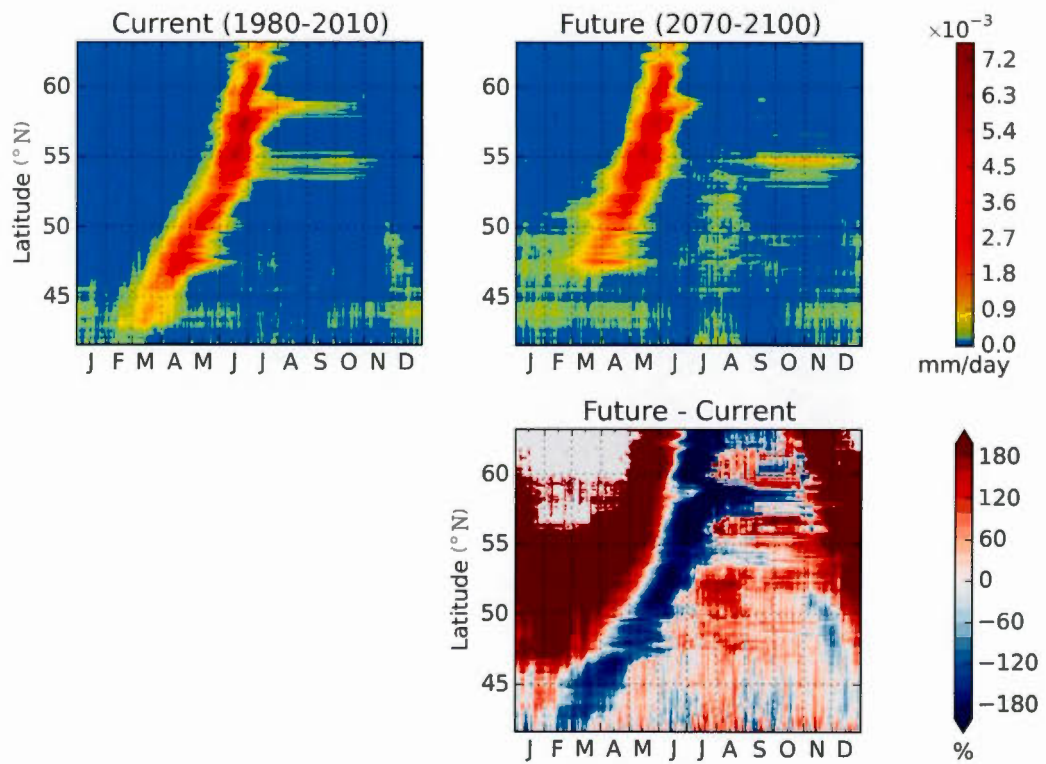


Figure 3.14: Zonally averaged interflow rates (for the first soil layer, mm/day) simulated by CanESM2-CRCM5-LI are shown for current (1980–2010) and future climates (2070–2100) (upper row). The difference between the future and current climate, i.e. projected changes, is shown in the second row.

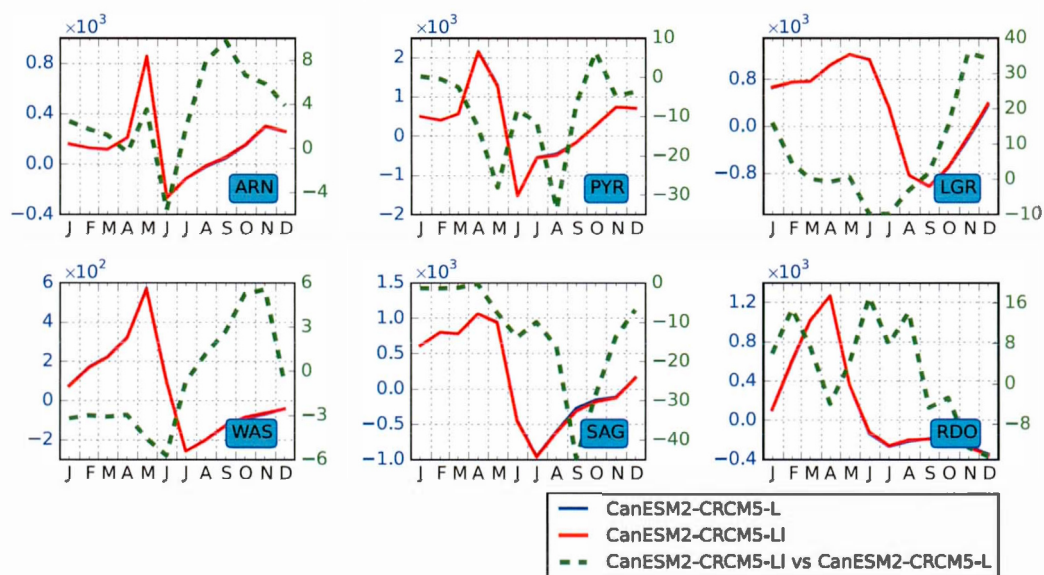


Figure 3.15: Projected changes to mean hydrographs at the outlets of the ARN, PYR, LGR, WAS, SAG, RDO basins for CanESM2-CRCM5-L (blue) and CanESM2-CRCM5-LI (red) simulations and the difference in projected changes (green). Northern (southern) basins are shown in the top (bottom) panel. All values are in m^3/s . The left axis indicates projected changes (red and blue lines) and the right axis indicates differences in projected changes.

the southern parts of the domain. The interflow effect on streamflows varies in sign. Increases in streamflow, caused by interflow, are often followed by decreases, caused by enhanced infiltration of water into soil due to soil moisture deficits created by interflow.

The lower latitudes show a decrease in the lateral flows during snowmelt periods (around 38%), possibly due to reduced snow cover and therefore reduced soil saturation levels for this region. A decrease in maximum interflow values (by approximately 8%) and shift in their timing to earlier in spring are noted in future climate (Fig. 3.14), which is in line with projected changes to the timing of snowmelt and to snow cover itself. The projected increases in interflow rates in future climate during summer and fall seasons could be associated with enhanced precipitation rates during these periods in future climate.

The impacts of interflow on the projected changes to surface and subsurface runoff, streamflow, soil moisture, and evaporation are modest for the study region. A look at the mean changes in hydrographs (plotted using monthly means) near selected basin outlets (Fig. 3.15) show that the maximum impact of interflow on projected changes to streamflow is approximately 1% of the maximum climate change signal at corresponding outlets. The higher positive impacts of interflow on projected changes to streamflow are noted at the outlet of RDO basin (Fig. 15) during summer (up to $16 \text{ m}^3/\text{s}$) and at the outlet of LGR (up to $35 \text{ m}^3/\text{s}$) during fall. Interflow attenuates projected changes to streamflow at the outlet of SAG basin during all seasons, with the maximum attenuation (around $45 \text{ m}^3/\text{s}$) occurring in September. These differences are indicators of projected changes to interflow contributions to streamflows, i.e. when they are positive (negative) the interflow contributions to streamflows are projected to increase (decrease) in future climate. The changes to interflow are controlled by changes in soil moisture driven by changes to SWE, precipitation and evaporation.

3.4 Conclusions

Since lakes and rivers are important components of the climate of Northeast Canada, and since the population heavily rely on the stability of these resources, it is important to understand well their impacts on the regional climate and how

the anticipated climate change might influence lake-river-atmosphere interactions. Therefore, the impact of lake-river-atmosphere interactions and of the interflow process on the regional climate, hydrology and CRCM5-simulated climate change signal are evaluated in this work. To this end, three transient climate change simulations are performed with CRCM5 driven by CanESM2 at the lateral boundaries for the 1950 to 2100 period, for the RCP8.5 scenario. The first simulation includes lakes, while the second one does not have lakes and the third simulation has both lakes and the interflow process. An additional simulation, driven by ERA-Interim reanalysis, for the 1980–2010 period, is performed in order to assess performance errors, i.e. errors due to the physics and dynamics of the regional model.

Performance errors associated with 2-m air temperature and precipitation fields are assessed by comparing with three different observation datasets: CRU, UDel and Hopkinson et al. (2011). All comparisons show similar results, although the performance errors are generally smaller when compared with the higher resolution dataset from Hopkinson et al. (2011). 2-m temperature performance errors are mostly positive in winter and summer. Negative biases appear only in the northern parts of the domain during spring and fall. Performance errors for precipitation are positive for all seasons. The above temperature and precipitation biases influence simulated SWE, which in turn causes overestimation of spring peak and winter flows.

Boundary forcing errors are generally of the same sign as performance errors, except for summer and fall precipitation in the central part of the domain, where the boundary forcing and performance errors are of opposite signs, which lead to smaller total streamflow biases in CanESM2-CRCM5-L than in ERAI-CRCM5-L during summer and fall seasons (Fig. 3.5b).

Assessment of projected changes to seasonal streamflows for the 2070–2100 period, compared to 1980–2010 suggests increases in winter and spring over the entire study domain, due to higher fraction of liquid to solid precipitation and to the projected increases in total precipitation. In summer, the mean streamflows are generally projected to decrease, due to higher evaporation and partly due to reduced precipitation in future climate. During fall, streamflows are projected to increase in the northern part of the domain, where precipitation increase seems

to overcome enhanced evaporation, although in the southerly regions streamflows are expected to decrease.

Projected changes to the 10- and 50-year 1-day high flow return levels are found to be not significant at the 5% significance level almost everywhere over the study domain. On the contrary, projected changes (mostly increases) to the 2- and 5-year 15-day low flow return levels are found to be significant almost everywhere over the domain, which confirms results previously reported by Huziy et al. (2013). It must be noted that Huziy et al. (2013) used a previous version of the model, which is entirely different to the version considered here, i.e. with respect to the physics and dynamics. The simulations were performed at a coarse resolution and did not include lake routing. The similarities, in spite of the model differences, indicate the robustness of the obtained results.

Comparison of projected changes from the two simulations with and without lakes suggests important impact of lakes. Lakes are found to attenuate projected increases to 2-m temperatures, due to their thermal inertia. Although, the maximum attenuation is noted in the vicinity of the lakes, the projected changes to 2-m air temperatures are dampened over the entire region, even in places with relatively smaller lake fractions. Results suggest that the impact of lakes on projected changes to streamflows during winter-spring season depends on the stage of the spring snowmelt. Therefore, the projected increases to winter streamflows are amplified in the northern and dampened in the southern part of the domain. The projected increases to spring streamflows are mostly dampened by the storage effect of lakes.

Based on the projected changes to lake levels, some conclusion could be made concerning lake-river interactions, particularly impacts of lakes on streamflow. Lake levels, and consequently impacts of lakes on rivers, are projected to decrease in future climate in the southern part of the domain throughout the year. In the larger northern part of the domain, the lake-river interactions are expected to decrease in summer and to be amplified in winter and spring, due to decreased and increased lake levels in future climate respectively.

As for the interflow, its impact on projected changes to streamflows is small

(Fig. 3.15) for the current domain and resolution. Its impact on projected changes to precipitation, soil moisture and humidity is also modest. The duration of the period when the interflow process is active in this region is probably too short to cause significant impacts on projected changes to the regional climate. More studies, covering other regions, with more accurate geographic data are required in order to state this with certainty.

The results presented here, although of innovative nature, are based on single simulations of various configurations. It would be useful to perform an ensemble of simulations per configuration to improve confidence in the presented results. The modelled streamflow could be further improved by improving the quality of geophysical fields used in the land surface scheme to calculate hydraulic conductivities, infiltration and surface runoff. The impact of vegetation on hydraulic conductivity might improve the representation of the interflow process. For the lakes, the implementation of the heat exchange with rivers might be beneficial for the correct representation of the energy balance. Work is underway to further improve the frozen soil parameterization and surface-groundwater interactions, which could further improve simulated streamflow and increase confidence in the projected changes simulated by CRCM5.

Acknowledgement

This research was carried out within the framework of the Canadian Network for Regional Climate and Weather Processes (CNRCWP) funded by the Natural Sciences and Engineering Research Council (NSERC) of Canada. The authors would like to thank the two anonymous reviewers whose comments helped further improve the paper.

CONCLUSION

The stability of freshwater resources in a changing climate is an important concern worldwide. RCMs, because of their higher spatial resolution compared to GCMs, are being increasingly used to provide detailed information required for water resources related mitigation and adaptation studies. Thus, it is important to represent realistically surface types and processes including those related to fresh water bodies such as lakes and rivers in climate models. This project, therefore, focusses on improving the representation of lake-river connectivity and interflow process in CRCM5, and to study lake-river-atmosphere interactions within a single regional modelling system, for both current and future climates, for Northeastern Canada. The results obtained during the course of the project, a summary of scientific contributions, current limitations and future work are discussed below.

Summary of results

Projected changes to streamflow characteristics over Northeastern Canada were assessed using transient climate change simulations from CRCM4 in the first part of the thesis. Analysis of the streamflow hydrographs for current climate indicated some model deficiencies such as underestimated low flows due to the lack of representation of lakes in the model. Lakes modulate streamflows for this region by storing snowmelt water, which is released gradually to rivers during the summer to winter seasons. Projected changes to mean annual and seasonal flows and selected high and low flow return levels were studied, assuming that the systematic errors cancel out when computing climate change signal. Results suggest statistically significant increases to mean annual streamflows nearly all over the study domain, while those for seasonal streamflows show increases/decreases depending on the season. Two- and five-year return levels of 15-day low flows are projected to increase significantly over most part of the study domain, although the changes are small in absolute terms. Based on the ensemble averaging approach, changes to 10- and 30-year return levels of high flows are not generally

found significant. However, when a similar analysis is performed using longer samples obtained by merging the different simulations for current and similarly for future climate, significant increases to high flow return levels are found mainly for the northernmost watersheds. This part highlights the need for longer samples, particularly for extreme events, in the development of robust projections. Although important information on projected changes to streamflow characteristics are developed, it is important to understand the physical mechanisms behind these projected changes. This led to further developments of the CRCM and sensitivity experiments to focus on important science questions.

Based on the findings from the experiments with the offline version of the river model, performed in the first part of the study, CRCM5 simulations with lakes and rivers, deeper soil configuration (60 m and 26 soil layers) and higher horizontal resolution (0.1°) were used in the remaining two parts of the thesis.

The influence of lake-atmosphere, lake-river interactions and of interflow on the regional climate and hydrology were studied in the second part of the thesis using a suite of CRCM5 simulations over northeastern Canada for the current period. Experiments with and without lakes demonstrate the thermal moderation effect of lakes, with warmer winter and cooler summer temperatures in the simulation with lakes. Lake-river interactions significantly improved the hydrographs, with lakes dampening the spring flows and providing water later during the year during low flows periods, and lake level variability. As for the interflow, its impact on regional climate and hydrology were modest for the study domain. It is mostly positive and is comparable (if one considers streamflow) to the effect of lake-atmosphere interactions.

Finally, the impact of climate change on lakes and regional hydrology as well as the influence of lakes on projected changes to regional climate and hydrology for northeastern Canada were studied in the third and final part of the thesis using transient climate change simulations spanning the 1950–2100 period, with and without lakes, for the RCP8.5 scenario. Comparison of projected changes based on the simulations with and without lakes suggests that lakes dampen projected changes to 2-m temperature for all seasons. As for streamflows, projected changes to spring streamflows were attenuated in the simulation with lakes and this is

due to the storage effect of lakes, despite the projected increase in precipitation for the spring season in future climate. Similarly, projected changes to summer streamflows were augmented in the simulation with lakes, due to the release of snowmelt water and larger amounts of precipitation stored in lakes from previous months.

Scientific contribution

The main scientific contribution of this study is the improved understanding of the role of lakes, rivers and their connectivity and interflow process on the regional climate and hydrology for northeastern Canada. Although previous studies have looked at some of these aspects in offline simulations of a river or a lake model, this study is innovative in that the above interactions have been assessed within a single regional modelling system. This involved significant developments to the model (implementation of the components and processes discussed above within a highly parallelized framework). This work is thus an important step towards Regional Earth System Modelling.

This study, again for the first time, quantifies the impact of lakes and lake-river connectivity on projected changes to the climate and hydrology for the region. The impacts on projected changes to streamflows are important and highlight the need to represent adequately surface types, including rivers and lakes, and related processes and their interactions in climate models.

This study also provides useful information on projected changes to extreme high and low flows, which are crucial to many economic sectors and thus makes this a valuable contribution to science and to the public in general.

Limitations and outlook

This study, irrespective of the size of lakes, used a 1-D lake model. The study domain considered in this study did contain some of the Great Lakes. One-dimensional models are not suited for large lakes and 3-D lake models are required to simulate the complex circulation patterns and mixing in these large lakes. Some efforts along those lines are already underway with respect to CRCM5. It would

be useful to perform a similar study, for the Great Lakes region, using 3-D lake models in CRCM5 to assess lake-river-atmosphere interactions for this region.

Modelled streamflows could be further improved by improving the quality of geophysical fields used in the land surface scheme to better estimate hydraulic conductivity, infiltration and surface runoff. Work is in progress to improve simulated runoff in CLASS, focusing on improving representation of soil hydraulic conductivity during frozen conditions and surface-groundwater interactions. The former has the potential of improving the timing of snowmelt peak flows in the region and the latter can have significant impacts on winter and summer low flows. The treatment of heat transport and ice processes were not considered in this study and it will be useful to include these in future.

Due to limited time and computing resources, only one transient climate change simulation per configuration, when driven by CanESM2, was considered in this thesis. To quantify the uncertainties, it would be useful to perform at least a small ensemble consisting of other driving GCMs and emission scenarios.

REFERENCES

- Ailliot, P., Thompson, C., and Thomson, P. (2011). Mixed methods for fitting the GEV distribution. *Water Resources Research*, 47(5).
- Arnell, N. W. (2011). Uncertainty in the relationship between climate forcing and hydrological response in uk catchments. *Hydrology and Earth System Sciences*, 15(3):897–912.
- Bechtold, P., Bazile, E., Guichard, F., Mascart, P., and Richard, E. (2001). A mass-flux convection scheme for regional and global models. *Quarterly Journal of the Royal Meteorological Society*, 127(573):869–886.
- Benjamini, Y. and Hochberg, Y. (1995). Controlling the false discovery rate - a practical and powerful approach to multiple testing. *Journal of the Royal Statistical Society Series B-Methodological*, 57:289–300.
- Bennington, V., Notaro, M., and Holman, K. D. (2014). Improving climate sensitivity of deep lakes within a regional climate model and its impact on simulated climate. *Journal of Climate*, 27(8):2886–2911.
- Benoit, R., Côté, J., and Mailhot, J. (1989). Inclusion of a tke boundary-layer parameterization in the canadian regional finite-element model. *Monthly Weather Review*, 117:1726–1750.
- Berrisford, P., Dee, D., Fielding, K., Fuentes, M., Kallberg, P., Kobayashi, S., and Uppala, S. (2009). The era-interim archive. Technical report, European Centre for Medium-Range Weather Forecasts.
- Bowling, L. C. and Lettenmaier, D. P. (2010). Modeling the effects of lakes and wetlands on the water balance of arctic environments. *Journal of Hydrometeorology*, 11:276–295.
- Brasnett, B. (1999). A global analysis of snow depth for numerical weather prediction. *Journal of Applied Meteorology*, 38:726–740.
- Brown, R. D., Brasnett, B., and Robinson, D. (2003). Gridded North American monthly snow depth and snow water equivalent for GCM evaluation. *Atmosphere-Ocean*, 41(1):1–14.

- Chanasyk, D. and Verschuren, J. (1983). An interflow model: I. model development. *Canadian Water Resources Journal*, 8(1):106–119.
- Clapp, R. B. and Hornberger, G. M. (1978). Empirical equations for some soil hydraulic properties. *Water Resources Research*, 14:601–604.
- Clavet-Gaumont, J., Sushama, L., Khaliq, M., Huziy, O., and Roy, R. (2013). Canadian rcm projected changes to high flows for québec watersheds using regional frequency analysis. *International Journal of Climatology*, 33(14):2940–2955.
- Coles, S. (2001). *An introduction to statistical modeling of extreme values*. Springer Series in Statistics.
- Collins, M., Knutti, R., Arblaster, J., Dufresne, J.-L., Fichefet, T., Friedlingstein, P., Gao, X., Gutowski, W., Johns, T., Krinner, G., et al. (2013). Long-term climate change: projections, commitments and irreversibility.
- Côté, J., Gravel, S., Methot, A., Patoine, A., Roch, M., and Staniforth, A. (1998). The operational CMC-MRB Global Environmental Multiscale (GEM) model. Part I: Design considerations and formulation. *Monthly Weather Review*, 126:1373–1395.
- Dadson, S. J., Bell, V. A., and Jones, R. G. (2011). Evaluation of a grid-based river flow model configured for use in a regional climate model. *Journal of Hydrology*, 411:238–250.
- Davies, H. C. (1976). A lateral boundary formulation for multi-level prediction models. *Quarterly Journal of the Royal Meteorological Society*, 102:405–418.
- de Elía, R., Caya, D., Côté, H., Frigon, A., Biner, S., Giguère, M., Paquin, D., Harvey, R., and Plummer, D. (2008). Evaluation of uncertainties in the crcm-simulated north american climate. *Climate Dynamics*, 30:113–132. 10.1007/s00382-007-0288-z.
- de Elia, R. and Côté, H. (2010). Climate and climate change sensitivity to model configuration in the Canadian RCM over North America. *Meteorologische Zeitschrift*, 19:325–339.
- Dee, D. P., Uppala, S. M., Simmons, A. J., Berrisford, P., Poli, P., Kobayashi, S., Andrae, U., Balmaseda, M. A., Balsamo, G., Bauer, P., Bechtold, P., Beljaars, A. C. M., van de Berg, L., Bidlot, J., Bormann, N., Delsol, C., Dragani, R., Fuentes, M., Geer, A. J., Haimberger, L., Healy, S. B., Hersbach, H., Hólm, E. V., Isaksen, L., Kållberg, P., Köhler, M., Matricardi, M., McNally, A. P., Monge-Sanz, B. M., Morcrette, J. J., Park, B. K., Peubey, C., de Rosnay, P.,

- Tavolato, C., Thépaut, J. N., and Vitart, F. (2011). The era-interim reanalysis: configuration and performance of the data assimilation system. *Quarterly Journal of the Royal Meteorological Society*, 137:553–597.
- Delage, Y. (1997). Parameterising sub-grid scale vertical transport in atmospheric models under statically stable conditions. *Boundary-Layer Meteorology*, 82:23–48.
- Delage, Y. and Girard, C. (1992). Stability functions correct at the free-convection limit and consistent for both the surface and ekman layers. *Boundary-Layer Meteorology*, 58:19–31.
- Dibike, Y. B. and Coulibaly, P. (2007). Validation of hydrological models for climate scenario simulation: the case of Saguenay watershed in Quebec. *Hydrological Processes*, 21:3123–3135.
- Döll, P., Kaspar, F., and Lehner, B. (2003). A global hydrological model for deriving water availability indicators: model tuning and validation. *Journal of Hydrology*, 270:105–134.
- Döll, P. and Lehner, B. (2002). Validation of a new global 30-min drainage direction map. *Journal of Hydrology*, 258:214–231.
- Dutra, E., Stepanenko, V. M., Balsamo, G., Viterbo, P., Miranda, P., Mironov, D., and Schär, C. (2010). An offline study of the impact of lakes on the performance of the ecmwf surface scheme. *Boreal environment research*, 15(2):100–112.
- Efron, B. and Tibshirani, R. (1993). *An introduction to the Bootstrap*. Chapman & Hall/CRC.
- Falloon, P., Betts, R., Wiltshire, A., Dankers, R., Mathison, C., McNeall, D., Bates, P., and Trigg, M. (2011). Validation of river flows in hadgem1 and hadcm3 with the trip river flow model. *Journal of Hydrometeorology*, 12(6):1157–1180.
- Fan, Y., Miguez-Macho, G., Weaver, C. P., Walko, R., and Robock, A. (2007). Incorporating water table dynamics in climate modeling: 1. water table observations and equilibrium water table simulations. *Journal of Geophysical Research-Atmospheres*, 112.
- Forzieri, G., Feyen, L., Rojas, R., Flörke, M., Wimmer, F., and Bianchi, A. (2014). Ensemble projections of future streamflow droughts in europe. *Hydrology and Earth System Sciences*, 18(1):85–108.

- Frigon, A., Music, B., and Slivitzky, M. (2010). Sensitivity of runoff and projected changes in runoff over Quebec to the update interval of lateral boundary conditions in the Canadian RCM. *Meteorologische Zeitschrift*, 19:399–399.
- Gal-Chen, T. and Somerville, R. C. J. (1975). On the use of a coordinate transformation for the solution of the navier-stokes equations. *Journal of Computational Physics*, 17(2):209 – 228.
- Garnaud, C. and Sushama, L. (2015). Biosphere-climate interactions in a changing climate over north america. *Journal of Geophysical Research: Atmospheres*, 120(3):1091–1108.
- Giorgi, F. and Bates, G. T. (1989). The climatological skill of a regional model over complex terrain. *Monthly Weather Review*, 117(11):2325–2347.
- Goyette, S., McFarlane, N., and Flato, G. M. (2000). Application of the canadian regional climate model to the laurentian great lakes region: Implementation of a lake model. *Atmosphere-Ocean*, 38(3):481–503.
- Graham, L., Andréasson, J., and Carlsson, B. (2007a). Assessing climate change impacts on hydrology from an ensemble of regional climate models, model scales and linking methods - a case study on the Lule River basin. *Climatic Change*, 81(0):293–307.
- Graham, L., Hagemann, S., Jaun, S., and Beniston, M. (2007b). On interpreting hydrological change from regional climate models. *Climatic Change*, 81(0):97–122.
- GREHYS (1996). Inter-comparison of regional flood frequency procedures for canadian rivers. *Journal of Hydrology*, 186(1-4):85–103.
- Gu, H., Jin, J., Wu, Y., Ek, M. B., and Subin, Z. M. (2013). Calibration and validation of lake surface temperature simulations with the coupled wrf-lake model. *Climatic Change*, 129(3-4):471–483.
- Hall, M. J., van den Boogaard, H. F. P., Fernando, R. C., and Mynett, A. E. (2004). The construction of confidence intervals for frequency analysis using resampling techniques. *Hydrology and Earth System Sciences*, 8(2):235–246.
- Harris, I., Jones, P., Osborn, T., and Lister, D. (2014). Updated high-resolution grids of monthly climatic observations—the cru ts3. 10 dataset. *International Journal of Climatology*, 34(3):623–642.
- Hartmann, D. L., Tank, A. M. G. K., Rusticucci, M., Alexander, L. V., Brönnimann, S., Charabi, Y., Dentener, F. J., Dlugokencky, E. J., Easterling, D. R.,

- Kaplan, A., Soden, B. J., Thorne, P. W., Wild, M., and Zhai, P. M. (2013). *Observations: Atmosphere and Surface*. In: *Climate Change 2013: The Physical Science Basis. Contribution of Working Group I to the Fifth Assessment Report of the Intergovernmental Panel on Climate Change*. Cambridge University Press, Cambridge, United Kingdom and New York, NY, USA.
- Held, I. M. and Soden, B. J. (2006). Robust responses of the hydrological cycle to global warming. *Journal of Climate*, 19(21):5686–5699.
- Hopkinson, R. F., McKenney, D. W., Milewska, E. J., Hutchinson, M. F., Papadopol, P., and Vincent, L. A. (2011). Impact of aligning climatological day on gridding daily maximum-minimum temperature and precipitation over canada. *Journal of Applied Meteorology and Climatology*, 50(8):1654–1665.
- Hosking, J. R. M. (1990). L-moments: analysis and estimation of distributions using linear combinations of order statistics. *Journal of the Royal Statistical Society, Series B*, 52:105–124.
- Hosking, J. R. M., Wallis, J. R., and Wood, E. F. (1985). Estimation of the Generalized Extreme-Value Distribution by the Method of Probability-Weighted Moments. *Technometrics*, 27(3):pp. 251–261.
- Hostetler, S. W., Bates, G. T., and Giorgi, F. (1993). Interactive Coupling of a Lake Thermal Model with a Regional Climate Model. *Journal of Geophysical Research*, 98(D3):5045–5057.
- Hurkmans, R., Terink, W., Uijlenhoet, R., Torfs, P., Jacob, D., and Troch, P. A. (2010). Changes in streamflow dynamics in the rhine basin under three high-resolution regional climate scenarios. *Journal of Climate*, 23(3):679–699.
- Huziy, O. and Sushama, L. (2015). Lake-river connectivity and interflow: impacts on the spatial and temporal distribution of water and energy fluxes over quebec. *TBD*.
- Huziy, O., Sushama, L., Khaliq, M., Laprise, R., Lehner, B., and Roy, R. (2013). Analysis of streamflow characteristics over northeastern canada in a changing climate. *Climate Dynamics*, 40(7-8):1879–1901.
- IPCC (2001). Climate change 2001: the scientific basis. In: Contribution of Working Group I to the Third Assessment Report of the Intergovernmental Panel on Climate Change.
- IPCC (2007). Climate Change 2007: The Physical Science Basis. Contribution of Working Group I to the Fourth Assessment Report of the Intergovernmental Panel on Climate Change.

- Jha, M., Pan, Z., Tackle, E., and Gu, R. (2004). Impacts of climate change on streamflow in the Upper Mississippi River Basin: A regional climate model perspective. *Journal of Geophysical Research D: Atmospheres*, 109(9):D09105 1–12.
- Kain, J. S. and Fritsch, J. M. (1990). A one-dimensional entraining detraining plume model and its application in convective parameterization. *Journal of the Atmospheric Sciences*, 47:2784–2802.
- Kay, A. L., Davies, H. N., Bell, V. A., and Jones, R. G. (2009). Comparison of uncertainty sources for climate change impacts: flood frequency in England. *Climatic Change*, 92(1-2):41–63.
- Kay, A. L., Jones, R. G., and Reynard, N. S. (2006a). RCM rainfall for UK flood frequency estimation. II. Climate change results. *Journal of Hydrology*, 318(1-4):163–172.
- Kay, A. L., Reynard, N. S., and Jones, R. G. (2006b). RCM rainfall for UK flood frequency estimation. I. Method and validation. *Journal of Hydrology*, 318(1-4):151–162.
- Kendon, E. J., Rowell, D. P., Jones, R. G., and Buonomo, E. (2008). Robustness of future changes in local precipitation extremes. *Journal of Climate*, 21(17):4280–4297.
- Khaliq, M. N., Ouarda, T. B. M. J., Gachon, P., and Sushama, L. (2008). Temporal evolution of low-flow regimes in canadian rivers. *Water Resources Research*, 44.
- Khaliq, M. N., Ouarda, T. B. M. J., Gachon, P., Sushama, L., and St-Hilaire, A. (2009). Identification of hydrological trends in the presence of serial and cross correlations: A review of selected methods and their application to annual flow regimes of canadian rivers. *Journal of Hydrology*, 368(1-4):117–130.
- Kourzeneva, E. (2010). External data for lake parameterization in numerical weather prediction and climate modeling. *Boreal environment research*, 15(2):165–177.
- Kuo, H.-L. (1965). On formation and intensification of tropical cyclones through latent heat release by cumulus convection. *Journal of the Atmospheric Sciences*, 22:40–63.
- Laprise, R. (1992). The euler equations of motion with hydrostatic pressure as an independent variable. *Monthly Weather Review*, 120:197–207.

- Laprise, R. (2008). Regional climate modelling. *Journal of Computational Physics*, 227(7):3641–3666.
- Lehner, B. and Döll, P. (2004). Development and validation of a global database of lakes, reservoirs and wetlands. *Journal of Hydrology*, 296(1-4):1 – 22.
- Lehner, B., Verdin, K., and Jarvis, A. (2008). New Global Hydrography Derived From Spaceborne Elevation Data. *Eos Transactions AGU*, 89:93.
- Leung, L. R., Qian, Y., Han, J., and Roads, J. O. (2003). Intercomparison of global reanalyses and regional simulations of cold season water budgets in the western united states. *Journal of Hydrometeorology*, 4(6):1067–1087.
- Li, J. and Barker, H. W. (2005). A radiation algorithm with correlated-k distribution. Part I: Local thermal equilibrium. *Journal of the Atmospheric Sciences*, 62:286–309.
- Lofgren, B. M. (1997). Simulated effects of idealized laurentian great lakes on regional and large-scale climate*. *Journal of Climate*, 10(11):2847–2858.
- Lucas-Picher, P., Arora, V. K., Caya, D., and Laprise, R. (2003). Implementation of a large-scale variable velocity river flow, routing algorithm in the canadian regional climate model (CRCM). *Atmosphere-ocean*, 41(2):139–153.
- Martins, E. S. and Stedinger, J. R. (2000). Generalized maximum-likelihood generalized extreme-value quantile estimators for hydrologic data. *Water Resources Research*, 36(3):737–744.
- Martynov, A., Laprise, R., Sushama, L., Winger, K., Šeparović, L., and Dugas, B. (2013). Reanalysis-driven climate simulation over cordex north america domain using the canadian regional climate model, version 5: model performance evaluation. 41(11-12):2973–3005.
- Martynov, A., Sushama, L., Laprise, R., Winger, K., and Dugas, B. (2012). Interactive lakes in the canadian regional climate model, version 5: the role of lakes in the regional climate of north america. *Tellus A*, 64(0).
- May, W. (2008). Potential future changes in the characteristics of daily precipitation in Europe simulated by the HIRHAM regional climate model. *Climate Dynamics*, 30:581–603.
- McFarlane, N. A. (1987). The effect of orographically excited gravity wave drag on the general circulation of the lower stratosphere and troposphere. *Journal of the Atmospheric Sciences*, 44:1775–1800.

- Mearns, L. O., Gutowski, W., Jones, R., Leung, R., McGinnis, S., Nunes, A., and Qian, Y. (2009). A regional climate change assessment program for north america. *Eos, Transactions American Geophysical Union*, 90(36):311–311.
- Mekonnen, M., Soulis, R., Fortin, V., Davison, B., Marin, S., and Wilson, R. (2012). WATDRN: Enhanced hydrology for CLASS. *Technical paper*.
- Minville, M., Brissette, F., Krau, S., and Leconte, R. (2009). Adaptation to climate change in the management of a Canadian water-resources system exploited for hydropower. *Water Resources Management*, 23:2965–2986.
- Minville, M., Brissette, F., and Leconte, R. (2008). Uncertainty of the impact of climate change on the hydrology of a nordic watershed. *Journal of Hydrology*, 358:70–83.
- Mironov, D., HEIST, E., Kourzeneva, E., Ritter, B., Schneider, N., and Terzhevik, A. (2010). Implementation of the lake parameterisation scheme flake into the numerical weather prediction model cosmo. *Boreal environment research*, 15(2):218–230.
- Mitchell, T. D. and Jones, P. D. (2005). An improved method of constructing a database of monthly climate observations and associated high-resolution grids. *International Journal of Climatology*, 25:693–712.
- Mladjic, B., Sushama, L., Khaliq, M. N., Laprise, R., Caya, D., and Roy, R. (2011). Canadian rcm projected changes to extreme precipitation characteristics over canada. *Journal of Climate*, 24(10):2565–2584.
- Monk, W. A., Peters, D. L., Allen Curry, R., and Baird, D. J. (2011). Quantifying trends in indicator hydroecological variables for regime-based groups of canadian rivers. *Hydrological Processes*, 25(19):3086–3100.
- Muerth, M., Gauvin St-Denis, B., Ricard, S., Velázquez, J., Schmid, J., Minville, M., Caya, D., Chaumont, D., Ludwig, R., and Turcotte, R. (2013). On the need for bias correction in regional climate scenarios to assess climate change impacts on river runoff. *Hydrology and Earth System Sciences*, 17(3):1189–1204.
- Music, B., Frigon, A., Slivitzky, M., Musy, A., Caya, D., Roy, R., Yilmaz, K., Yucel, I., Gupta, H., Wagener, T., et al. (2009). Runoff modelling within the canadian regional climate model (crcm): analysis over the quebec/labrador watersheds. In *New approaches to hydrological prediction in data-sparse regions. Proceedings of Symposium HS. 2 at the Joint Convention of The International Association of Hydrological Sciences (IAHS) and The International Association of Hydrogeologists (IAH) held in Hyderabad, India, 6-12 September 2009.*, pages 183–194. IAHS Press.

- Nash, J. E. and Sutcliffe, J. V. (1970). River flow forecasting through conceptual models part I — A discussion of principles. *Journal of Hydrology*, 10:282–290.
- Niu, G. Y., Yang, Z. L., Dickinson, R. E., Gulden, L. E., and Su, H. (2007). Development of a simple groundwater model for use in climate models and evaluation with gravity recovery and climate experiment data. *Journal of Geophysical Research-Atmospheres*, 112.
- Notaro, M., Holman, K., Zarrin, A., Fluck, E., Vavrus, S., and Bennington, V. (2013a). Influence of the laurentian great lakes on regional climate. *Journal of Climate*, 26:789–804.
- Notaro, M., Zarrin, A., Vavrus, S., and Bennington, V. (2013b). Simulation of heavy lake-effect snowstorms across the great lakes basin by regcm4: Synoptic climatology and variability*,+. *Monthly Weather Review*, 141(6):1990–2014.
- Paquin, J.-P. and Sushama, L. (2015). On the arctic near-surface permafrost and climate sensitivities to soil and snow model formulations in climate models. *Climate Dynamics*, pages 1–26.
- Patterson, J. and Hamblin, P. (1988). Thermal simulation of a lake with winter ice cover. *Limnology and Oceanography*, 33(3):323–338.
- Pitman, A. (2003). The evolution of, and revolution in, land surface schemes designed for climate models. *International Journal of Climatology*, 23(5):479–510.
- Poitras, V., Sushama, L., Seglenieks, F., Khaliq, M. N., and Soulis, E. (2011). Projected changes to streamflow characteristics over western Canada as simulated by the Canadian RCM. *Journal of Hydrometeorology*.
- Quilbé, R., Rousseau, A. N., Moquet, J.-S., Trinh, N. B., Dibike, Y., Gachon, P., and Chaumont, D. (2008). Assessing the Effect of Climate Change on River Flow Using General Circulation Models and Hydrological Modelling – Application to the Chaudière River, Québec, Canada. *Canadian Water Resources Journal*, 33(1):73–94.
- Rudolf, B., Becker, A., Schneider, U., Meyer-Christoffer, A., and Ziese, M. (2010). The new “GPCC full data reanalysis version 5” providing high-quality gridded monthly precipitation data for the global land-surface is public available since December 2010. Technical report, Germany.
- Samuelsson, P., Kourzeneva, E., and Mironov, D. (2010). The impact of lakes on the European climate as simulated by a regional climate model. *Boreal Environment Research*, 15:113–129.

- Šeparović, L., Alexandru, A., Laprise, R., Martynov, A., Sushama, L., Winger, K., Tete, K., and Valin, M. (2013). Present climate and climate change over north america as simulated by the fifth-generation canadian regional climate model. *Climate Dynamics*, 41(11-12):3167–3201.
- Smakhtin, V. U. (2001). Low flow hydrology: a review. *Journal of Hydrology*, 240:147–186.
- Soulis, E., Snelgrove, K., Kouwen, N., and Seglenieks, F. (2000). Towards Closing the Vertical Water Balance in Canadian Atmospheric Models: Coupling of the Land Surface Scheme CLASS with the Distributed Hydrological Model WATFLOOD. *Atmosphere-ocean*, 38(1):251–269.
- Stedinger, J. R., Vogel, R. M., and Foufoula-Georgiou, E. (1993). *Frequency analysis of extreme events*. In: *Handbook of hydrology*. McGraw-Hill Book Co., Inc., New York.
- Subin, Z. M., Riley, W. J., and Mironov, D. (2012). An improved lake model for climate simulations: model structure, evaluation, and sensitivity analyses in cesm1. *Journal of Advances in Modeling Earth Systems*, 4(1).
- Sundqvist, H., Berge, E., and Kristjánsson, J. E. (1989). Condensation and cloud parameterization studies with a mesoscale numerical weather prediction model. *Monthly Weather Review*, 117:1641–1657.
- Sushama, L., Laprise, R., Caya, D., Frigon, A., and Slivitzky, M. (2006). Canadian Regional Climate Model projected climate-change signal and its sensitivity to model errors. *International Journal of Climatology*, 26(15):2141–2159.
- Sushama, L., Laprise, R., Caya, D., Larocque, M., and Slivitzky, M. (2004). On the variable-lag and variable-velocity cell-to-cell routing schemes for climate models. *Atmosphere-Ocean*, 42(4):221.
- Te Chow, V. (1959). Open channel hydraulics.
- Uppala, S. M., Kallberg, P. W., Simmons, A. J., Andrae, U., Bechtold, V. D., Fiorino, M., Gibson, J. K., Haseler, J., Hernandez, A., Kelly, G. A., Li, X., Onogi, K., Saarinen, S., Sokka, N., Allan, R. P., Andersson, E., Arpe, K., Balmaseda, M. A., Beljaars, A. C. M., Van De Berg, L., Bidlot, J., Bormann, N., Caires, S., Chevallier, F., Dethof, A., Dragosavac, M., Fisher, M., Fuentes, M., Hagemann, S., Holm, E., Hoskins, B. J., Isaksen, I., Janssen, P. A. E. M., Jenne, R., McNally, A. P., Mahfouf, J. F., Morcrette, J. J., Rayner, N. A., Saunders, R. W., Simon, P., Sterl, A., Trenberth, K. E., Untch, A., Vasiljevic, D., Viterbo, P., and Woollen, J. (2005). The ERA-40 re-analysis. *Quarterly Journal of the Royal Meteorological Society*, 131:2961–3012.

- Vallis, G. K., Zurita-Gotor, P., Cairns, C., and Kidston, J. (2014). Response of the large-scale structure of the atmosphere to global warming. *Quarterly Journal of the Royal Meteorological Society*.
- Verseghy, D. L. (1991). Class-A Canadian land surface scheme for GCMS. I. Soil model. *International Journal of Climatology*, 11(2):111–133.
- Verseghy, D. L. (1996). Local climates simulated by two generations of canadian gcm land surface schemes. *Atmosphere-Ocean*, 34(3):435–456.
- Verseghy, D. L. (2009). CLASS –the canadian land surface scheme (version 3.4) technical documentation (version 1.1). Technical report, Environment Canada, Climate Research Division, Science and Technology Branch, Downsview, Ontario, Canada.
- Walpole, R. E. and Myers, R. H. (1985). *Probability and Statistics for Engineers and Scientists*. Macmillan, New York, 3 edition.
- Webb, R. S., Rosenzweig, C. E., and Levine, E. R. (1993). Specifying land surface characteristics in general-circulation models - soil-profile data set and derived water-holding capacities. *Global Biogeochemical Cycles*, 7:97–108.
- Weiland, F. S., Van Beek, L., Kwadijk, J., and Bierkens, M. (2012). On the suitability of gcm runoff fields for river discharge modeling: A case study using model output from hadgem2 and echam5. *Journal of Hydrometeorology*, 13(1):140–154.
- Welch, B. L. (1947). The generalization of student's problem when several different population variances are involved. *Biometrika*, 34(1/2):28–35.
- Wen, L., Wu, Z., Lu, G., Lin, C. A., Zhang, J., and Yang, Y. (2007). Analysis and improvement of runoff generation in the land surface scheme CLASS and comparison with field measurements from China. *Journal of Hydrology*, 345(1):1–15.
- Willmott, C. J. and Matsuura, K. (1995). Smart interpolation of annually averaged air-temperature in the united-states. 34:2577–2586.
- Wood, A. W., Leung, L. R., Sridhar, V., and Lettenmaier, D. P. (2004). Hydrologic implications of dynamical and statistical approaches to downscaling climate model outputs. *Climatic Change*, 62:189–216. 10.1023/B:CLIM.0000013685.99609.9e.
- Yakimiw, E. and Robert, A. (1999). Validation Experiments for a Nested Grid-Point Regional Forecast Model. *Atmosphere-Ocean*, 28:466–472.

- Yeh, K. S., Côté, J., Gravel, S., Methot, A., Patoine, A., Roch, M., and Staniforth, A. (2002). The CMC-MRB global environmental multiscale (GEM) model. part III: Nonhydrostatic formulation. *Monthly Weather Review*, 130:339–356.
- Yuan, X. and Liang, X.-Z. (2011). Evaluation of a conjunctive surface–subsurface process model (cssp) over the contiguous united states at regional–local scales. *Journal of Hydrometeorology*, 12(4):579–599.
- Zadra, A., McTaggart-Cowan, R., and Roch, M. (2012). Recent changes to the orographic blocking. *Seminar presentation, RPN, Dorval, Canada*, 2013.
- Zadra, A., Roch, M., Laroche, S., and Charron, M. (2003). The subgrid-scale orographic blocking parametrization of the gem model. *Atmosphere-Ocean*, 41:155–170.